



The Flower Constellation Set and its Possible Applications

Final Report

Authors: Marina Ruggieri¹, Mauro De Sanctis¹, Tommaso Rossi¹,
Marco Lucente¹, Daniele Mortari², Christian Bruccoleri²,
Pietro Salvini¹, Valerio Nicolai¹
Affiliation: (1) University of Roma "Tor Vergata", (2) External Consultant

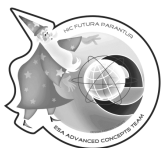
ESA Research Fellow/Technical Officer: Dario Izzo

Contacts:

Marina Ruggieri
Tel: +39 (0)6 7259 7451
Fax: +39 (0)6 7259 7455
e-mail: ruggieri@uniroma2.it

Mauro De Sanctis
Tel: +39 (0)6 7259 7767
Fax: +39 (0)6 7259 7455
e-mail: mauro.de.sanctis@uniroma2.it

Dario Izzo
Tel: +31(0)71 565 3511
Fax: +31(0)71 565 8018
e-mail: act@esa.int



Available on the ACT website
<http://www.esa.int/act>

Ariadna ID: 05/4108
Study Duration: 6 months
Contract Number: 19700/06/NL/HE

Abstract

Currently there are several satellite constellations that allow generating a particular group of satellites with desired features. Walker constellations, probably the most notable example, are created from a set of circular orbits with a given number of satellites in each orbit plane. Removing some constraints on this set of constellations can lead to a more efficient set of constellations suitable for different applications ranging from telecommunications and navigation to Earth and Deep Space Observation. The Flower Constellation set is one important example of such constellations. In fact this set of constellations is not constrained to circular orbits, while, on the other hand, all the satellites belonging to the same Flower Constellation show the same repeating space track. This set of constellations can support both global, regional or spot areas services.

This report complete and update the already known theory of Flower Constellations and develop novel applications of FCs proving the effectiveness of constellation design by means of FCs.

Contents

1	Theoretical Background	1
1.1	Introduction	1
1.2	Orbit compatibility	6
1.3	Flower Constellation phasing	8
1.3.1	Phasing discussion	9
1.3.2	ECEF compatible orbits	11
1.4	Dual-Compatible Flower Constellations	15
1.5	Numerical Example	17
1.5.1	Secondary Paths and Equivalency	21
1.5.2	Symmetric Schemes	22
1.5.3	Restricted Schemes	23
1.5.4	Non-symmetric Schemes	23
1.5.5	Incomplete Schemes	24
1.6	Secondary Closed Paths - Existence and Uniqueness	24
1.7	Secondary Open Paths	30
1.8	Restricted Phasing Secondary Paths	32
1.9	Constructing Secondary Paths	35
1.10	Angular velocity of a secondary path	36
1.11	Equivalent Satellite Distributions	38
1.11.1	Families of Flower Constellations	39
1.11.2	The Contiguous Flower Constellation	41
1.11.3	Finding the Fundamental Distribution	42
	References	43

2	Design of Flower Constellations	58
2.1	Optimisation of Flower Constellations	58
2.1.1	Methodology for the Design of FCs	58
2.1.1.1	Objective Function	63
2.1.1.2	Optimisation process	65
	References	74
3	Applications and Benefit Analysis	75
3.1	Telemedicine	75
3.1.1	Telemedicine Services	76
3.1.2	Constellation Design for Telemedicine	78
3.1.2.1	Flower Constellation Design	78
3.1.2.2	Walker Constellation Design	79
3.1.3	Performance Comparison	82
3.1.4	Conclusion	84
3.2	Martian Constellation of Orbiters	84
3.2.1	Interplanetary Internet And Martian Missions	86
3.2.1.1	Mission Needs	86
3.2.2	Communication Architecture	87
3.2.3	FC Optimization	88
3.2.3.1	Spot Coverage	90
3.2.3.2	Regional Coverage	91
3.2.3.3	Performance Evaluation and Comparison	92
3.2.3.4	Spot Coverage - Single FC parameters	92
3.2.3.5	Spot Coverage - Double FC parameters	94
3.2.3.6	Regional Coverage - Single FC parameters	94
3.2.3.7	Regional Coverage - Double FC parameters	94
3.2.4	Performance Comparison	98
3.2.5	Conclusions	100
3.3	Interferometric Imaging	101
3.3.1	Introduction	101
3.3.2	Optical Interferometric Imaging	102
3.3.3	Flower Constellations for Interferometry	105

CONTENTS

3.3.4	Numerical Optimization Results	106
3.4	Global Navigation Services	109
	References	109
4	Feasibility	112
4.1	Control and Maintenance	112
4.1.1	Orbital Perturbations	112
4.1.2	Perturbations in Flower and Walker Constellations	115
4.1.3	Control and Maintenance Solutions	125
4.2	Constellation Positioning	131
4.3	Deployment	135
4.4	Reconfigurability	140
5	Conclusions	149
A	Flower Constellation Toolbox	150

List of Figures

1.1	Time $t = 0.0$ days	18
1.2	Time $t = 60.3$ days	18
1.3	Time $t = 123.1$ days	19
1.4	Time $t = 185.9$ days	19
1.5	Time $t = 248.7$ days	20
1.6	Time $t = 311.5$ days	20
1.7	Time $t = 374.3$ days	20
1.8	Time $t = 437.1$ days	20
1.9	Comparison of the sequence of allowable values for the RAAN and mean anomaly angles.	25
1.10	When specific choices of parameters are made, then the pattern of pairs of RAAN and mean anomaly angles will repeat before the complete range is filled.	47
1.11	By graphing the RAAN versus mean anomaly over $\text{mod}(2\pi)$, one can see that as the satellites are placed, distinct banding can appear depending upon the values of A and B	48
1.12	Here the RAAN is plotted versus mean anomaly over $\text{mod}(2\pi)$ in a polar plot.	49
1.13	Case 1: A 3-1 FC, Case 2: A 769-257 FC.	50
1.14	Case 1: A 3-1 Flower Constellation with 50 satellites, Case 2: A 769-257 Flower Constellation with 50 satellites.	50
1.15	Secondary closed paths can form on top of the relative orbit. . . .	51
1.16	The Lone Star Constellation - a 38-23-77-23-77 Flower Constellation with $i = 0^\circ$, $\omega = 270^\circ$, and $h_p = 1300 \text{ km}$. Note that the depictions of satellites are not to scale.	52

LIST OF FIGURES

1.17	A secondary path consisting of a single closed loop.	53
1.18	A secondary path consisting of four distinct closed loops.	54
1.19	A secondary path with $N_{al} = 10$ and $N_{pl} = 5$	55
1.20	A graphical example of the allowable circular permutations for the $N = 3$ case. In this example, there are three admissible positions on a given orbit, and there are $(3 - 1)! = 2$ unique sequences that define the order of placement.	55
1.21	A graphical example of the allowable circular permutations for the $N = 4$ case. In this example, there are four admissible positions on a given orbit, and there are $(4 - 1)! = 6$ unique sequences that define the order of placement.	56
1.22	A comparison of satellite node spacing for a <i>Contiguous</i> Flower Constellation, $\Delta\Omega_c$, and an arbitrary node spacing $\Delta\Omega$ when $F_d = 8$	57
1.23	A comparison of satellite mean anomaly spacing for a <i>Contiguous</i> Flower Constellation, ΔM_c , and an arbitrary node spacing ΔM when $N_d = 4$	57
2.1	Input dialog for the optimization process.	60
2.2	Example of points distribution obtained with the function <i>region-grid.m</i> over Texas.	62
2.3	Optimisation process diagram.	66
2.4	Ground track plot for Example 1	67
2.5	Three-dimensional relative path in ECEF coordinates for Example 1.	68
2.6	Solution for continuous coverage of Texas with 6 satellites.	69
2.7	Ground track plot of best solution found in Example 3.	70
2.8	Percentage of visible sites as function of time for the solution found in Example 3.	70
2.9	Best and mean population fitness during GA optimization for example 3.	71
2.10	Ground track plot of best solution found in Example 4.	72
2.11	Ground track plot of best solution found in Example 4.	72
2.12	Ground track plot of best solution found in Example 3.	73

LIST OF FIGURES

3.1	Repeating ground track of the FC for telemedicine.	80
3.2	Relative orbit of the FC for telemedicine (view from the pole). . .	81
3.3	Relative orbit of the FC for telemedicine (orthographic view). . .	81
3.4	Chain access availability percentage performance comparison for all service customers.	83
3.5	Mean access time performance comparison for all service customers.	83
3.6	Ground track of the FC-MARS-single.	93
3.7	Ground track of the FC-MARS-double.	96
3.8	Ground track of the FC-MARS-singleR.	97
3.9	Ground track of the FC-MARS-doubleR.	99
3.10	Spatial physical plane	103
3.11	Spatial frequency plane	104
3.12	Pixels plane	105
3.13	Genetic Algorithm for 10×10 pixels: Coverage = 97.72%	107
3.14	Particle Swarm Optimization for 10×10 pixels: Coverage = 97.72%	107
3.15	Genetic Algorithm for 12×12 pixels: Coverage = 87.87%	108
3.16	Particle Swarm Optimization for 12×12 pixels: Coverage = 83.33%	108
4.1	Satellite constellations cost drivers.	114
4.2	Orbital elements of telemedicine FC.	117
4.3	Orbital elements of telemedicine Walker constellation.	118
4.4	Ground track shift of the Flower Constellation over one month. . .	119
4.5	J_2 effect on RAAN and mean anomaly.	119
4.6	RAAN time progression for Flower and Walker constellations. . .	120
4.7	RAAN evolution for the Flower satellite.	121
4.8	Semimajor axis evolution for the Flower satellite.	122
4.9	Perigee argument evolution for the Flower satellite.	123
4.10	Eccentricity evolution for the Flower satellite.	124
4.11	Inclination evolution for the Flower satellite.	125
4.12	Mean anomaly evolution for the Flower satellite.	126
4.13	Differences between maximum and minimum values of the orbital elements over one year for the Flower constellation.	127

LIST OF FIGURES

4.14 Differences between maximum and minimum values of the orbital elements over one year for the Walker constellation.	128
4.15 RAAN evolution for the Walker satellite.	129
4.16 Semimajor axis evolution for the Walker satellite.	130
4.17 Inclination evolution for the Walker satellite.	131
4.18 Eccentricity evolution for the Walker satellite.	132
4.19 Mean anomaly evolution for the Walker satellite.	133
4.20 Transfer orbits for three satellites.	137
4.21 Common orbit forming (starting from blue, through reds until the black is reached).	138
4.22 Common orbit Eccentricity and Semi major axis evolution.	138
4.23 Common orbit orientation angles evolution.	139
4.24 Eccentricity and Semi major axis.	140
4.25 Orientation angles.	141
4.26 Time evolution of eccentricity and semi-major axis.	143
4.27 Time evolution of shape and orientation errors.	143
4.28 Time evolution of RAAN, inclination and argument of perigee.	144
4.29 Time evolution of satellite mass and delta V	145
4.30 Satellite path from initial to the final orbit.	145
4.31 Shape and Orientation error when multiply factor is 100.	146
4.32 Shape and Orientation error for multiply factor equal to 1 (no effect).	146
4.33 Shape and Orientation error for multiply factor equal to 10.	147
4.34 Shape and Orientation error for multiply factor equal to 100.	148

Chapter 1

Theoretical Background

1.1 Introduction

During the last three decades, the general trend of proposing the substitution of a single large satellite with a set of smaller satellites working in cooperation has pervaded almost all aspects of space research and applications. Some of these fields implicitly require the use of many satellites (e.g., telecommunication, global/regional coverage and navigation systems) while for others, the performance gain obtained using satellite formation schemes or constellations,¹ such as those related to Earth or deep-space observation missions, has been largely proved to be more efficient. To that end, several new measurement technologies have been developed and will most likely be continually developed and improved. Unfortunately, the type of satellite constellations and satellite formations proposed and used today are based on the existing design capability, which can be considered still in its infancy. Reference [1] highlights this aspect and contains an excellent and detailed description of the satellite constellations history, including the well-known Walker constellations [2, 3] and other not-so-well established design methodologies. This is the state of the art as dated in 2004. The most important historical contributions, which can be found in References [4, 5, 6, 7, 8, 9, 10, 11, 12, 13, 14] are detailed summarized and discussed in Reference [1].

¹In this report we consider formation flying as a subset of the general satellite constellations set that is, in turn, unconstrained by satellite distances to guarantee each satellite being visible from all the others.

Constellation design is generally a very difficult problem because each orbit has an infinite number of choices for the six orbital parameters, so for many satellites, the problem is of exceedingly high dimensionality. In the authors' view, this is the primary reason why the art of constellation design is presently suffering from a deep technology development delay. In order to solve this complex problem, satellite constellation designers adopt very limiting assumptions preventing the discovery and development of new, useful solutions. For instance, the assumption of circular orbits, while simplifying the problem from one side, strongly limits the varieties of potential configurations.

Also formations around planets have received a great deal of attention. But to date, only simple string-of-pearl type formations have been flown in Earth observing missions. The challenge lies in the difficulty and high cost of maintaining non-trivial formations which has prevented this technology from blossoming. Satellite formations that have been studied to date tend to be relatively simple (e.g. rotating triangles). Most notably these configurations tend to be in nearly circular orbits, with all orbits lying on the same inertial plane. With Flower Constellation, these simple solutions have been extended to more interesting 3-Dimensional solutions.

The art of designing orbits, satellite constellations and formations will have a large impact on the future mission architectures and concepts. Therefore, the need for covering this evident and existing technological gap implies that new methodologies need to be constructed to design new orbits and satellite constellations. Incidentally, this is now considered in the NASA and ESA strategic road-maps to benefit the NASA and ESA future space missions. In particular, satellite constellations requiring less fuel for control and maintenance than more conventional formations should take advantage of the natural orbital dynamics.

To satisfy the above requirements, some novel methodologies to efficiently design new satellite constellations have been recently proposed. The results obtained in this area during the last few years, especially the development of the Flower Constellations theory, represent a dramatic step forward with wide-ranging mission design impact, both for future geocentric missions and the goals to move to the Moon, Mars, and beyond. In fact, this new and more effective satellite constellation design methodology strongly benefits many of the key strategic

focus areas identified by NASA and ESA. In particular, we have identified direct beneficiaries such as the Robotic and human lunar expeditions, the sustained, long-term robotic and human exploration of Mars, the robotic exploration across the solar system, the development of advanced telescopes searching for Earth-like planets and habitable environments, and the exploration of the Universe, of the dynamic Earth system, and of the Sun-Earth system. Moreover, those mission concepts requiring distributed space systems, telecommunication, deep-space observation, and/or reconnaissance and surveillance can be thought of in new and unique ways through the Flower Constellations. Practical applications such as these will be the focus of detailed work in future publications.

This section contains an extended summary of two articles (Refs. [15], and [16]) to appear in the *IEEE Transactions on Aerospace and Electronic Systems*. These articles and this section, contain the theory of the Flower Constellations as up today's knowledge. The Flower Constellations theory is a truly fundamental breakthrough in satellite constellation and formation design that overcomes these shortcomings in existing methods by adopting *compatible* orbits and an associated *phasing* mechanism. Since the compatibility can be designed with respect to any rotating reference frame, this assumption is not restrictive.

Flower Constellations are special satellite constellations whose satellites follow the same 3-dimensional space track with respect to assigned rotating reference frame. This section presents the theoretical foundation of compatibility and phasing of the Flower Constellations. Compatibility is the synchronization property of a Flower Constellations with respect to a rotating reference frame while phasing dictates the satellite distribution property. Compatibility and phasing, which are ruled by a set of five independent integer parameters, constitute the two main properties of the Flower Constellations. In particular, the Dual-Compatible Flower Constellations theory, which allows a simultaneous synchronization of the Flower Constellation dynamics with two independent rotating reference frames, are explained. Potential applications are briefly discussed in other sections of this final report.

The Flower Constellations constitute an infinite set of satellite constellations characterized by periodic dynamics. They were discovered on the way to the generalization of the concept of some existing satellite constellations. The dynamics

of a Flower Constellations identify a set of implicit rotating reference frames on which the satellites follow the same closed-loop relative trajectory. In particular, when one of these rotating reference frames is “Planet Centered, Planet Fixed”, then all the orbits become compatible (resonant) with the Planet, and consequently, the projection of the relative trajectory on the planet becomes a repeating ground track.

As a particular case, the Flower Constellations can be designed as J_2 compliant in an Earth Centered Earth Fixed (ECEF) frame. That is to say, the orbits are chosen with a compatibility that takes into account the linear effects of the J_2 perturbation. By considering the J_2 effect on these relative trajectories, it is possible to identify a set of critical inclinations associated with dynamically repeating relative trajectories, in this instance called repeating ground track orbits. Because the Earth is a natural object of study, the authors have found numerous applications and specific types of Flower Constellations pertinent to Earth study.

For instance, one can identify so called “two-way” orbits that have identical and parallel perigee and apogee ground tracks. This property allows us to design constellations observing the same geographical region simultaneously from apogee and perigee. In another case, the recently proposed *Synodic* and *Relative* Flower Constellations, which use dual compatible orbits as well as the results obtained in designing reconnaissance orbits for Earth sites, constitute key initial conditions for many potential research proposals because some of these designs would allow both long-term, stand-off surveillance, and episodic close-in inspection.

The relative trajectories in rotating reference frames, which depend on five independent parameters, constitute a continuous, closed-loop, symmetric pattern reminiscent of flower petals. These five parameters are: two integer parameters, N_p and N_d , the angular velocity of the rotating reference frame, the orbit eccentricity (or the perigee altitude), and the orbit inclination. Different values of the first right ascension of the ascending node have just the effect of rigidly rotating the whole relative trajectory about the Earth spin axis. In particular N_p and N_d establish the orbit period, while the three other parameters (ω , e , and i) the shape of the relative trajectory. Finally, the additional three phasing integer parameters (F_n , F_d , and F_h) distribute the satellites into an upper bounded number of admissible positions along the relative trajectory. One of the most important

consequences of the Flower Constellation theory is that, for a particular set of the five integer parameters, the satellite distribution highlights the existence of *Secondary Paths*. These Secondary Paths, which exhibit many beautiful and intricate dynamics and mysterious properties, are close to being fully understood [16], and the prediction of them appears to be linked to real algebraic geometry. Finally, the possibilities of re-orienting the Flower Constellation axis and playing with multiple Flower Constellations allow the design of a constellation of constellations and constellations of formation flying schemes.

The Flower Constellation theory has been developed at Texas A&M University. Along with the theory, the Flower Constellations Visualization and Analysis Tool (FCVAT) has been developed and coded. The FCVAT software represents a truly fundamental breakthrough in satellite constellation design methodology, because it makes easier to see and to understand the complicated satellite dynamics as well as allowing one to see the effects of the variations of the design parameters on the constellation. This allows users to easily find different types of satellite formations which have heretofore been very difficult to construct using current methods. It is important to emphasize that, in order to design a Flower Constellation, a program like FCVAT must be first developed. Without such a specific program, or equivalent, the design (and the understanding) of a Flower Constellation dynamics becomes very difficult or almost impossible.

Flower Constellations represent a breakthrough in the difficult art (and science) of satellite constellation design. The Flower Constellations described here provide a new capability for global 3-D spatial observations around the planets. Flower Constellations also provide new and unique avenues for addressing the ever-present problem of constellation maintenance. Background on Flower Constellations can be found in [17, 18, 19]. The Flower Constellation theory, which required over two years of effort, is presented here at today's mature stage. As for applications, the theory has already been successfully applied to design GPS-like Global Navigation Systems for Earth [20, 21]. In particular, constellation design software, written in Java and Java-3D, has already been developed to assist in visualizing and building new Flower Constellations [22].

This report summarizes important properties of the Flower Constellations and introduces the theory of Dual-Compatible Flower Constellations. Flower

Constellation Phasing is first discussed in brief. We also introduce an additional parameter not present in earlier developments, the phasing step F_h , that further enlarges the dimensionality of the potential solutions. Finally, the theory of Dual-Compatible Flower Constellations is introduced and some examples are given.

1.2 Orbit compatibility

Flower Constellations are built using compatible (or resonant) orbits. The word compatible associated with two rotating reference frames characterizes a synchronization property between them. From a mathematical point of view, two rotating reference frames, \mathcal{F}_1 and \mathcal{F}_2 , are identified as *compatible* or as *resonant*, if their constant angular velocities, ω_1 and ω_2 (or periods T_1 and T_2), satisfy the condition

$$N_1 T_1 = N_1 \frac{2\pi}{\omega_1} = N_2 T_2 = N_2 \frac{2\pi}{\omega_2} \quad (1.1)$$

where N_1 and N_2 can be any integers.

If the angular velocities ω_1 and ω_2 are not constant, then \mathcal{F}_1 and \mathcal{F}_2 are still identified as compatible if and only if $\omega_1(t)$ and $\omega_2(t)$ are periodic functions of periods T_1 and T_2 , respectively. In this specific case, the compatibility is mathematically defined by the relationship

$$N_1 \int_0^{T_2} \omega_2(t) dt = N_2 \int_0^{T_1} \omega_1(t) dt \quad (1.2)$$

where T_1 and T_2 are the periods of the rotating frames.

The orbit periodicity is characterized by a fictitious constant angular velocity $n = \frac{2\pi}{T}$, called the orbit mean motion. Therefore, the orbit compatibility, with respect to a reference frame \mathcal{F} rotating with angular velocity ω , is ruled by the relationship:

$$N_p T = N_p \frac{2\pi}{n} = N_d \frac{2\pi}{\omega} \quad (1.3)$$

where N_p and N_d are two positive integers characterizing the compatibility mechanism. Alternatively, the definition of a compatible orbit can be expressed by saying that an orbit is compatible when the ratio of its orbital period with that of the rotating reference frame is rational. In the Flower Constellations theory, N_p

and N_d have been identified as the *Number of Petals* and the *Number of Days*. In fact, when the rotating reference frame is chosen to be the Earth-Centered Earth-Fixed (ECEF) frame, then N_d really represents the number of days. The *Number of Petals*, N_p , that actually represent the number of orbit revolutions, finds its origin because of the petal-like shape of the relative trajectory.

Equation (1.3) simply states that after N_p orbital periods the rotating reference frame has performed N_d complete rotations and, consequently, the satellite and the rotating reference frame come back to their initial positions. This implies that, in the rotating reference frame, the spacecraft follows a closed-loop trajectory that can be seen as a closed 3-Dimensional space track. The orbiting satellite completes this closed-loop trajectory in the repetition time

$$T_r = N_p T \quad (1.4)$$

Alternatively, the definition of a compatible orbit can be expressed by saying that an orbit is compatible when the ratio of its orbital period with the rotational period of the rotating reference frame is rational. In particular, when the rotating reference frame is chosen to be Earth-Fixed Earth-Centered (ECEF) frame, then the projection of the 3-Dimensional closed-loop trajectory on the Earth is what it is termed “repeating ground track.”

It is important to emphasize that the concept of compatibility does not uniquely identify a specific rotating reference frame but rather an infinite set of rotating reference frames. In fact, an orbit satisfying Equation (1.3) is also compatible with all the reference frames \mathfrak{F}' rotating with angular velocity:

$$\omega' = \omega \left(\frac{N'_d}{N'_p} \right) \left(\frac{N_p}{N_d} \right) \quad (1.5)$$

where N'_p , N'_d , and ω' , satisfy the compatibility condition:

$$N'_p T = N'_d \frac{2\pi}{\omega'} \quad (1.6)$$

In total, Flower Constellations are identified by eight parameters. Five are integer parameters. Thus far, we have discussed the *Number of Petals* (N_p) the *Number of Days* (N_d). In the following discussion, we introduce three more integers to rule the phasing (F_n , F_d , and F_h). Keep in mind that common to

all satellites in a Flower Constellation are three orbit parameters: the argument of perigee (ω), the orbit inclination (i), and the perigee altitude (h_p) or the eccentricity (e).

1.3 Flower Constellation phasing

Flower Constellations are built using orbits that are compatible with respect to assigned rotating reference frames. In particular, in the Flower Constellations design methodology, all the satellites follow the same 3-D relative trajectory in the rotating reference frame. In order to obtain this result, the values of the right ascension of the ascending node, Ω , and the mean anomaly, M , cannot be independent. Once Ω is assigned, then there is a subset of mean anomalies (M), called “admissible,” that can be selected. This constitutes the Flower Constellations phasing rule.

Mathematically, one is free to choose the placement of the first satellite at $(\Omega_1, M_1) = (0, 0)$ and adopt the satellite distribution with the following sequence of orbit node lines

$$\Omega_{k+1} = \Omega_k - 2\pi \frac{F_n}{F_d} \quad (1.7)$$

where F_n and F_d are two independent integer parameters that can be freely chosen. Equation (1.7) can be written as

$$\Omega_k = 2\pi \frac{F_n}{F_d} (1 - k), \quad (1.8)$$

where $k = 1, 2, \dots, N_s$ and N_s is the total number of satellites constituting the Flower Constellation.

Now, in order to place the satellites in the same 3-D relative trajectory, the mean anomaly must be selected as

$$M_{k+1} = M_k + 2\pi \frac{F_n N_p + F_d F_h}{F_d N_d} \quad (1.9)$$

or, alternatively, Equation (1.9) can be written as

$$M_k = 2\pi \frac{F_n N_p + F_d F_h}{F_d N_d} (k - 1) \quad (1.10)$$

where $F_h \in \{0, 1, \dots, N_d - 1\}$ is an integer parameter that can be freely chosen called the phasing step parameter.

1.3.1 Phasing discussion

Among all possible freely chosen integer values for N_p and N_d , we make the non-restrictive hypothesis that N_p and N_d have no common factors besides themselves and 1. That is to say, N_p and N_d are relatively prime, expressed as

$$N_p \perp N_d \quad (1.11)$$

In fact, in the case that they do have common factors, we can always substitute N_p and N_d with $N_p^* = \frac{N_p}{C_t}$ and $N_d^* = \frac{N_d}{C_t}$, respectively, where $C_t = \text{gcd}(N_p, N_d)$ is the Greatest Common Divisor (gcd) of the two integers. This transformation leaves the ratio N_p/N_d invariant and, consequently, the orbit period T remains invariant. Similarly, the integer parameters F_n and F_d are also assumed to be relatively prime ($F_n \perp F_d$). Furthermore, we can assume that $\frac{F_n}{F_d} \leq 1$. In fact, if $F_n > F_d$, then we can always substitute F_n with $F'_n = F_n \pmod{F_d}$, since Ω and $(\Omega + 2k\pi)$ identify the same orbit node.

The sequence of the orbit node lines described by Equations (1.7) and (1.8) is such that when the index of the sequence k is equal to $F_d + 1$ then the orbit node line coincides with the first orbit node line and a second satellite is allocated on the first orbit. In fact, we have

$$\Omega_{F_d+1} = 2\pi F_n \quad (1.12)$$

is a multiple of 2π . This implies that F_d represents the total number of distinct orbits used to build the constellation.

It is interesting to point out that, in order to belong to the same relative trajectory, the step parameter F_h does not have to be necessarily constant, that is, invariant with respect to the index k , but just to be set to any integer from 0 to $(N_d - 1)$. This property is a consequence of the fact that compatible orbits have N_d admissible orbital locations displaced one from another by the mean anomaly $\Delta M = 2\pi/N_d$. By selecting a rule for F_h , as for instance $F_h = \text{constant}$, or $F_h = (F_{h0} + k) \pmod{N_d}$ or, in general

$$F_h = f(k) \pmod{N_d} \quad (1.13)$$

1.3 Flower Constellation phasing

where $f(k)$ identifies an assigned numerical sequence (e.g., the Fibonacci's sequence) we obtain “harmonic” satellite distributions and dynamics. However, a specifically ordered sequence is not required by the theory and even a random distribution, such as $F_h(k) = \text{rand}(N_d)$ where $\text{rand}(N_d)$ identifies a function providing non-uniform random integer numbers in the range $[0, N_d - 1]$, is admissible. However, when $f(k)$ is selected to be random, the harmonic dynamics and distribution is, in general, lost.

Equations (1.9) and (1.10) govern the sequence of the mean anomalies, which is dictated by the rational parameter $(F_n N_p + F_d F_h)/(F_d N_d)$. This ratio might be further simplified. To this end, let $C = \text{gcd}(F_n N_p + F_d F_h, F_d N_d)$. This implies that Equations (1.9) and (1.10) can be re-written in the following simplified way

$$M_k = 2\pi \frac{F_n N_p + F_d F_h}{F_d N_d} (k - 1) = 2\pi \frac{R_n}{R_d} (k - 1), \quad (1.14)$$

where $k = 1, 2, \dots, N_s$ and where

$$R_n = \frac{F_n N_p + F_d F_h}{C} \quad \text{and} \quad R_d = \frac{F_d N_d}{C} \quad (1.15)$$

Equations (1.8) and (1.14) implies that when we come back to the initial orbit with the sequence index $k = F_d + 1$, then the mean anomaly of the second satellite belonging to the first inertial orbit is

$$M_{F_d+1} = 2\pi \frac{R_n}{R_d} F_d \quad (1.16)$$

Let $C_r = \text{gcd}(F_d, R_d)$. Therefore, the integer

$$N_{so} = \frac{R_d}{C_r} \leq N_d \quad (1.17)$$

represents the number of satellites per orbit for the chosen distribution sequence and constellation. As a consequence, the total number of satellites will be

$$N_s = N_{so} F_d \leq N_d F_d \quad (1.18)$$

The parameter N_{so} also represents the number of loops around the Earth that are completed while placing satellites in a Flower Constellation. That is to say, if one places a single satellite in each of F_d orbits, it will take you N_{so} cycles

1.3 Flower Constellation phasing

around to place all the satellites. Now, since N_d represents the overall number of admissible locations in one orbit, then N_{so} tells you how many of the N_d locations are filled in a given satellite distribution. Therefore, if $N_{so} = N_d$, then all the available admissible spots are filled, while if $N_{so} = 1$, then only one admissible spot (per orbit) is used. If $N_{so} < N_d$, then we define $N_s \equiv N_{so} F_d$ and describe the satellite distribution as forming a N_{so}/N_d *Secondary Path*.

Associated with a given distribution sequence there is always an upper limit for the number of admissible locations where one can locate satellites. This implies that a single Flower Constellation (not a *Flower Group*, which is a constellation of Flower Constellations) is made with no more than N_s satellites, where

$$N_s \leq N_d F_d \quad (1.19)$$

However, for an assigned sequence distribution, there exists the possibility that the sequence distribution does not fill all the $N_d F_d$ admissible locations. This happens when, during the satellite distribution, a satellite should be placed onto the initial location of the first satellite, location that has already been occupied. When this happens the satellites are distributed along a *secondary path*, which is associated with a sequence distribution that create a premature closing loop. Depending upon the number of satellites per orbit N_{so} constituting this particular distribution, a classification of the secondary paths is given. Thus, a secondary path having N_{so} satellite per orbit is called “secondary path of order N_{so} ”. See sections 2.3 and 2.4 of this report.

1.3.2 ECEF compatible orbits

For the specific application of finding precise repeating orbits in Earth’s gravity field, one must write the perturbative quantities $\dot{\Omega}$ and \dot{M}_0 using the well documented spherical harmonic expansion. The symmetric phasing scheme that has been adopted for use in the Flower Constellations, including perturbative quantities, can be expressed as

$$\Omega_{k+1} = \Omega_k - 2\pi \frac{F_n}{F_d} \quad (1.20)$$

1.3 Flower Constellation phasing

and

$$M_{k+1}(0) = M_k(0) + 2\pi \frac{F_n}{F_d} \left(\frac{n + \dot{M}_0}{\omega_{\oplus} + \dot{\Omega}} \right) \quad (1.21)$$

where $k \in \{1, 2, \dots, N_s - 1\}$. Note that Equation (1.21) is a function of the orbit mean motion. In order to find the mean motion, which is a function of the semi-major axis a , one must first find the anomalistic orbit period by solving the equation

$$T = \frac{2\pi}{\omega_{\oplus}} \frac{N_d}{N_p} \left(1 + 2\xi \frac{n}{\omega_{\oplus}} \cos i \right)^{-1} \chi, \quad (1.22)$$

where $\omega_{\oplus} = 7.2921158553 \cdot 10^{-5}$ rad/sec is the Earth spin rate. The expression for χ and ξ appearing in Equation (1.22) are

$$\chi = 1 + \xi \left[4 + 2\sqrt{1 - e^2} - (5 + 3\sqrt{1 - e^2}) \sin^2 i \right], \quad (1.23)$$

where e and i are the orbit eccentricity and inclination, respectively, and

$$\xi = \frac{3R_{\oplus}^2 J_2}{4p^2} \quad (1.24)$$

where $R_{\oplus} = 6378.1363$ Km is the equatorial Earth radius, $J_2 = 1.0826269 \cdot 10^{-3}$ the Earth oblateness constant, and $p = a(1 - e^2)$ the orbit semilatus rectum.

Equation (1.22) has been analytically expressed up to $O(J_2)$.² Equation (1.22) is the most general equation governing the anomalistic orbit period of the Flower Constellation. The mean motion must be isolated on the left hand side of the equation, which leads to an equation of the following form:

$$n = \frac{\omega_{\oplus} [1 + A(\xi)]^{-1}}{\tau - 2\xi [1 + A(\xi)]^{-1} \cos i} \approx \frac{\omega_{\oplus} [1 - A(\xi)]}{\tau - 2\xi \cos i} \quad (1.25)$$

where

$$A(\xi) = \xi \left[4 + 2\sqrt{1 - e^2} - (5 + 3\sqrt{1 - e^2}) \sin^2 i \right] \quad (1.26)$$

and

$$\tau = \frac{N_d}{N_p} \quad (1.27)$$

Note that the approximation given in Equation (1.25) results from two simplifications. Terms that are $O(\xi^2)$ have been ignored, and the approximation,

²This equation can be expressed to any order or degree but the analytic complexity increases significantly.

1.3 Flower Constellation phasing

$(1+x)^n \approx 1+nx$ for sufficiently small x , has been utilized. However, if one will consider higher order perturbations, such as J_3 and J_4 that are generally $O(\xi^2)$, then this simplification can not be made.

Returning back to Equation (1.21), the perturbative quantities $\dot{\Omega}$ and \dot{M}_0 can be expressed as a function of the J_2 perturbation and known parameters by incorporating Equation (1.25)

$$\dot{\Omega} = -2\xi n \cos i \approx \frac{-2\xi\omega_{\oplus}[1-A(\xi)]\cos i}{\tau - 2\xi \cos i} \quad (1.28)$$

and

$$\begin{aligned} \dot{M}_0 &= -\xi n \sqrt{1-e^2}(3\sin^2 i - 2) \approx \\ &\approx \frac{-\xi\omega_{\oplus}[1-A(\xi)]\sqrt{1-e^2}(3\sin^2 i - 2)}{\tau - 2\xi \cos i} \end{aligned} \quad (1.29)$$

Note that the simplified form of Equation (1.25) has been used because only the J_2 effect is being considered at this point.

By substituting Equations (1.28), (1.29), and (1.25) into Equation (1.21), we obtain

$$M_{k+1}(0) = M_k(0) + \frac{2\pi F_n}{\tau F_d} \beta_1 \quad (1.30)$$

where

$$\beta_1 = \frac{[1-A(\xi)][1-\xi\sqrt{1-e^2}(3\sin^2 i - 2)]}{1-4\xi \cos i/\tau} \quad (1.31)$$

or

$$M_{k+1}(0) = M_k(0) + \frac{2\pi F_n N_p}{F_d N_d} \beta_2 \quad (1.32)$$

where

$$\beta_2 = \frac{1-A(\xi) - \xi\sqrt{1-e^2}(3\sin^2 i - 2)}{1-4\xi \cos i/\tau} \quad (1.33)$$

and where in Equation (1.32) the terms of $O(\xi^2)$ have been ignored.

Assuming that the orbit inclination has been specified, Equation (1.22) is essentially a single equation in terms of a single unknown, the semi-major axis. All of the other variables (n, ξ, p, T) can be resolved in terms of a . In particular, the orbit eccentricity can be written as a function of the semi-major axis a and of the perigee altitude h_p

$$e = 1 - \frac{R_{\oplus} + h_p}{a} \quad (1.34)$$

1.3 Flower Constellation phasing

This allows us to write the semi-parameter only in terms of the unknown a

$$p = a(1 - e^2) = 2(R_{\oplus} + h_p) - \frac{(R_{\oplus} + h_p)^2}{a} \quad (1.35)$$

The anomalistic period and mean motion are given by

$$T = \frac{2\pi}{n} = 2\pi \sqrt{\frac{a^3}{\mu}} \quad (1.36)$$

where $\mu = 398,600.4415 \text{ Km}^3/\text{sec}^2$. Using any standard numerical solver, one can now solve for the semi-major axis. Once the semi-major axis has been established, we can obtain the required eccentricity and the anomalistic period.

With a specific choice of inclination, one can mitigate the movement of the line of apsides. The critical inclinations 63.4° and 116.6° allow one to “freeze” the precession of the line of apsides. Choosing either of these inclinations significantly reduces the control effort required to maintain the overall constellation geometry.

However, it is also possible to choose inclinations where the constellation deforms in a regular way returning back to its original configuration. In this manner, we choose to work with Mother Nature rather than fight her. First recall that the rate of change in the argument of perigee due to the J_2 effect is represented as:

$$\dot{\omega} = \frac{3R_{\oplus}^2 J_2}{4p^2} n (4 - 5 \sin^2 i) \quad (1.37)$$

Here we allow the line of apsides to rotate at a specified rate but modified with an integer parameterization.

$$K_d \dot{\omega} = K_n \dot{\omega}_c \quad (1.38)$$

where $\dot{\omega}_c$ is a specified desired angular velocity, K_n is a positive integer parameter and K_d is an independent (positive or negative) integer parameter. In the case that $\dot{\omega}_c = \frac{2\pi}{T_{\oplus}}$, this equation states that, in K_d Earth orbit periods, the orbit apsidal line precesses (clockwise or counter-clockwise) $|K_n|$ times. Equation (1.38) also generalizes Equation (1.37) that, in turn, can be obtained by setting $K_n = K_d = 1$.

1.4 Dual-Compatible Flower Constellations

This section analyzes some particular Flower Constellations whose orbits are simultaneously compatible with two rotating reference frames. As it will be demonstrated later, for these special Flower Constellations, we are no longer free to choose where to locate the orbit apsidal lines (i.e the subsequent values of Ω_k). In other words, we are no longer free to choose the two phasing parameters F_n and F_d (F_h has no longer meaning), establishing the $\Delta\Omega = 2\pi F_n/F_d$ between two subsequent apsidal lines. In fact, for these special Flower Constellations, the value of $\Delta\Omega$ is directly derived from the dual compatibility constraint. Furthermore, the overall number of admissible locations strongly depend on the design parameters.

An orbit is Dual-Compatible (or dual-resonant) if, assigned the four integers N_{p1}, N_{d1}, N_{p2} , and N_{d2} , its orbital period T satisfies the two relationships

$$N_{p1} T = N_{d1} T_1 \quad \text{and} \quad N_{p2} T = N_{d2} T_2 \quad (1.39)$$

where

$$T_1 = \frac{2\pi}{\omega_1} \quad \text{and} \quad T_2 = \frac{2\pi}{\omega_2} \quad (1.40)$$

are the periods associated with two reference frames rotating with angular velocities ω_1 and ω_2 , respectively.

Based on the above definition, any orbit characterized by orbit period T , is compatible with an infinity of rotating reference frames characterized by the set of angular velocities

$$\omega_k = \frac{2\pi}{T} \frac{N_{dk}}{N_{pk}} = n \frac{N_{dk}}{N_{pk}} \quad (1.41)$$

In order to find out where to locate the satellite of a Dual-Flower Constellation, let us evaluate the RAAN variation, as provided by Equations (1.7) and (1.8)

$$\Delta\Omega = \Omega_{k+1} - \Omega_k = -2\pi \frac{F_n}{F_d}, \quad (1.42)$$

which tells one where to allocate one orbit ($k+1$) with respect to the previous orbit (k). The satellite in the $(k+1)$ -th orbit will have a variation of the mean

1.4 Dual-Compatible Flower Constellations

anomaly with respect to the value of the previous satellite that can be evaluated using Equations (1.9) and (1.10). The ΔM expression is

$$\Delta M = M_{k+1} - M_k = 2\pi \frac{F_n N_p + F_d F_h}{F_d N_d} = \Delta\Omega \frac{N_p}{N_d} - 2\pi \frac{F_h}{N_d}. \quad (1.43)$$

We can evaluate the variation ΔM using both sequences, $\mathfrak{F}_1 \triangleq \{N_{p1}, N_{d1}, F_n, F_d, F_h\}$ and $\mathfrak{F}_2 \triangleq \{N_{p2}, N_{d2}, F_n, F_d, F_h\}$. These two distributions, \mathfrak{F}_1 and \mathfrak{F}_2 , must provide values for ΔM that can only differ by an amount $2\pi\ell$, where ℓ can be any integer. Therefore, we can write that

$$\Delta M = \Delta\Omega \frac{N_{p1}}{N_{d1}} + 2\pi \frac{F_h}{N_{d1}} = \Delta\Omega \frac{N_{p2}}{N_{d2}} + 2\pi \frac{F_h}{N_{d2}} + 2\pi\ell \quad (1.44)$$

This equation allows us to obtain an expression for $\Delta\Omega$ that is a function of the integer parameter ℓ

$$\Delta\Omega_\ell = 2\pi \frac{F_h(N_{d2} - N_{d1}) + \ell N_{d1} N_{d2}}{N_{d1} N_{p2} - N_{d2} N_{p1}} = 2\pi \frac{G_\ell}{G_d} \quad (1.45)$$

which allows us to evaluate the values (therefore, the sequence) of the right ascension of the ascending nodes, Ω_k , where the two distributions locate satellites with the same values of the mean anomaly (same orbital position).

In order to use Equation (1.45), the condition $G_d \neq 0$, that is

$$N_{d1} N_{p2} \neq N_{d2} N_{p1} \quad (1.46)$$

must be satisfied. This condition implies that the case $T_1 = T_2$ must be avoided. This is intuitive because the point of this exercise is to study two reference frames that are rotating with respect to each other and having identical rotation periods would preclude this. In addition, the values of ℓ satisfying

$$\ell N_{d1} N_{d2} = F_h(N_{d1} - N_{d2}) \iff G_\ell = 0, \quad (1.47)$$

which are associated with the condition $\Delta\Omega_\ell = 0$, allow us to obtain the sequence of all the solutions per orbit. This sequence can also be obtained for the values of ℓ giving $\Delta\Omega_\ell = 2\pi m$, which is satisfied when

$$\gcd(G_\ell, G_d) = G_d \quad (1.48)$$

For each value of $\Delta\Omega_\ell$ provided by Equation (1.45), we have an associated value for ΔM_ℓ

$$\Delta M_\ell = -\Delta\Omega_\ell \frac{N_{p1}}{N_{d1}} - 2\pi \frac{F_h}{N_{d1}} = -\Delta\Omega_\ell \frac{N_{p2}}{N_{d2}} - 2\pi \frac{F_h}{N_{d2}} + 2\pi \ell \quad (1.49)$$

Summarizing, a dual-compatible Flower Constellation is built using the phasing sequence

$$\Omega_{k+1} = \Omega_k + \Delta\Omega_\ell \quad \text{and} \quad M_{k+1} = M_k + \Delta M_\ell \quad (1.50)$$

where $k = 1, 2, \dots$, and $\Delta\Omega_\ell$ and ΔM_ℓ are provided by Equations (1.45) and (1.49), respectively.

1.5 Numerical Example

“Single”-compatible Flower Constellations have been presented in previous publications such as [17, 18, 20, 21, 23, 24, 25] as well as in the companion work [16], showing how the design parameters affect the configuration. These publications highlight the versatility and the wide range of potential applications characterizing the Flower Constellation design methodology. For this reason, an example of Dual Flower Constellation is presented in the following.

In order to understand the dynamics of a Dual Flower Constellation, some subsequent displacements of the satellites and of the rotating relative trajectories are given in Figures 1 through 8, using a time step of approximately $\Delta t = 2$ months. This Dual Flower Constellation is obtained using the Sun as a central body, orbit eccentricity $e = 0.4$, orbit inclination $i = 0^\circ$, the parameter $\ell = 0$, and the following specific design parameters:

N_{p1}	N_{d1}	N_{p2}	N_{d2}	F_n	F_d	F_h
4	3	3	1	1	13	1

Table 1.1: Dual Flower Constellation design parameters

In these Figures the Dual Flower Constellation is provided by a sequence of subsequent time instants highlighting the configuration dynamics. Satellites are marked with “O” symbols. At each time instant, one can see how the intersections

1.5 Numerical Example

of the two relative trajectories (where the satellites are located) move. Not all the relative trajectories intersections are admissible locations but just a small subset of them, characterized by $\Delta\Omega_\ell$ and ΔM_ℓ , provided by Equations (1.45) and (1.49), respectively.

The admissible locations of a Dual Flower Constellation is the intersection set of the admissible location sets of the two relative trajectories. Mathematically, this implies that the number of admissible locations for a Dual Flower Constellation is $G_d N_{d1}$.

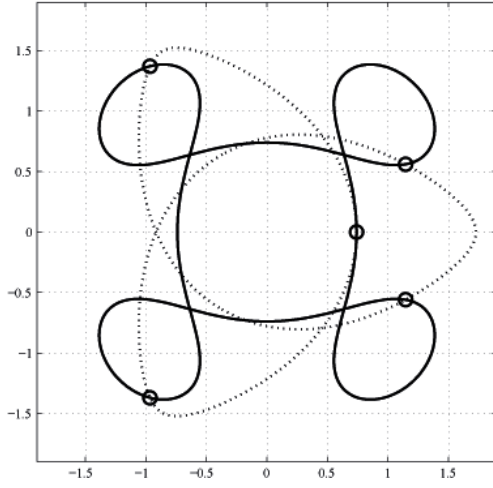


Figure 1.1: Time $t = 0.0$ days

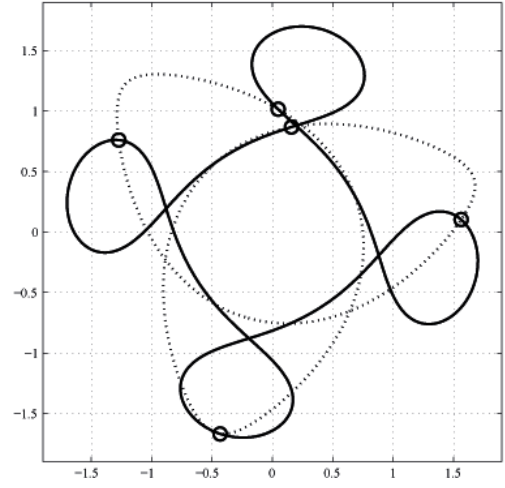


Figure 1.2: Time $t = 60.3$ days

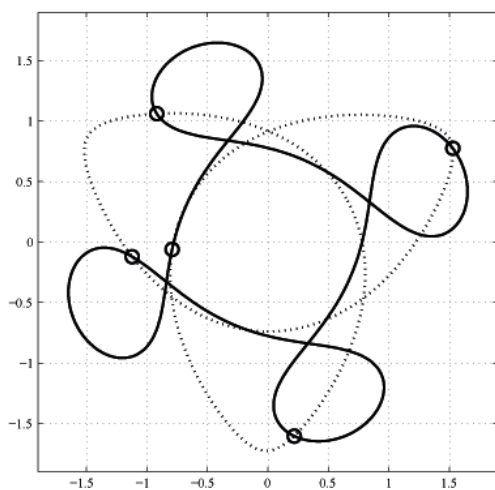


Figure 1.3: Time $t = 123.1$ days

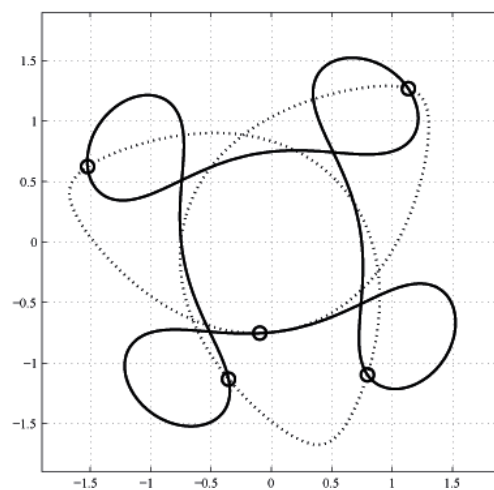


Figure 1.4: Time $t = 185.9$ days

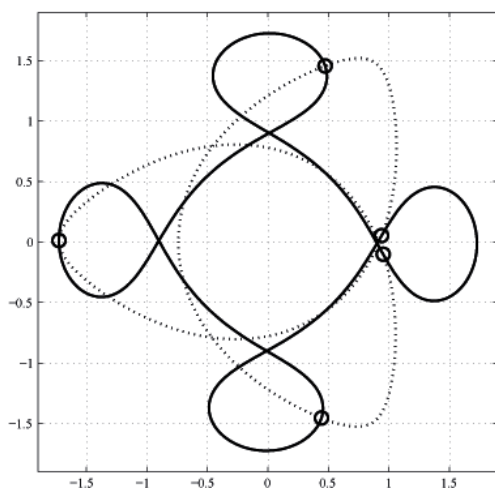


Figure 1.5: Time $t = 248.7$ days

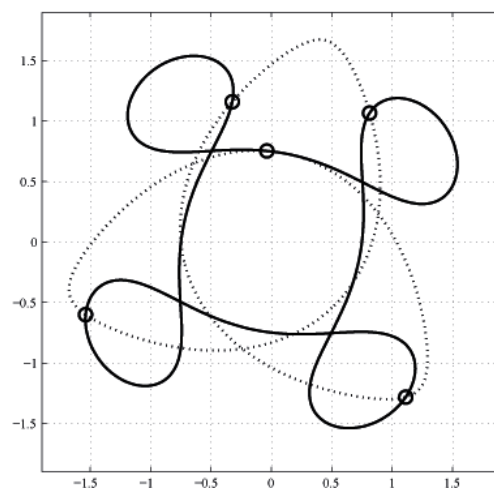


Figure 1.6: Time $t = 311.5$ days

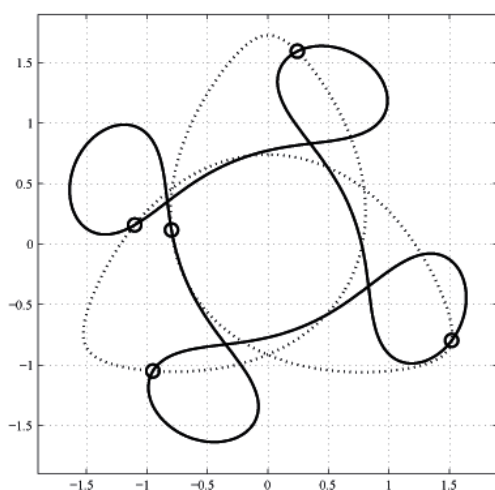


Figure 1.7: Time $t = 374.3$ days

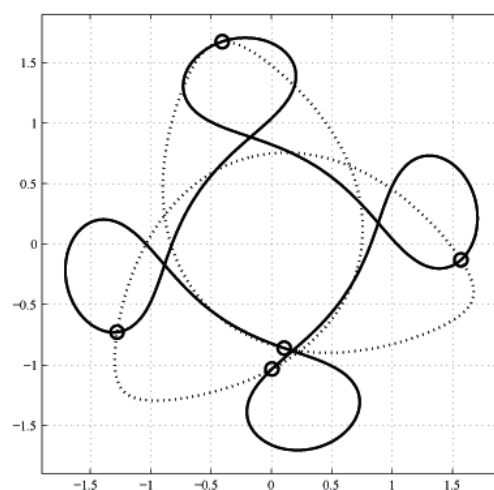


Figure 1.8: Time $t = 437.1$ days

1.5.1 Secondary Paths and Equivalency

In the previous developments, the Flower Constellation Set theory was introduced but specific details left out. In the following sections, the particular phasing theory that we have adopted is discussed in full. As a consequence of this choice of parametrization, a new class of orbit theory has emerged: secondary paths. The theory of secondary paths is developed and proved in this work. Examples of secondary paths are presented and discussed.

Furthermore, we discuss the equivalency of Flower Constellations and resolve how certain disparate choices of integer parameters can generate identical satellite distributions.

Flower Constellations present an interesting and unique mathematical theory for the design of constellations and formations of satellites. As previously discussed, to establish a *Flower Constellation* (FC), one must specify the semi-major axis and eccentricity through a choice of parameters (N_p, N_d, h_p) , the orbit inclination, and the argument of perigee, which are all common values for each satellite belonging to that Flower Constellation. The remaining two parameters, the right ascension of the ascending node (RAAN) and the mean anomaly, must be determined through a phasing rule for each satellite.

In our previous work for the *Flower Constellation Set* theory, we developed a functional relationship between the right ascension of the ascending node and the mean anomaly of a given satellite such that its relative trajectory in an arbitrary rotating reference frame will precisely coincide with the relative trajectory of another satellite in that frame. We did not elaborate on a specific choice of this functional relationship because the functional choice is largely an arbitrary choice. However, we made a specific choice for the parametrization, and a new class of orbit theory has emerged, *secondary paths* (SPs).

1.5.2 Symmetric Schemes

The symmetric phasing scheme that has been adopted for use in the Flower Constellations, characterized by N_s satellites, is obtained by the phasing rule

$$\Omega_{k+1} = \Omega_k - 2\pi \frac{F_n}{F_d} \quad (1.51)$$

$$M_{k+1}(0) = M_k(0) + 2\pi \frac{F_n}{F_d} \left(\frac{n + \dot{M}_0}{\omega_s + \dot{\Omega}} \right) \quad (1.52)$$

where $k = 1, \dots, N_s - 1$, ω_s is the angular velocity of the arbitrary rotating reference frame, $\dot{\Omega}$ and \dot{M}_0 are perturbations to the RAAN and mean anomaly angles, F_n and F_d are two integer parameters that can be freely chosen provided that $F_n \in \mathbb{Z}$ and $F_d \in \mathbb{N}$, and where $M_1(0)$ and Ω_1 (which are assigned) dictate the initial position of the first satellite and the angular shifting of the relative orbit, respectively.³ Flower Constellations have an axis of symmetry that is coincident with the direction of the total angular momentum vector of all the satellite orbits that constitute the constellation.

Equation (1.21) has a more simplified form that allows for more extensive analysis. If perturbations are ignored, then the most simplified version of the phasing relationships are given by

$$\Delta\Omega = -2\pi \frac{F_n}{F_d} \quad (1.53)$$

$$\Delta M = 2\pi \frac{F_n N_p}{F_d N_d} = -\Delta\Omega \frac{N_p}{N_d} = -\Delta\Omega \frac{1}{\tau} \quad (1.54)$$

where $\tau \equiv \frac{N_d}{N_p}$.

Note that $\Delta\Omega$ and ΔM as expressed in Equation (1.53) and Equation (1.54) are both rational, constructible numbers. It becomes clear here that the maximum number of satellites in a given Flower Constellation is

$$N_s^* = F_d N_d \quad (1.55)$$

³Note that this choice can be somewhat limiting in that irrational numbers are excluded. To avoid this limitation, F_n/F_d should be substituted by a single decimal parameter, F , where $F \in \mathbb{R}$. With this choice, all the currently known possible types of symmetric phasing are encompassed. As more investigation is completed, additional symmetric schemes may become apparent.

and that the sequence of right ascension of the ascending node values will repeat N_d times. This is due to the fact that a single RAAN and mean anomaly value will be assigned in sequence to each satellite in a unique pairing. Since the mean anomaly steps by $F_d N_d$, then it will take a total of $F_d N_d$ steps in order to complete the assignments. It follows from $\Delta\Omega F_d N_d$ that the unique values of $\Delta\Omega$ will repeat N_d times. Note that Equation (1.55) is an upper bound on the number of satellites. One is not required to completely fill out a Flower Constellation but rather can selectively choose where to place satellites once the phasing scheme has been established. Therefore,

$$N_s \leq F_d N_d \quad (1.56)$$

1.5.3 Restricted Schemes

Consider now that, for some mission design reason, the RAAN angle is constrained to fall within a certain range. These constellations are built with orbit node lines uniformly distributed in a limited range $[\Omega_1^*, \Omega_2^*]$ instead of $[0, 2\pi]$. In this case, the phasing rules given in Eqs. (1.20) and (1.21) are specialized as follows

$$\Omega_{k+1} = \Omega_k - (|\Omega_2^* - \Omega_1^*|) \frac{F_n}{F_d} = \Delta\Omega_R \frac{F_n}{F_d} \quad (1.57)$$

$$M_{k+1}(0) = M_k(0) + \Delta\Omega_R \frac{F_n}{F_d} \left(\frac{n + \dot{M}_0}{\omega_s + \dot{\Omega}} \right) \quad (1.58)$$

with $\Omega_1 = \Omega_2^*$ and $M_1 = M_1(0)$. Because the RAAN angle is decremented, one must remember to set Ω_1 to the maximum value in the range of allowable values for the restricted RAAN scheme.

1.5.4 Non-symmetric Schemes

Building upon the concept of the restricted phasing scheme, the phasing relationships can also be expressed as

$$\Omega_{k+1} = \Omega_k - \Delta\Omega_k \quad (1.59)$$

$$M_{k+1}(0) = M_k(0) + \Delta\Omega_k \left(\frac{n + \dot{M}_0}{\omega_s + \dot{\Omega}} \right) \quad (1.60)$$

1.6 Secondary Closed Paths - Existence and Uniqueness

with Ω_1 and $M_1(0)$ assigned. This implies that the difference in node value between any two satellites in the placement sequence can be arbitrary provided that the mean anomaly is selected appropriately.

1.5.5 Incomplete Schemes

Based upon the developments of the previous section, it is clear that changing the number of satellites in the constellation does not have any dramatic effect on the overall dynamics of the Flower Constellation, which, in turn, is dictated by the overall structure (parameters N_p and N_d) and the phasing rules (parameters F_n and F_d). Once a desired dynamic is achieved by a proper choice of the constellation parameters, then it becomes an easy task to find out the minimum number of satellites required to accomplish a specific mission objective. If it is desirable to remove a portion of the satellites but maintain the overall dynamics, one must generate the *Flower Constellation* as if the complete number of satellites were going to be placed and then selectively remove the undesirable number of satellites. That is to say, once the orbit elements have been generated for all possible satellites, the mission designer can selectively choose sets of parameters from the list. This procedure is necessary because of the way that the phasing rules are mathematically constructed. Doing this leads to an incomplete Flower Constellation.

1.6 Secondary Closed Paths - Existence and Uniqueness

In the previous section, a method for generating a single closed path - the relative path - is described. All the satellites belonging to a particular Flower Constellation belong to that single relative path. In order for this to occur, each satellite is assigned a unique pairing of RAAN and mean anomaly angles ($\Omega_i, M_i(0)$) while their remaining orbit parameters are identical (a, e, i , and ω). Ignoring perturbations, Equation (1.53) and Equation (1.54) define the allowable values for these pairs.

1.6 Secondary Closed Paths - Existence and Uniqueness

Considering Equation (1.54), the maximum value of $M(0)$ is $M_f(0) = 2\pi F_n N_p$. One can also see that there are a maximum of $F_d N_d$ unique mean anomaly angles. This is graphically illustrated in Figure 1.9. Furthermore, examining Equation (1.53), one can see that the maximum value of RAAN is $2\pi F_n$. However, since there are more available mean anomaly angles to assign, the RAAN must cycle until a value has been assigned to each corresponding value of the mean anomaly. Therefore, the final value of RAAN will be $\Omega_f = \Delta\Omega F_d N_d = -2\pi F_n N_d$.

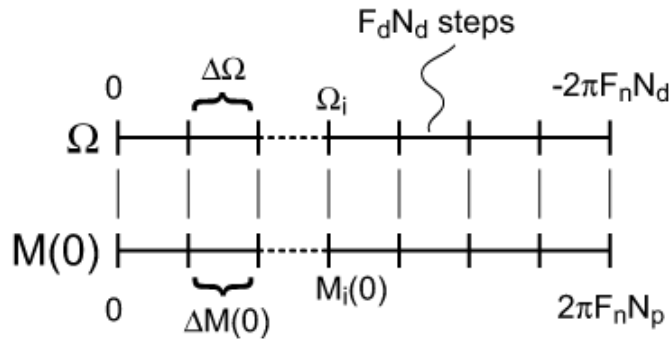


Figure 1.9: Comparison of the sequence of allowable values for the RAAN and mean anomaly angles. Each mark on the number line corresponds to a unique pair of RAAN and mean anomaly angles that specifies a location for the i^{th} satellite to be placed in an orbit. All other orbit parameters have been specified by the design of the Flower Constellation.

Now consider the possibility that the pairs of RAAN and mean anomaly angles will repeat before $(\Omega_f, M_f(0))$ is reached. In this case, there exists only a subset of angle pairs that are unique. This subset of unique angle pairs is what is termed a *secondary closed path* (SCP). If one were to continue placing satellites in the standard fashion, they would be placed physically on top of one another. While this might be a mathematical possibility, it is a physically unrealizable condition! Thus, the secondary closed path is a unique pattern of satellites that lies *on top of* the original relative path. A satellite belonging to a secondary closed path also belongs to the original relative path.

A question is now posed. What values of the Flower Constellation design parameters will cause a secondary closed path to occur?

1.6 Secondary Closed Paths - Existence and Uniqueness

Theorem 1. *For N_p sufficiently large, a symmetric Flower Constellation secondary closed path occurs when $N_d = 1$ or $F_n = kN_d$ for $k \in \mathbb{N}$.*

Remark 2 (Theorem 1). *N_p is the number of “petals” in the relative path of a Flower Constellation. In order for a secondary closed path to be distinguishable, the number of petals must be large enough that they overlap sufficiently to allow for the closed path to be obvious. The choice of N_p and the relative merit of “sufficiently large” is left up to the mission designer.*

Proof. In order for the $(\Omega_i, M_i(0))$ pairs to repeat and form a unique subset, the mean anomaly angle must be an integer multiple of 2π less than $M_f(0)$. Assume that there are a maximum of N_s^* satellites in this subset. This leads to

$$\Delta M m = 2\pi n_1 \tag{1.61}$$

Likewise, for the RAAN, one can write

$$\Delta \Omega m = 2\pi n_2 \tag{1.62}$$

where m , n_1 and n_2 are unknown integers.

This can be written out in equation form as

$$-2\pi m \frac{F_n}{F_d} = 2\pi n_1 \tag{1.63}$$

$$2\pi m \frac{F_n}{F_d} \frac{N_p}{N_d} = 2\pi n_2 \tag{1.64}$$

which reduces to

$$-m \frac{F_n}{F_d} = n_1 \tag{1.65}$$

$$m \frac{F_n}{F_d} \frac{N_p}{N_d} = n_2 \tag{1.66}$$

It has already been established that F_n and F_d must be relatively prime for a unique Flower Constellation as must be N_p and N_d . Examining Equation (1.65), one can immediately say by the division lemma that, since $F_n \perp F_d$, $F_d \mid m$ for n_1 to be an integer (i.e. $m = jF_d$ for $j \in \mathbb{N}$).⁴ The smallest integer value of F_d

⁴Read $F_d \mid m$ as “ F_d divides m ,” which means that m is an integer multiple of F_d .

1.6 Secondary Closed Paths - Existence and Uniqueness

that divides m is required for a unique base pattern due to the simple fact that multiples of m will only result in multiples of the base secondary closed path. Therefore, $m = F_d$, and, consequently, $n_1 = -F_n$.

Equation (1.66) can be analyzed in a similar way. Here, $(F_d N_d) \mid (m F_n N_p)$. However, since it was just established that $m = F_d$, this reduces to $N_d \mid (F_n N_p)$. From this condition and the division lemma, one can easily see that, since $N_p \perp N_d$, either $N_d = 1$ or $N_d \mid F_n$. In other words, a unique secondary closed path is formed when F_n is an integer multiple of N_d (i.e. $F_n = k N_d$ for $k \in \mathbb{N}$). When $k > 1$, then a unique set of multiple base paths will form. These requirements are graphically depicted in Figure 1.10. Note that when $F_n = N_d$, then $n_1 = -F_n = -N_d$ and $n_2 = N_p$. Likewise, when $N_d = 1$, $n_2 = F_n N_p$. \square

Corollary 3 (Theorem 1). *For N_p sufficiently large, a Flower Constellation secondary closed path can also occur when $F_n \mid N_d$ (i.e. $N_d = r F_n$ for $r \in \mathbb{N}$).*

Proof. In Theorem 1, it was shown that a secondary closed path occurs when $N_d \mid F_n$ which is equivalent to saying that F_n is an integer multiple of N_d . If one rearranges this requirement to show that $F_n/k = N_d$, one can see immediately that N_d can only be an integer when $k \mid F_n$. Therefore, a secondary closed path can also occur when $N_d = r F_n$ where $r \in \mathbb{N}$. \square

One can see clearly now that the secondary closed path subset of RAAN and mean anomaly pairs will repeat after F_d pairs. Thus, the maximum number of satellites in a secondary closed path is

$$N_s^* = F_d \tag{1.67}$$

Note that $N_s \leq F_d$ with $N_s = F_d$ in order to completely visualize the entire secondary closed path. At this point, not much has been said about the actual values of N_p , N_d , or F_d . From previous developments, N_p and N_d determine the anomalistic orbit period of the satellites. Thus, these values would generally be established by mission design requirements. F_d , however, has no such constraints and, in general, can be any non-zero positive integer (i.e. $F_d \in \mathbb{N}$). Given an infinity of choices for the value of F_d , we can choose F_d in a specific way that allows one to predict the resultant secondary path shape.

1.6 Secondary Closed Paths - Existence and Uniqueness

Theorem 4. For N_p sufficiently large, and assuming that Theorem 1 has been satisfied, the phasing denominator can be expressed as $F_d = AN_d + BN_p$ where $F_d \in \mathbb{N}$, N_p and N_d are specified according to Flower Constellation theory, and given arbitrary $A, B \in \mathbb{Z}$ such that A and B have the physical meaning of the integer number of times the mean anomaly and the RAAN are divisible by 2π .

Proof. Examine Equation (1.53) and Equation (1.54) now written for the specific case of the secondary closed path:

$$\Delta\Omega = -\frac{2\pi N_d}{F_d} \quad (1.68)$$

$$\Delta M_0 = \frac{2\pi N_p}{F_d} \quad (1.69)$$

In order to determine the form of F_d , one must demonstrate that the form of either Equation (1.68) or Equation (1.69) can be constructed. Since Equation (1.68) and Equation (1.69) are dependent, we only have to prove one of the equations. First consider

$$\Delta M_0 \equiv C \pmod{2\pi} \quad (1.70)$$

$$\Delta\Omega \equiv D \pmod{2\pi} \quad (1.71)$$

where the symbol \equiv means *congruent*. According to the definition of congruency,

$$a \equiv c \pmod{b} \Leftrightarrow b \mid (a - c). \quad (1.72)$$

Therefore, one can write that

$$2\pi \mid (\Delta M_0 - C) = A \quad (1.73)$$

$$2\pi \mid (\Delta\Omega - D) = B \quad (1.74)$$

where A and B are integers (i.e. $A, B \in \mathbb{Z}$) and C and D are real numbers (i.e. $C, D \in \mathbb{R}$).

From Equation (1.54), one can express ΔM in terms of $\Delta\Omega$. This leads to

$$2\pi \mid \left(-\Delta\Omega \frac{N_p}{N_d} - C \right) = A \quad (1.75)$$

$$2\pi \mid (\Delta\Omega - D) = B \quad (1.76)$$

1.6 Secondary Closed Paths - Existence and Uniqueness

which can also be written as

$$2\pi A = \left(-\Delta\Omega \frac{N_p}{N_d} - C \right) \quad (1.77)$$

$$2\pi B = (\Delta\Omega - D). \quad (1.78)$$

Solving for 2π and then equating to the two equations results in

$$\frac{A}{B} (\Delta\Omega - D) = -\Delta\Omega \frac{N_p}{N_d} - C \quad (1.79)$$

Collecting terms,

$$\Delta\Omega \left(\frac{A}{B} + \frac{N_p}{N_d} \right) = \frac{A}{B} D - C \quad (1.80)$$

Finding the common denominator of the term in parentheses,

$$\Delta\Omega \left(\frac{AN_d + BN_p}{BN_d} \right) = \frac{A}{B} D - C \quad (1.81)$$

Multiplying through,

$$\Delta\Omega (AN_d + BN_p) = ADN_d - BCN_d = (AD - BC)N_d \quad (1.82)$$

which leads to

$$\Delta\Omega = \frac{(AD - BC)N_d}{AN_d + BN_p} = -\frac{2\pi N_d}{F_d} \quad (1.83)$$

where it is now clear comparing Equation (1.83) to Equation (1.68) that $F_d = AN_d + BN_p$ and A and B represent the integer number of times that the RAAN and the mean anomaly are divisible by 2π . \square

What is most interesting is that the values selected for A and B have physical meaning. One can think of B as the number of times the secondary closed path will intersect itself or twist over onto itself. A is the whole number of times that the node angle will be swept through 2π . One can see this clearly by plotting the RAAN (Ω) versus the mean anomaly (M) in cartesian coordinates for various values of A and B . Figure 1.11 shows 6 cases where $(A, B) \in \{(0, 3) (3, 0) (2, 3) (3, 2) (-1, 3) (3, -1)\}$.

For an arbitrary choice of F_d , the plot of RAAN and mean anomaly can have a sparse scatter-plot appearance. This is in large part due to the fact

that the maximum number of satellites is controlled by F_d (assuming N_d is a defined mission parameter). However, when F_d is chosen to have the form given in Theorem 4, then the scattered points will coalesce into distinct bands. Therefore, it is important to consider that while Theorem 1 guarantees a secondary closed path will exist, Theorem 4 determines in large part if the secondary closed path is *distinguishable* to the human eye. Furthermore, we can conclude that the categories of Flower Constellations discussed in our previous work[18] are merely human interpretations of a mathematical phenomena.

1.7 Secondary Open Paths

Referring back to Equation (1.54), recall that the ratio of N_p and N_d is defined as τ . Keeping the values of N_p and N_d in proportion to one another is important for realizable constellations and formations to be generated. For a given value of N_d , as $N_p \rightarrow \infty$, $\tau \rightarrow 0$, the anomalistic orbit period also goes to zero (which is physically unrealizable). Conversely, for a given value of N_p , as $N_d \rightarrow \infty$, $\tau \rightarrow \infty$, the anomalistic orbit period goes to infinity. This is also generally unacceptable. Therefore, even though N_p and N_d may individually be quite large, provided that the overall ratio, τ is kept in a reasonable range, the resultant Flower Constellation will be plausible.

Table 1.2: Lower bound on τ as a function of minimum altitude with respect to the Earth.

$h_{min}(km)$	τ_{min}
90	6.0083×10^{-2}
400	6.4454×10^{-2}
600	6.7328×10^{-2}
800	7.0243×10^{-2}
1000	7.3050×10^{-2}
10000	2.4209×10^{-1}

Note that a lower bound for τ can be found as a function of some minimum

allowable perigee altitude. This lower bound can be expressed as

$$\tau \geq \omega_s \sqrt{\frac{(R_p + h_{min})^3}{\mu_p}} \quad (1.84)$$

where h_{min} is the minimum altitude above the planet, R_p is the mean planet radius, and μ_p is the gravitational parameter of the planet under consideration. Table 1.2 shows the resultant minimum value for τ for some specific values of the minimum altitude h_{min} . Here we have written the equations in a general way to reference any planet to remind the reader that the Flower Constellations can be designed with respect to any planet or rotating reference system.

Because Flower Constellations are geometrically symmetrical about the axis of symmetry, as the number of petals increases while the number of days to repeat the pattern stays the same, the petals begin to overlap each other. As N_p grows large, the relative orbit begins to look less like distinct flower petals and more like a surface. Figure 1.14 shows two cases to illustrate this point. The first case shows a $N_p = 3$, $N_d = 1$ Flower Constellation ($\tau = 0.3333$) while the second case has $N_p = 769$, $N_d = 257$ ($\tau = 0.3342$).

Now, remove the relative orbits that are depicted in Figure 1.13 and, instead, increase the number of satellites to fill out the pattern. When one views both of these cases from the North pole of the Earth without the relative orbits (Figure 1.14), one will see something rather unexpected. Both constellations look almost identical.

In fact, there is only one subtle difference between the two patterns of satellites. In Case 1, the pattern fits exactly on the relative path and, thus, is a closed path (this is the trivial *secondary closed path* case). In Case 2, there are two "paths" for the satellites to follow. The first "path" is the relative orbit depicted in Figure 1.13. The secondary path is generated by the pattern that you see in Figure 1.14. The secondary path, for this particular case, is open ended. That is, if you follow a particular satellite from the starting point to the end point of the pattern, those points do not coincide. As the number of petals is decreased (while maintaining the appropriate τ ratio), this disconnection will become more and more pronounced.

Note that, in general, secondary paths can be closed or open. Part of the constellation design process will focus on selecting patterns of satellites that are either on closed or open secondary paths. *Secondary open paths* are formed when τ is perturbed slightly and all other design parameters remain constant.

1.8 Restricted Phasing Secondary Paths

The orbit distribution as provided by Eqs. (1.53) and (1.54) is evenly distributed about a complete 2π rotation. When the orbit node lines are restricted to lie within a particular range, then the existence of secondary paths must be revisited. As will be seen, the mathematical possibilities become very limited if the orbits are not arrayed about 2π .

Theorem 5. *For N_p sufficiently large and in the special case when one restricts the right ascension of the ascending node of each orbit to lie within the range $[\Omega_2^*, \Omega_1^*]$, a Flower Constellation secondary closed path occurs when $F_d = N_o$, $N_d = F_n = 1$, and $N_p = kN_\Omega \ \forall \ k \in \mathbb{N}$ where N_o is the number of orbit planes and $\Delta\Omega_R = |\Omega_2^* - \Omega_1^*|$ is chosen to have the functional form $\Delta\Omega_r = 2\pi/N_\Omega$, $N_\Omega \in \mathbb{N}$.*

Remark 6. *Note that this choice of functional form for $\Delta\Omega_r$ restricts the values that $\Delta\Omega_r$ can be assigned.*

Proof. In our previous work, we showed that the relationship between RAAN and the mean anomaly is

$$\Delta M = -\Delta\Omega \frac{N_p}{N_d} = 2\pi \frac{F_n N_p}{F_d N_d} \quad (1.85)$$

where

$$\Delta\Omega = -2\pi \frac{F_n}{F_d} \quad (1.86)$$

This provides for a Flower Constellation that has orbits whose RAAN are evenly arrayed about 2π . However, we may desire to have orbits that are restricted to be arrayed within a smaller range of RAAN values, $\Delta\Omega_R$. In this case, while Equation (1.85) remains the same, Equation (1.86) becomes

$$\Delta\Omega = -\Delta\Omega_R \frac{F_n}{F_d} \quad (1.87)$$

1.8 Restricted Phasing Secondary Paths

where

$$\Delta\Omega_R = \frac{2\pi}{N_\Omega} \quad (1.88)$$

For example, if one desires to restrict the RAAN to a span of 60° , then $N_\Omega = 6$. Now, let's re-write Equation (1.87) as

$$\Delta\Omega = -\Delta\Omega_R \frac{F_n}{F_d} = -\frac{|F_n\Omega_2^* - F_n\Omega_1^*|}{F_d} \quad (1.89)$$

while Equation (1.85) becomes

$$\Delta M = -\Delta\Omega \frac{N_p}{N_d} = 2\pi \frac{F_n N_p}{N_\Omega F_d N_d} \quad (1.90)$$

Notice here that, for $F_n > 1$, the value of $\Omega_i|_{i=N_s}$ is not Ω_2^* as we had originally intended. Therefore, if one desires to restrict all orbits to $\Omega_1^* < i < \Omega_2^* \forall i \leq N_s$, then $F_n \equiv 1$.

$$\Delta\Omega = -\frac{\Delta\Omega_R}{F_d} = -\frac{2\pi}{N_\Omega F_d} \quad (1.91)$$

and

$$\Delta M = 2\pi \frac{N_p}{N_\Omega F_d N_d} \quad (1.92)$$

Pay close attention to Equation (1.91). There are two equally valid representations depicted. However, we must choose

$$\Delta\Omega = -\frac{\Delta\Omega_R}{F_d} \quad (1.93)$$

and remember to set $\Omega_{i+1} = \Omega_2^* + \Delta\Omega$ when $\Omega_i = \Omega_1^*$. If we had chosen the latter representation, then we would have ended up with an Flower Constellation arrayed about 2π again.

Now, the question becomes, what values of the remaining Flower Constellation parameters will result in a secondary closed path on a restricted RAAN set. As discussed in earlier, SCP's form when a unique subset of RAAN and mean anomaly pairs repeat an integer number of times within the allowable range of discrete mean anomaly values. However, there are some subtle differences with the restricted RAAN case. In order for the $(\Omega_i, M_i(0))$ pairs to repeat and form a unique subset, the mean anomaly angle must be an integer multiple of 2π less than $M_f(0)$. Likewise, since we have restricted the RAAN, the RAAN angle must

1.8 Restricted Phasing Secondary Paths

be an integer multiple of $\Delta\Omega_R$. Assume that there are a maximum of N_s^* satellites in this subset. This leads to

$$-m \Delta\Omega = \Delta\Omega_R n_1 \quad \text{and} \quad m \Delta M = 2\pi n_2 \quad (1.94)$$

Substituting in the relationships for $\Delta\Omega$ and ΔM from the above equations, we obtain

$$-m \frac{\Delta\Omega_R}{F_d} = \Delta\Omega_R n_1 \quad (1.95)$$

and

$$2\pi m \frac{N_p}{N_\Omega F_d N_d} = 2\pi n_2 \quad (1.96)$$

Examining Equation (1.95) in detail, we see that

$$-\frac{m}{F_d} = n_1 \quad (1.97)$$

which implies that $F_d \mid m$ for n_1 to be an integer. Furthermore, for a base SCP, $F_d = m$. Substituting this result into Equation (1.96), we get the following:

$$\frac{N_p}{N_\Omega N_d} = n_2 \quad (1.98)$$

It follows that, for n_2 to be an integer, $N_\Omega N_d \mid N_p$. It has been well established that $N_d \perp N_p$. That is to say, N_d and N_p are relatively prime. Therefore, the only possible solution that will result in n_2 being an integer is the case when $N_d = 1$. This gives the final requirement that $N_\Omega \mid N_p$. Gathering all the requirements together:

$$F_d = N_o \quad (1.99)$$

$$N_d = 1 \quad (1.100)$$

$$F_n = 1 \quad (1.101)$$

$$N_p = k N_\Omega \quad \forall \quad k \in \mathbb{N} \quad (1.102)$$

where N_o is the desired number of orbits in the restricted Flower Constellation. In this case, $N_s^* = N_\Omega F_d$ is the maximum number of satellites allowable. \square

Since there are F_d orbits, there are exactly N_Ω permissible locations in which to place satellites per orbit. Curiously, F_n just so happens to equal N_d as was the requirement for a standard SCP arrayed about 2π . Could we have started out with that assumption from the outset? The answer is no. The logic required to solve the restricted case is different and requires re-evaluating the governing equations from first principles resulting in a different solution path.

1.9 Constructing Secondary Paths

The developments of the previous sections have shown that there are specific requirements on the choice of parameters in order to ensure that a secondary path is formed. Figure 1.15 provides a sample of four constellations that have been generated using the concept of secondary closed paths.

The Lone Star Constellation

This section will examine how to create an example secondary closed path that is called the *The Lone Star Constellation*. Looking at Figure 1.9, one can see that this constellation forms the shape of a five pointed star. This constellation closely resembles the star on flag of the State of Texas, hence the name. When viewing this constellation in motion, one would see the whole star spin about the axis of symmetry, which in this case is the spin axis of the Earth. Figure 1.9 and Figure 1.9 show the relative orbit and the ECI orbits, respectively, for this constellation.

Based upon the developments previously described, the construction of the Lone Star Constellation is relatively simple. In this case, five secondary petals are desired to form on top of the relative path already in place. To effect this design, the value of F_d must be chosen appropriately based upon the value of τ and for a particular choice of A and B. Looking back at Theorem 4, one can immediately determine the appropriate values for A and B simply by noting that, if we want five points on the star, we require five loops in mean anomaly for one loop in RAAN about the Earth. This leads to $A = 5$ and $B = 1$.

However, A and B can be positive or negative. Therefore, we must resolve the question of appropriate sign. Generally, F_d is chosen to be positive because

1.10 Angular velocity of a secondary path

negative values for F_d simply reverse the sign on $\Delta\Omega$ and ΔM in Eqs. (1.53) and (1.54). Therefore, we choose A to be positive. The sign of B has physical connotations and can be determined by looking at how the five points of the star are created. When $B = -1$, we get the *Lone Star Constellation* pictured in Figure 1.16. However, when $B = 1$, the inverse pattern is created with five larger overlapping circles creating intersections where the vertices of the star would have been in the $B = -1$ case. Therefore, to obtain the desired constellation shape, we require

$$F_d = 5N_d - N_p \quad (1.103)$$

The values of N_d and N_p can be freely chosen to achieve a desired orbit period (i.e. a particular value of τ). In order to make the points of the star fairly sharp, $N_d = 23$ and $N_p = 38$ were found to be acceptable, which leads to $F_d = 5(23) - 38 = 77$. This particular constellation is rather large, and smaller stars can be found by adjusting the values of N_d and N_p .

The inclination of the *Lone Star Constellation* is set to be zero. This is done to maintain the sharp points of the constellation. Other values for the inclination will still yield a constellation with five points when viewed from the polar axis, but the points will be significantly rounded. For the equatorial *Lone Star Constellation*, the choice of argument of perigee is arbitrary.

1.10 Angular velocity of a secondary path

When all the admissible locations of a Flower Constellation are filled (especially when the number of these locations are many), the Flower Constellation dynamics reveals the shape of the relative trajectory by clearly showing the number of petals (i.e. the apogees of the relative trajectory). In this case the whole constellation appears to be rotating, as a rigid body, with the angular velocity of the planet, assuming that the orbit period is commensurate with the planet's spin rate. Sometimes, however, the phasing does not allow us to fill out all the admissible locations, and it happens that the satellite distribution sequence comes back to the first position ($\Omega = 0$ and $M = 0$) before all the admissible locations are filled. When this happens, the Flower Constellation dynamics highlights the

1.10 Angular velocity of a secondary path

existence of *Secondary Paths* that have unexpected and beautiful shapes that are time invariant.

The immobility of the printed figure does not allow us to demonstrate the resulting complex shape-preserving dynamic. While complete Flower Constellations spin with a prescribed angular velocity (i.e. the same rate as that of the rotating reference frame), the spin rate of a secondary path should be quantified. Note that the angular velocity of a secondary path is *apparent* and not real. That is to say, the apparent angular rotation is not a motion that can be described by any particular dynamical relationship but rather is an artifact of the mathematics that generates a Flower Constellation. In other words, the appearing angular rotation is not continuous but rather *appears* continuous. Furthermore, the continuity is not discrete, as in the effect of the fast flow of photograms of motion pictures, because the satellites motion IS continuous. In effect, the angular motion arises because of a particular combination of the continuous motion of a satellite along its orbit and the discrete separation of contiguous orbits.

In general, SPs are made with single ($N_\ell = 1$) or multiple ($N_\ell > 1$) loops.⁵ Figures (1.17) and (1.18) show a single and a four-loop SP, respectively. The angular velocity of a SP does not depend on N_ℓ , but on the four integer parameters characterizing the loop(s): the number of apogees per loop, N_{al} , the number of perigees per loop, N_{pl} , and two jumping-petal step parameters, J_{al} and J_{pl} . The jumping-petal step parameters indicate that the satellite moves from the petal apogee or perigee k to the petal apogee or perigee $(k+J_{al})$ or $(k+J_{pl})$, respectively. In each case, the petal apogees and perigees are counted counter clockwise and the jumping-step parameters are restricted to $0 \leq J_{al} < N_{al}$ and $0 \leq J_{pl} < N_{pl}$. Figure (5) shows a SP having $N_{al} = 10$ and $N_{pl} = 5$.

For a majority of SPs, we have $N_{al} = N_{pl}$ and, for symmetry, $J_{al} = J_{pl}$.

In the following, let us first consider the simple and common case of $N_{al} = N_{pl}$, and identify as “petal” indifferently, petal-apogee or petal-perigee. In a SP, the time required from a satellite to move from a petal to the next petal is one orbit period. Therefore, in general, after one orbit period the satellite comes back to

⁵The shape of the loops in multiple-loop SPs are all identical. They are just rotated one from another by an angle $2\pi/N_\ell$.

1.11 Equivalent Satellite Distributions

its initial position, but on a different petal of its loop.⁶ After N_{al} orbit periods, the satellite has visited all the petals of its loop. In the case the SP has one loop ($N_\ell = 1$), two petals ($N_{al} = 2$), and a unitary jumping-petal step parameter ($J_{al} = 1$), then after N_{al} orbit periods the SP is rotated by an angle 2π and, therefore, the SP angular velocity is $\omega = 2\pi/(N_{al}T)$. From these considerations, the intuitive solution for the general case, when the SP loop is characterized by any values for N_{al} and J_{al} can be determined.

There are two possible solutions associated with a clockwise or counter clockwise rotation

$$\omega_{a\odot} = \frac{2\pi}{T} \cdot \frac{N_{al} - J_{al}}{N_{al}} \quad \text{and} \quad \omega_{a\odot} = -\frac{2\pi}{T} \cdot \frac{J_{al}}{N_{al}} \quad (1.104)$$

In the general case, when $N_{al} \neq N_{pl}$ (and $J_{al} \neq J_{pl}$), there are an additional two angular velocities associated with the petal-perigee motion

$$\omega_{p\odot} = \frac{2\pi}{T} \cdot \frac{N_{pl} - J_{pl}}{N_{pl}} \quad \text{and} \quad \omega_{p\odot} = -\frac{2\pi}{T} \cdot \frac{J_{pl}}{N_{pl}} \quad (1.105)$$

1.11 Equivalent Satellite Distributions

The phasing theory of Flower Constellations generates a family of RAAN and mean anomaly angle pairs. Each pair of angles, called an element, is denoted $\{d_i\}_{i \in I}$ where d_i is i^{th} member of the family and I is a nonempty index set. This family gives rise to the set $\mathfrak{D} = \{d_i \mid i \in I\}$. Flower Constellation distribution sets are multisets. Multisets are set-like objects in which each element of the set is unique and the order of the elements is ignored. For instance, the multisets $\{1, 2, 3\}$ and $\{2, 1, 3\}$ are equivalent but $\{1, 1, 3, 2\}$ and $\{2, 3, 1\}$ are different.

This follows from the physical meaning of the Flower Constellation distribution. When one places a satellite at a particular RAAN and mean anomaly position in a given orbit, it does not matter if that is the first satellite placed or the 3^{rd} satellite placed - it is still the only satellite that is placed in that particular location.

⁶If it comes back on the same petal, then the problem is trivial because the angular velocity of the SP is identical to that of the rotating reference frame.

1.11 Equivalent Satellite Distributions

Given an arbitrary Flower Constellation phasing distribution of finite length, one can choose to place the satellites in a particular order in a finite number of ways. In general, the number of Flower Constellation multisets of length k on n elements is called n *multichoose* k , expressed as $\binom{n}{k}$. This can be calculated as

$$\binom{n}{k} = \binom{n+k-1}{k} = (n-1, k)! \quad (1.106)$$

where $(n-1, k)!$ is a multinomial coefficient. Multinomial coefficients are calculated as

$$(n_1, n_2, \dots, n_k)! = \frac{(n_1 + n_2 + \dots + n_k)!}{n_1! n_2! \dots n_k!} \quad (1.107)$$

Therefore, the finite number of rearrangements of N_s elements of an arbitrary Flower Constellation distribution of length N_s is $\frac{(2N_s-1)!}{(N_s-1)! N_s!}$ where N_s is the number of satellites in the Flower Constellation. This number is important because it tells us something rather interesting. Until now, we have known that particular choices of the Flower Constellation parameters N_p and N_d will generate identical Flower Constellations (all other things being equal). With this development, we now can state that certain choices of F_n and F_d also produce identical Flower Constellations with all other things being equal.

This brings up the rather obvious question: Which choices of F_n and F_d will result in equivalent Flower Constellation multisets? Recognize that each choice of the phasing parameters really represents a choice of permutation of a fundamental Flower Constellation distribution, which we named previously a *Contiguous Flower Constellation*.

1.11.1 Families of Flower Constellations

Recall Eqs. (1.53) and (1.54) now written in a slightly different way.

$$\Delta\Omega = \frac{-2\pi}{F_d} F_n = \Delta\Omega_c F_n \quad (1.108)$$

$$\Delta M_0 = \frac{2\pi}{F_d N_d} F_n N_p = \Delta M_c F_n N_p = \Delta M_c F_s \quad (1.109)$$

where it is clear that $F_s = F_n N_p \in \{1, 2, \dots, F_d N_d - 1\}$. Note that in general, the quantity $F_n N_p$ will not be able to represent all allowable values of F_s . N_p is

1.11 Equivalent Satellite Distributions

generally not a “free” parameter in this regard because N_p , in conjunction with N_d , specifies the orbit period. Therefore, our only option is to choose a value for F_n . However, it is clear that the product of F_n and N_p can not reproduce the set of allowable values of F_s for arbitrary N_p .

We desire to keep the phasing and shape considerations separate. Therefore, to encompass all possible values of F_s , we must rewrite Equation (1.109). The simplest choice is a linear form

$$F_s = F_n^* N_p + F_h F_d \quad (1.110)$$

where $F_h \in \{1, 2, \dots, N_d - 1\}$. Here we must solve for the value of $F_n^* = f(F_h)$ and obtain an equivalent Flower Constellation by setting $F_n = F_n^*$.

Furthermore, one can deduce that

$$\Delta M_c = -\frac{\Delta \Omega_c}{N_d}. \quad (1.111)$$

In Equation 1.109, there is a sequencing parameter for the mean anomaly that we have introduced in this study as F_s . In our previous work, the existence of this parameter was not appreciated. Therefore, we have modified our phasing relationships to account for the fact that one can choose the ordering of the placement of satellites not only in terms of the right ascension of the ascending node but also in terms of the mean anomaly. However, this choice is not wholly independent as we shall demonstrate. F_s , along with F_n , represent quantities that describe families of Flower Constellations. The reason for this has to do with circular permutation theory.

A circular permutation is the number of ways in which one can arrange N distinct objects around a fixed closed planar path (e.g. a circle, ellipse, etc). By fixed we mean to say that the closed path cannot be picked up off the plane and turned over (i.e. clockwise and counterclockwise have different meanings). Another way to envisage this is to imagine seating people around the dinner table. A circular permutation is the number of unique ways that you can arrange people around the table after the first person has chosen a seat. Please refer to Figures 1.20 and 1.21 for examples.

As discussed earlier, a Flower Constellation has precisely F_d orbits arrayed about 2π . The first orbit is chosen to be placed at Ω_0 , typically equal to 0° .

1.11 Equivalent Satellite Distributions

Therefore, according to circular permutation theory, there are $P = (F_d - 1)!$ possible unique sequences of choices where one can place a satellite on subsequent orbits. The choice of sequence is controlled by the choice of F_n .

When $F_n = 1$, then $\Delta\Omega = \frac{2\pi}{F_d} = \Delta\Omega_c$, and satellites will be placed sequentially from one orbit to the next in a monotone increasing manner (see Figure 1.22). That is to say, $\Omega_c \in \frac{2\pi}{F_d}\{1, 2, 3, \dots, F_d - 1\}$. This is the first sufficient condition for what we shall call a *Contiguous* Flower Constellation. When $F_n \neq 1$, then the sequence of orbit choices will be shuffled and one might end up with, for example, $\Omega \in \frac{2\pi}{F_d}\{1, F_d - 3, 2, F_d - 1, \dots, F_d - 6\}$.

Note that in each case, the first value of RAAN will always be Ω_0 or, in the set theory sequence, one. Additionally, this complete pattern will repeat $N_{so} \leq N_d$ times until all satellites have been placed in unique RAAN and mean anomaly pairings.

Similarly, when $F_s = 1$, then

$$\Delta M = \frac{2\pi}{F_d N_d} = \Delta M_c, \quad (1.112)$$

and satellites will be placed in monotone increasing mean anomaly locations (See Figure 1.23). That is to say,

$$M_c \in \frac{2\pi}{F_d N_d}\{1, 2, 3, \dots, F_d N_d - 1\}. \quad (1.113)$$

This is a second sufficient condition to generate what we call a *Contiguous* Flower Constellation. Recognize though that a Flower Constellation can be contiguous with respect to either RAAN or mean anomaly but not both simultaneously.

1.11.2 The Contiguous Flower Constellation

Contiguous distributions have the property of distributing subsequent satellites in subsequent continuous orbits. This characteristic, as it will be clear later, allows us to evaluate the spin rate of the secondary path. A *Contiguous* Flower Constellation is generated by a family of elements $\{d_i\}_{i \in \mathbb{N}}$ where \mathbb{N} is the set of positive integers. Such a family is called a sequence and is a totally ordered set. A total order is a set plus a particular relation on the set such that any elements $a, b \in \mathfrak{D}$ are governed by either $a \leq b$ or $b \leq a$.

1.11 Equivalent Satellite Distributions

Under the non-restrictive hypothesis that the distribution starts with $\Omega_1 = M_1 = 0$, then the second satellite ($k = 2$) is placed on an orbit with RAAN values of $\Omega_2 = \Delta\Omega$ or $\Omega_2 = \Delta\Omega_c$ for the contiguous case. Recall that there are F_d orbits that must be arrayed about the earth. We can write $\Omega_{F_d} = \Delta\Omega F_d = 2\pi F_n$. However, we know that for the contiguous distribution $\Delta\Omega_c F_d = 2\pi$. It follows from the fact that $F_n \perp F_d$ that, for the contiguous distribution, $F_n \equiv 1$. Alternatively, one can perform a similar analysis using the mean anomaly. The simplest case requires $F_n N_p \equiv 1$. It is clear that the product of F_n and N_p can only be identically one for $F_n = 1$ and $N_p = 1$. It is necessary that either the RAAN or mean anomaly step sequentially to construct a *Contiguous* Flower Constellation.

1.11.3 Finding the Fundamental Distribution

Consider now two arbitrary Flower Constellation distributions \mathfrak{D}_1 and \mathfrak{D}_2 . We assume here that the orbit periods for each arbitrary Flower Constellation are the same. In order to say that they are equivalent (i.e. $\mathfrak{D}_1 = \mathfrak{D}_2$), we first require that \mathfrak{D}_1 and \mathfrak{D}_2 are equipollent. That is to say, there is a one-to-one function (a bijection) from \mathfrak{D}_1 onto \mathfrak{D}_2 . Inherent in this requirement is that each set be of equal length.⁷

As stated earlier, a given distribution \mathfrak{D} is a permutation of a more fundamental, *contiguous*, distribution \mathfrak{D}_c . Therefore, if we can state conclusively that the fundamental distributions of two arbitrary distributions are equivalent, then the two distributions are themselves equivalent.

Let

$$\mathfrak{F}\mathfrak{C}_1 \triangleq \{ N_{p1}, N_{d1}, F_{n1}, F_{d1}, F_{h1} \}$$

and

$$\mathfrak{F}\mathfrak{C}_2 \triangleq \{ N_{p2}, N_{d2}, F_{n2}, F_{d2}, F_{h2} \}$$

be two integer sets characterizing two satellite distributions, \mathfrak{D}_1 and \mathfrak{D}_2 , respectively.

⁷This does not exclude the possibility that either set \mathfrak{D}_1 or \mathfrak{D}_2 is a k -subset of a larger Flower Constellation distribution.

It follows from Eqs. (1.108) and (1.109) that in order for two arbitrary distributions to be equipollent, we require that $\Delta\Omega_1 \equiv \Delta\Omega_2 \pmod{2\pi}$ and $\Delta M_1 \equiv \Delta M_2 \pmod{2\pi}$. This implies that $F_{d1} = F_{d2}$, $N_{d1} = N_{d2}$ as a necessary condition for having equal numbers of satellites and orbit planes. F_d can be found as the length of the set divided by N_d , which should already be specified as part of the orbit period.

Trivially, if $F_{n1} = F_{n2}$ and $F_{s1} = F_{s2}$, then the two distributions are equivalent. However, here we utilize a particular form of set theory, Zermelo-Fraenkel Set Theory, which provides a formal system of axioms expressed in first order predicate logic [26]. Of particular interest is the Axiom of Replacement which states that, if F is a function, then there exists a set $Y = F[X] = \{ F(x) : x \in X \}$ [27]. By establishing that $F_{d1} = F_{d2}$, we can immediately choose $Y = \Omega/GCD(\Omega) = \{ x/GCD(X) : x \in X \}$. Therefore, if $\forall y (y \in Y_1 \equiv y \in Y_2) \Rightarrow Y_1 = Y_2$ by the Axiom of Extensionality.

Note that $\frac{2\pi F_n}{F_d} = GCD(\Omega)$. F_d has already been found and we can solve for F_n . A similar analysis can be performed to extract the GCD of the mean anomaly distribution, which is equivalent to $F_n N_p$. In the general case, $F_{n1} \neq F_{n2}$ and $F_{s1} \neq F_{s2}$. Therefore, by extracting the greatest common divisor from a given distribution, one can easily check to see if the fundamental distributions of each constellation constitute identical sets. If the sets are identical, then we can say that the two constellations are themselves identical.

References

- [1] 55th International Astronautical Congress, IAC-04-A.5.01, Vancouver, Canada, Satellite Constellations, 2004, The Breakwell Memorial Lecture. 1
- [2] J. G. Walker, *Some circular orbit patterns providing continuous whole earth coverage*, British Interplanetary Journal Soc., vol. 24, 369384, 1971. 1
- [3] J. G. Walker, *Satellite Constellations*, British Interplanetary Journal Soc., vol. 37, pp. 559572, 1984. 1

BIBLIOGRAPHY

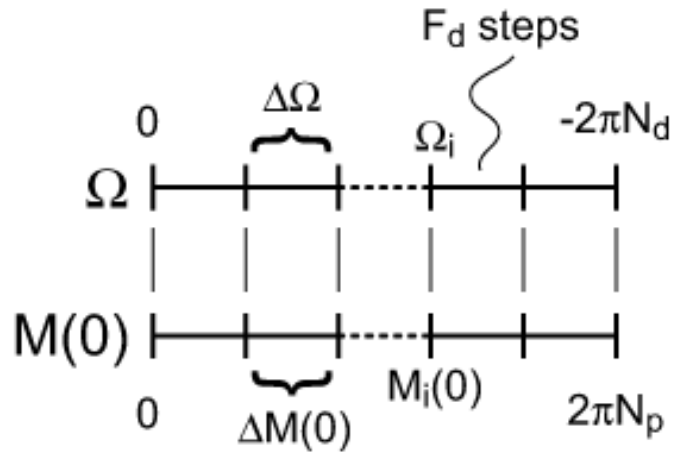
- [4] A. E. Turner, *Non-Geosynchronous oOrbits for Communications to off-load Daily Peaks in Geostationary Traffic*, AAS Paper 87-547, 1987. 1
- [5] J. Nugroho, J. E. Draim, Hudyarto, *A Satellite System Concept for Personal Communications for Indonesia*, Paper Presented at the United Nations Indonesia Regional Conference on Space Science and Technology, Bandung, Indonesia, 1993. 1
- [6] D. Beste, *Design of Satellite Constellations for Optimal Continuous Coverage*, IEEE Transactions on Aerospace and Electronic Systems, vol. 14, no. 3, 466473, 1978. 1
- [7] R. Proulx, J. Smith, John E. Draim, Paul Cefola, *Ellipso Gear Array - Coordinated Elliptical/Circular Constellations*, AAS Paper 98-4383, 1998. 1
- [8] John E. Draim, *Elliptical Orbit MEO Constellations: A Cost-Effective Approach for Multi-Satellite Systems*, 1996. 1
- [9] G. Solari, R. Viola, M-HEO: the Optimal Satellite System for the Most Highly Populated Regions of the Northern Hemisphere, Integrated Space/Terrestrial Mobile Networks Action Final Summary, ESA COST 227 TD, vol. 92, no. 37, 1992. 1
- [10] G. Pennoni, L. Bella, *JOCOS: A Triply Geosynchronous Orbit for Global Communications an Application Example*, Tenth International Conference on Digital Satellite Communications 2 (1995), 646652. 1
- [11] D. Rouffet, *The SYCOMORES System (Mobile Satellite Communications)*, IEE Colloquium on Highly Elliptical Orbit Satellite Systems (Digest No.86), pp. 6/1- 6/20, 1989. 1
- [12] P. Dondl, LOOPUS Opens a Dimension in Satellite Communications, International Journal of Satellite Communications, vol. 2, pp. 241250, First published 1982 in German, 1984. 1
- [13] J. R. Norbury, *The Mobile Payload of the UK T-Sat Project*, IEE Colloquium on Highly Elliptical Orbit Satellite Systems (Digest No.86), pp. 7/1-7/7, 1989. 1

BIBLIOGRAPHY

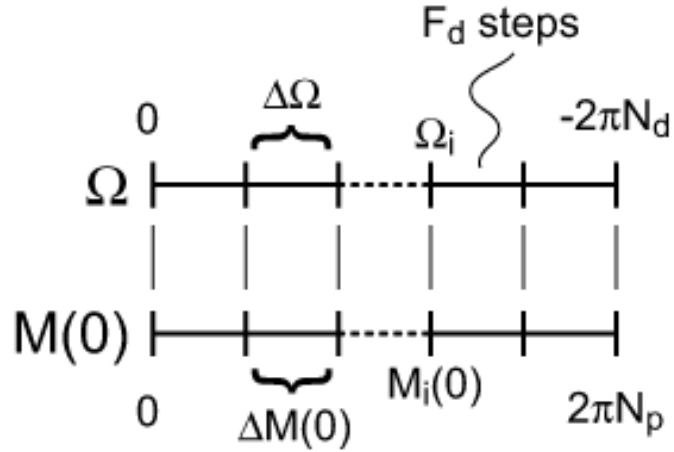
- [14] John E. Draim, R. Inciardi, Paul Cefola, Ron Proulx, David Carter, *Demonstration of the COBRA Teardrop Concept Using Two Smallsats in 8-hr Elliptic Orbits*, 15th Annual/USU Conference on Small Satellites, SSC01-II-3, 2001. [1](#)
- [15] Daniele Mortari, Matthew Paul Wilkins, *The Flower Constellation Set Theory Part I: Compatibility and Phasing*, 2006, accepted for publication. [1](#)
- [16] Matthew Paul Wilkins, Daniele Mortari, *The Flower Constellation Set Theory Part II: Secondary Paths and Equivalency*, 2006, accepted for publication. [1](#), [1.5](#)
- [17] Daniele Mortari, Matthew Paul Wilkins, Christian Bruccoleri, *The Flower Constellations*, Journal of the Astronautical Sciences 52 (2004), no. 1 and 2, 107 127, Special Issue: The John L. Junkins Astrodynamics Symposium. [1](#), [1.5](#)
- [18] Matthew Paul Wilkins, Christian Bruccoleri, Daniele Mortari, *Constellation Design Using Flower Constellations*, Paper AAS 04-208 of the 2004 Space Flight Mechanics Meeting Conference, February 913, 2004. [1](#), [1.5](#), [1.6](#)
- [19] Daniele Mortari, Ossama Omar Abdelkhalik, Christian Bruccoleri, *Synodic and Relative Flower Constellations with Applications for Planetary Explorations*, Paper AAS 05-151 of the 2005 Space Flight Mechanics Meeting Conference, January 2327 2005. [1](#)
- [20] Keun Joo Park, Matthew Paul Wilkins, Christian Bruccoleri, Daniele Mortari, *Uniformly Distributed Flower Constellation Design Study for Global Positioning System*, Paper AAS 04-297 of the 2004 Space Flight Mechanics Meeting Conference, February 913, 2004. [1](#), [1.5](#)
- [21] Keun Joo Park, Marina Ruggieri, Daniele Mortari, *Comparisons Between GalileoSat and Global Navigation Flower Constellations*, Paper of the 2005 IEEE Aerospace Conference, March 512 2005. [1](#), [1.5](#)

BIBLIOGRAPHY

- [22] Christian Bruccoleri, Daniele Mortari, *The Flower Constellation Visualization and Analysis Tool*, Paper of the 2005 IEEE Aerospace Conference, March 512 2005. 1
- [23] Ossama Omar Abdelkhalik, Daniele Mortari, *Two-Way Orbits*, Celestial Mechanics and Dynamic Astronomy 94 (2006), no. 4, 399410. 1.5
- [24] Daniele Mortari, *Flower Constellations as Rigid Objects in Space*, ACTA Futura 2 (2006), 722. 1.5
- [25] Matthew Paul Wilkins, Daniele Mortari, *Constellation Design via Projection of an Arbitrary Shape onto a Flower Constellation Surface*, Paper of the 2004 AIAA/AAS Astrodynamics Specialist Conference, August 1619, 2004. 1.5
- [26] Eric W. Weisstein, Zermelo-fraenkel set theory, From MathWorldA Wolfram Web Resource. <http://mathworld.wolfram.com/Zermelo-FraenkelSetTheory.html>, Accessed January 10, 2006. 7
- [27] Eric W. Weisstein, Axiom of replacement, From MathWorldA Wolfram Web Resource, <http://mathworld.wolfram.com/AxiomofReplacement.html>, Accessed January 10, 2006. 7



(a) $F_n = N_d$



(b) $N_d = 1$

Figure 1.10: When specific choices of parameters are made, then the pattern of pairs of RAAN and mean anomaly angles will repeat before the complete range is filled.

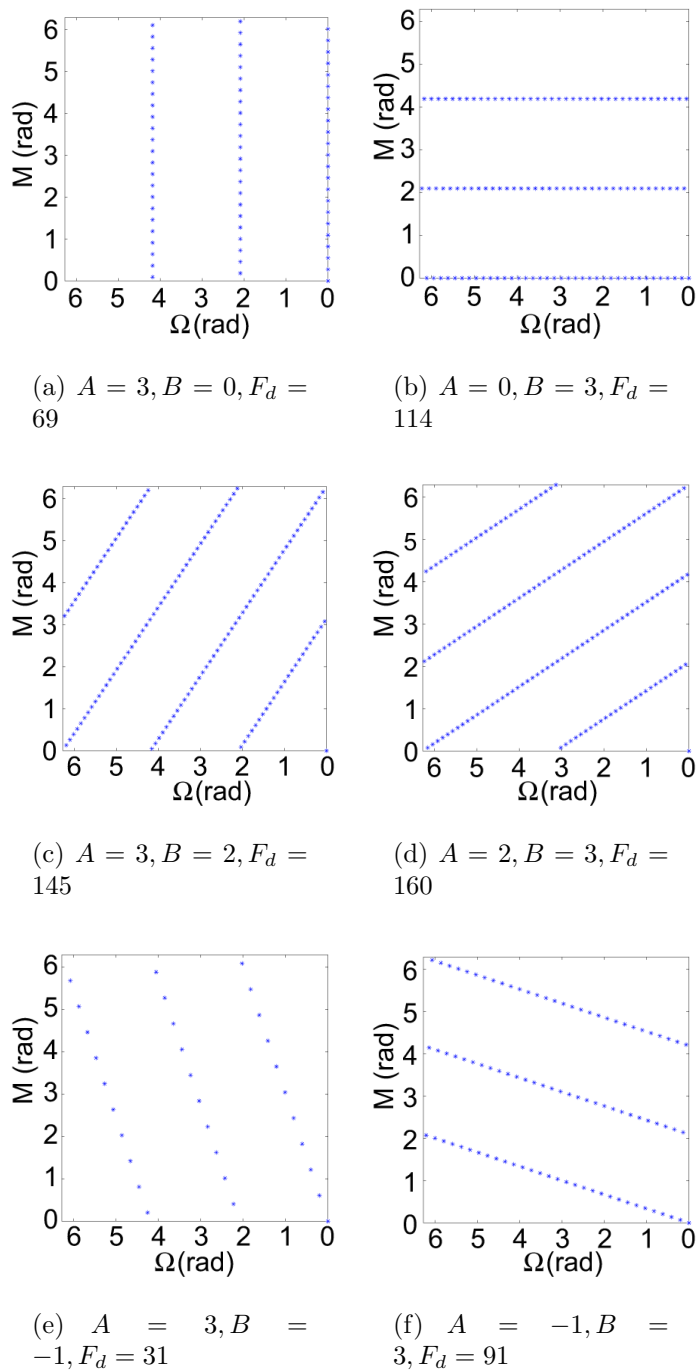


Figure 1.11: By graphing the RAAN versus mean anomaly over $\text{mod}(2\pi)$, one can see that as the satellites are placed, distinct banding can appear depending upon the values of A and B . A 38-23- F_d -23- F_d Flower Constellation is used for each plot where the naming convention follows N_p - N_d - N_s - F_n - F_d for the sake of brevity.

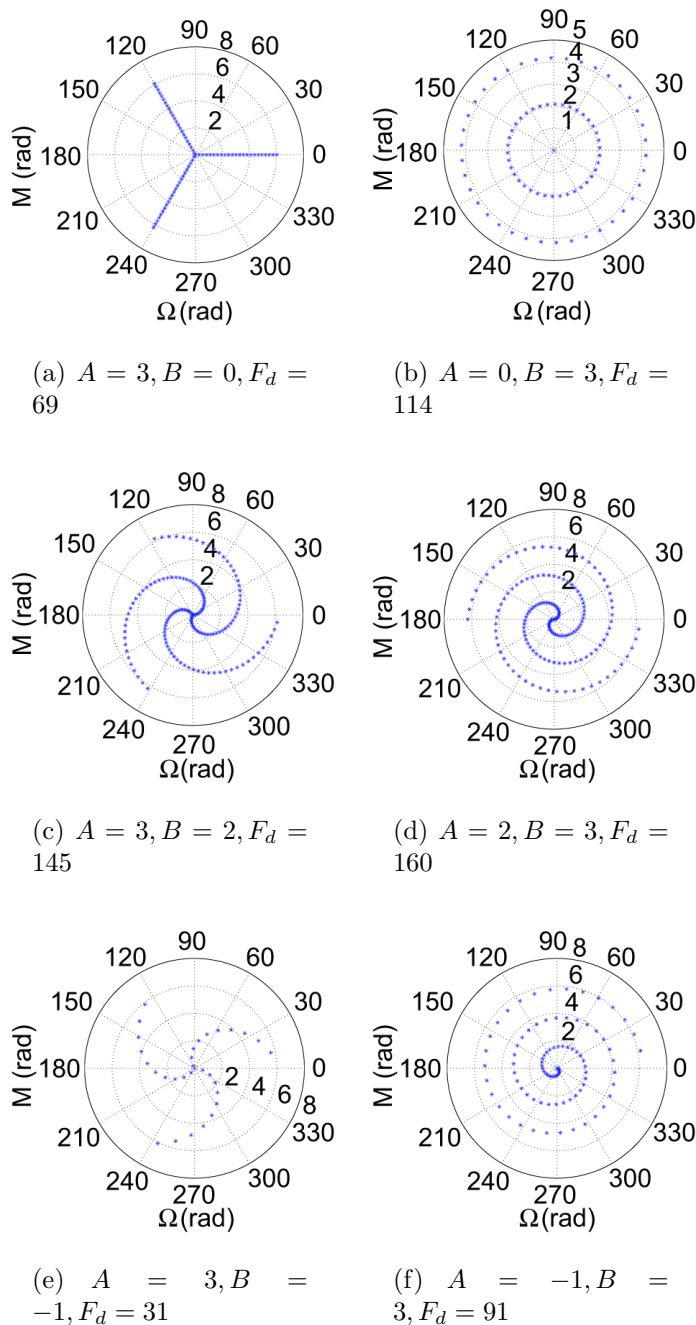


Figure 1.12: Here the RAAN is plotted versus mean anomaly over $\text{mod}(2\pi)$ in a polar plot. Ω is the angle and M is the radius on the polar plot. Notice the distinct branches that appear for specific values of A and B as well as the direction of the branches according to the sign of A and B . A 38-23- F_d -23- F_d Flower Constellation is used for each plot.

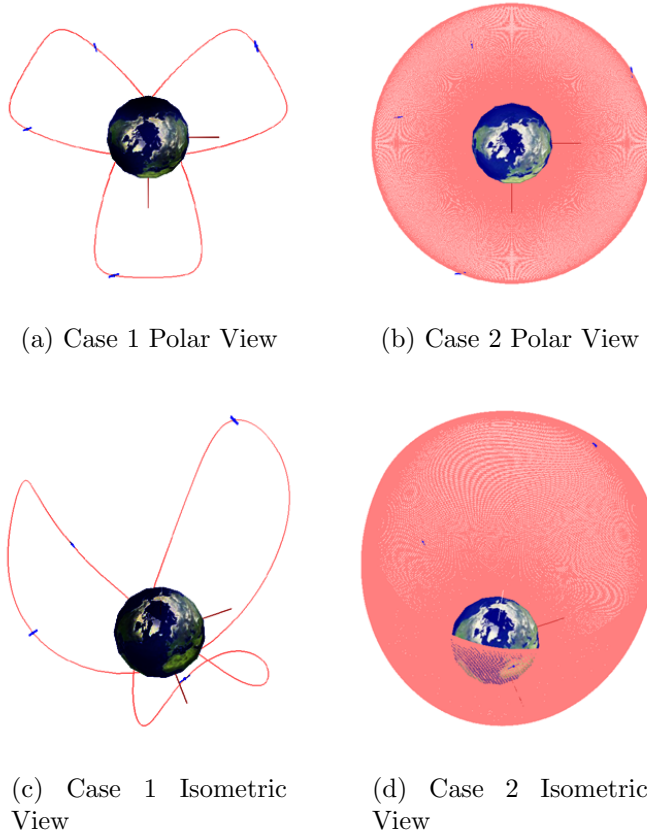


Figure 1.13: Case 1: A 3-1 FC, Case 2: A 769-257 FC.

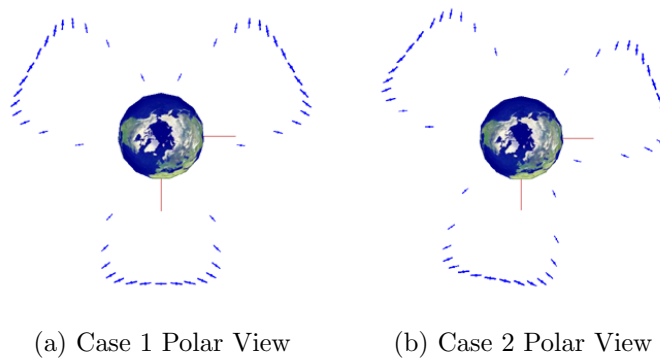
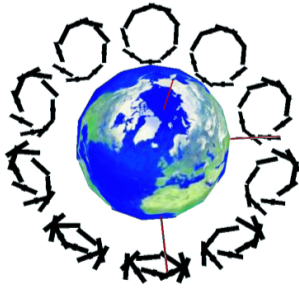
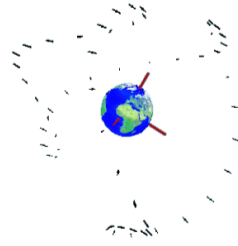


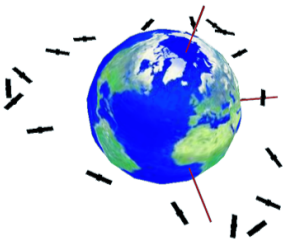
Figure 1.14: Case 1: A 3-1 Flower Constellation with 50 satellites, Case 2: A 769-257 Flower Constellation with 50 satellites. For both cases, each satellite has been placed into its own orbit (i.e. $F_n/F_d = 1/N_s$). Note that the satellite depictions are not to scale.



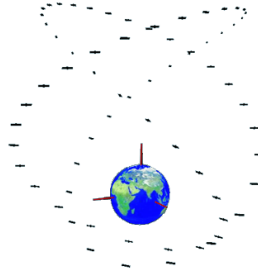
(a) 8-1-90-1-90 FC, $i = 165^\circ$, $\omega = 270^\circ$, $h_p = 3000 \text{ km}$



(b) 31-18-57-6-19 FC, $i = 63.4^\circ$, $\omega = 270^\circ$, $h_p = 22,967.988 \text{ km}$

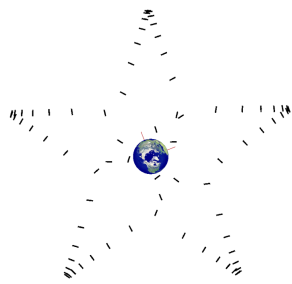


(c) 15-2-18-1-18 FC, $i = 180^\circ$, $\omega = 270^\circ$, $h_p = 3000 \text{ km}$

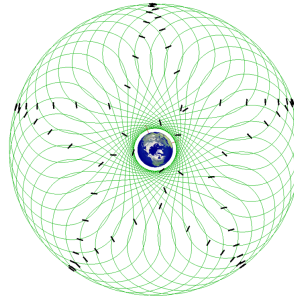


(d) 8-1-90-1-90 FC, $i = 165^\circ$, $\omega = 270^\circ$, $h_p = 3000 \text{ km}$

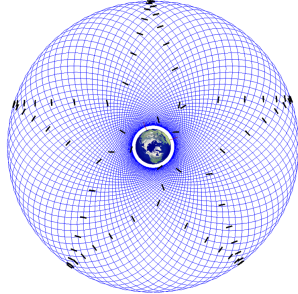
Figure 1.15: Secondary closed paths can form on top of the relative orbit. These secondary closed paths rigidly rotate about the axis of symmetry while the relative path is fixed in the rotating reference frame. Note that the depictions of satellites are not to scale.



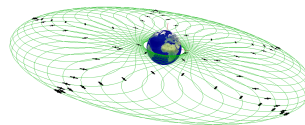
(a) North Pole view of the satellites only



(b) North Pole view of the relative orbit



(c) North Pole view of the ECI orbits



(d) Isometric view of the relative orbit

Figure 1.16: The Lone Star Constellation - a 38-23-77-23-77 Flower Constellation with $i = 0^\circ$, $\omega = 270^\circ$, and $h_p = 1300 \text{ km}$. Note that the depictions of satellites are not to scale.

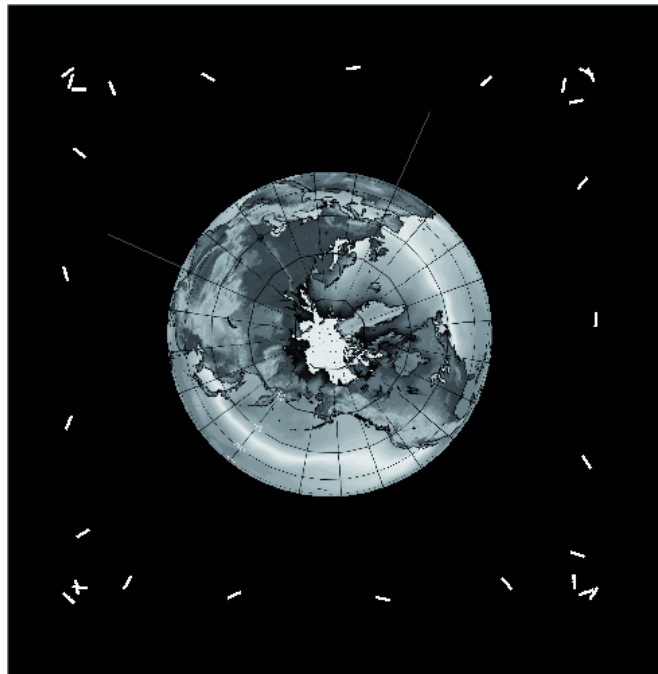


Figure 1.17: A secondary path consisting of a single closed loop.

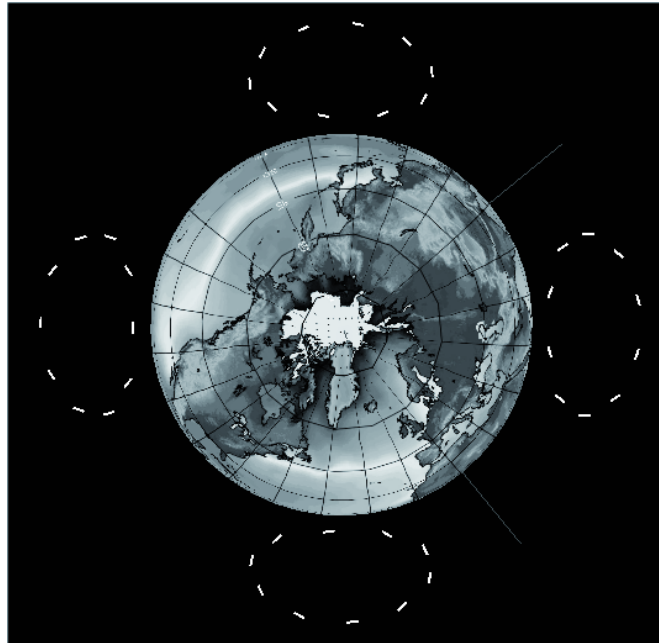


Figure 1.18: A secondary path consisting of four distinct closed loops.

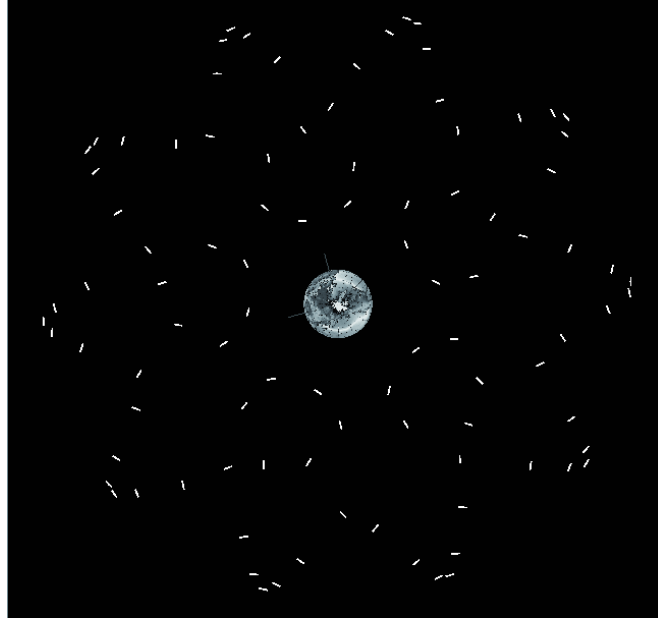


Figure 1.19: A secondary path with $N_{al} = 10$ and $N_{pl} = 5$

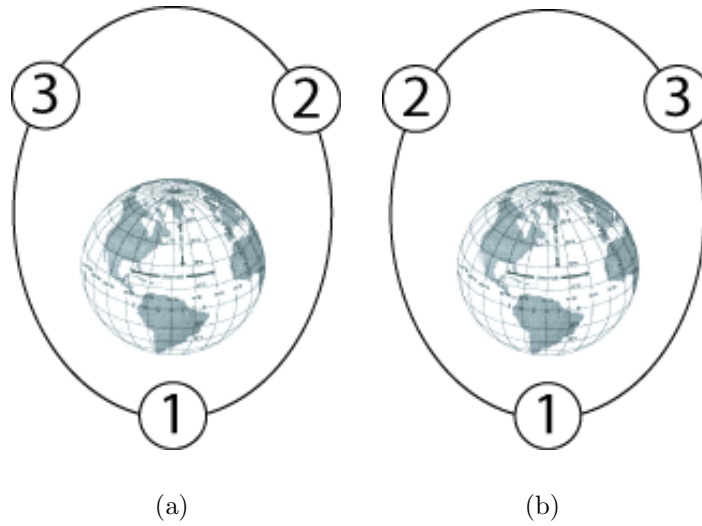


Figure 1.20: A graphical example of the allowable circular permutations for the $N = 3$ case. In this example, there are three admissible positions on a given orbit, and there are $(3 - 1)! = 2$ unique sequences that define the order of placement.

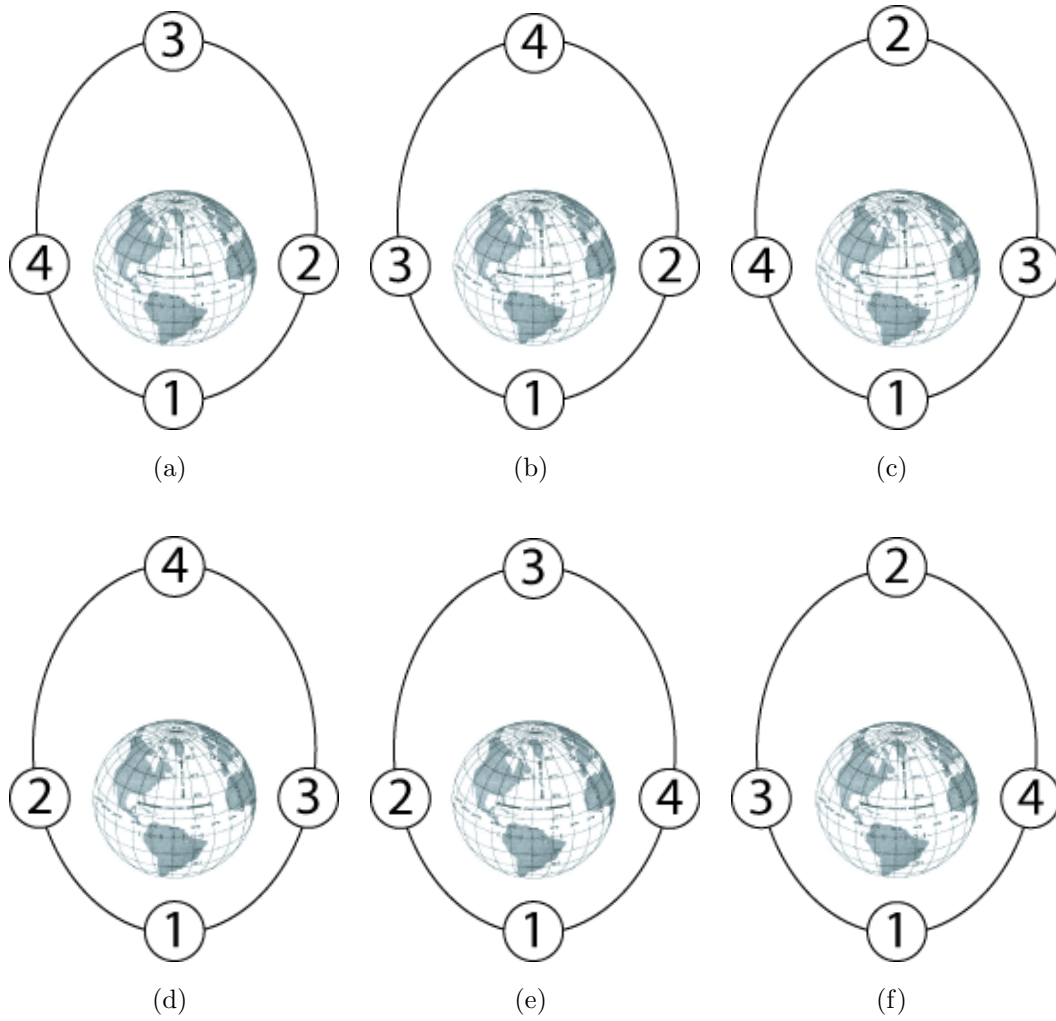


Figure 1.21: A graphical example of the allowable circular permutations for the $N = 4$ case. In this example, there are four admissible positions on a given orbit, and there are $(4 - 1)! = 6$ unique sequences that define the order of placement.

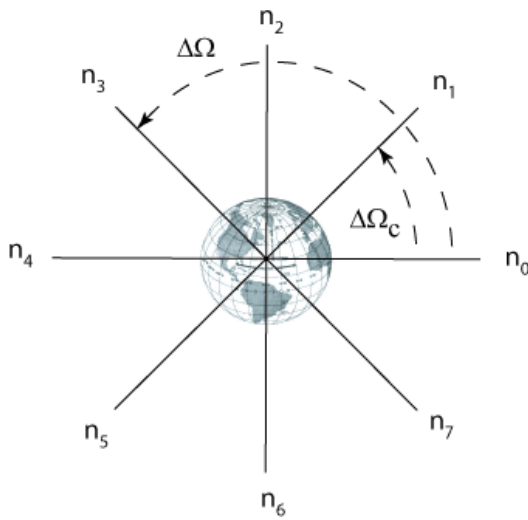


Figure 1.22: A comparison of satellite node spacing for a *Contiguous* Flower Constellation, $\Delta\Omega_c$, and an arbitrary node spacing $\Delta\Omega$ when $F_d = 8$.

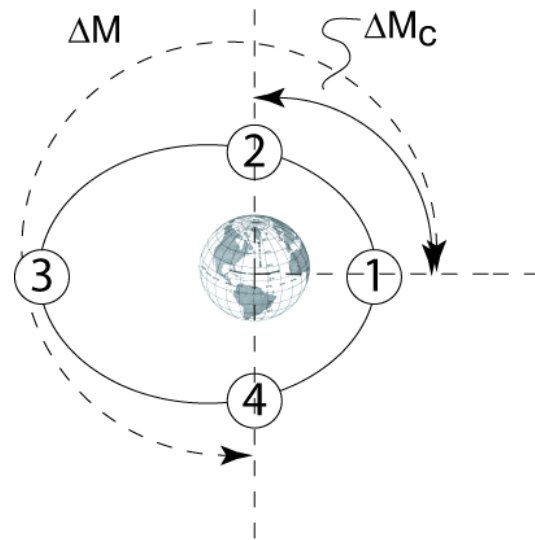


Figure 1.23: A comparison of satellite mean anomaly spacing for a *Contiguous* Flower Constellation, ΔM_c , and an arbitrary node spacing ΔM when $N_d = 4$.

Chapter 2

Design of Flower Constellations

2.1 Optimisation of Flower Constellations

A methodology for the optimisation of Flower Constellations for Continuous Regional Coverage has been conceived during this project and its feasibility has been demonstrated with simulations.

A Genetic Algorithm (GA) has been utilized to carry out the optimisation process because of the difficulty of determining a starting point in the design space and the presence of both integer and real parameters in the optimization space.

Wertz in [1] says that there is no defined process for constellation design since it is a process that varies significantly with the mission objectives. Although we recognize the truth of this statement we have also tried to maintain the maximum flexibility in the general method. By utilizing genetic algorithms, that by design do not require specific knowledge of the problem of interest, similar coverage problems can be analyzed by simply changing the cost function used by the GA. This also allows for a greater modularity of the implemented MATLAB code. Given the focus of this study, some example are provided in the following sections to demonstrate the validity of the approach.

2.1.1 Methodology for the Design of FCs

The first step in the design of FC optimisation with GAs is to select which parameters are assigned by the user a priori and which parameters are being

2.1 Optimisation of Flower Constellations

optimised. The constellation design process is usually a multi objective problem in which the different facets of constellation design must be weighed with the specific mission objectives; on the other hand it is useful to devise a methodology that is as general as possible. The choice of using GAs as the methodology for constellation optimization helps in maintaining generality since GAs do not require knowledge of the problem or an initial guess of the starting point for the optimization.

During constellation design the preferred solutions are those that satisfy the mission requirements while minimizing the cost of putting satellites in orbit. As a consequence it is desired that the minimum number of satellites to accomplish the mission objectives is employed. Another important cost factor is the number of orbital planes utilized: putting satellites on different orbital planes requires multiple launches and launch is a major cost factor. For these reasons the approach taken in this study is to leave the choice of the number of satellites and orbital planes to the user: it is reasonable to expect that the mission designer will know in advance how many spacecrafts can be utilized for a given project. The computer program will then seek an optimal solution for the given number of satellites.

A constellation for continuous regional coverage must satisfy the requirement that a given region of the earth (or Mars, or other planet) is being observed continuously by at least one spacecraft at all times. One obvious and trivial way to satisfy such requirement is to have one or more geostationary satellites above the regions of interest. A geostationary satellite has a circular orbit with a semi-major axis of 42.164 Km and will remain almost stationary over the region since it is orbiting with the same angular velocity of the earth. The merits of geostationary satellites will not be repeated here, but it is sufficient to say that they are, to date, the preferred solution for telecommunications and for continuous regional coverage in general. Their major drawback is however cost: launching a geostationary satellite is very expensive and a constellation of such satellites would be prohibitive.

Another reason for seeking alternative solutions is robustness. Geostationary satellites are being built with high redundancy to maintain the spacecraft operational in case of failure of some parts in the hard geo orbit environment. This is

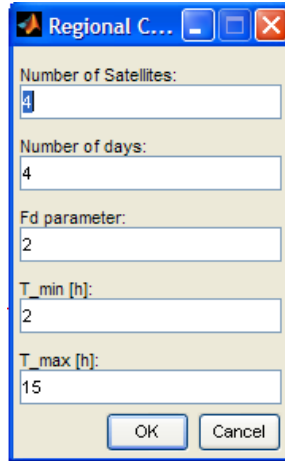
2.1 Optimisation of Flower Constellations

another cost driver since functionality, redundancy, low volume, power efficiency, and low weight are competing requirements in spacecraft design.

During the last decade there have been many proposals to move from the current framework in which access to space is very expensive and realized with few spacecrafts towards a framework of economy of scale. If satellites become more reliable, lighter, smaller, then the cost of access to space could be lowered. In this concept, the FCs could be utilized to provide novel solutions for continuous regional coverage that employ a larger number of less expensive spacecrafts in LEO to MEO orbits, trying to exploit the characteristics of elliptical orbits that are easily generated through the FCs parameters.

An optimization process for continuous coverage that leaves the choice of the orbit to the optimizer will, almost certainly, produce a very high (up to geo) orbit. For this reason the choice of the range of the allowed orbit periods should be a user input parameter.

The other two parameters, shown in Figure 2.1, are specific to the FCs: N_d is the number of days required to repeat the ground track, and F_d specifies how many satellites are distributed per orbital plane. More details on these parameters can be found in the chapter regarding the FCs theory. The orbit height chosen is



The image shows a standard Windows-style dialog box with a title bar that says "Regional C...". Inside the dialog, there are five labeled input fields stacked vertically. The first field is "Number of Satellites:" with the value "4". The second is "Number of days:" with the value "4". The third is "Fd parameter:" with the value "2". The fourth is "T_min [h]:" with the value "2". The fifth is "T_max [h]:" with the value "15". At the bottom right of the dialog are two buttons: "OK" and "Cancel".

Figure 2.1: Input dialog for the optimization process.

also a function of the sensor characteristics: if the sensor is a camera and a given minimum resolution is desired then there is a maximum orbit height requirement

2.1 Optimisation of Flower Constellations

that determines the maximum orbital period (T_{max} in Figure 2.1), the minimum orbital period (T_{min}) allowed has a lower bound that has been chosen assuming a minimum perigee height of 250 *Km*. A summary of the meaning of the input parameters entered in the dialog in Figure 2.1 is provided in Table 2.1.1.

Parameter	Description	Units
N_s	Total number of spacecrafts in the constellation	Non dim.
N_d	Number of days needed to repeat the ground-track	Non dim.
F_d	FC parameter: defines number of satellites per orbit	Non dim.
T_{min}	Lower Limit for the orbital period	Hours
T_{max}	Upper limit for the orbital period	Hours

Table 2.1: Summary of user parameters in the input dialog

The chosen sensor also has a limited field of view which obviously affects the coverage characteristics. The sensor parameters and the specification of the region of interest are done in the Matlab script that drives the optimization process, *regional_coverage_driver.m*, since these parameters don't need to be changed often while different configurations are examined.

The specification of the region of interest can be done in two ways: by using a discrete number of points (sites) on the earth surface that approximate the region, or as a small circle, i.e. the smallest circle that encloses the desired area. The discretized set of points approach is the one taken in this study since it allows for a finer analysis of the coverage.

In order to simplify the data input process the user is only required to provide the vertices of the closed spherical polygon that define the region boundaries and the number of points with which the region should be approximated. A function, *regiongrid.m*, is provided to further simplify this process: since Matlab already contains a polygonal description of the political boundaries of the United States and the geographical boundaries for the rest of the world, the selection of the region of interest can be done simply by using the name of the desired region as it is shown in Figure 2.2.

2.1 Optimisation of Flower Constellations

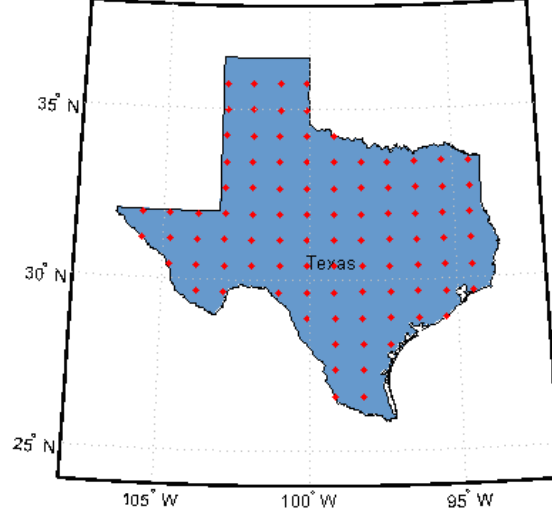


Figure 2.2: Example of points distribution obtained with the function *region-grid.m* over Texas.

The user will also have to select the simulation duration; by default this is taken to be equal to the number of days to ground-track repetition, N_d , expressed in seconds. Furthermore a starting date of simulation is needed to compute the hour angle of the earth at the specified simulation date, also known as Greenwich Sidereal time. Routines converting the calendar date to Julian date and then to compute the Greenwich Average Sidereal Time (GAST) hour angle¹ are also provided.

The remaining parameters needed to uniquely identify a FCs are left to the optimizer and are then encoded into a vector, chromosome in the context of GAs, that is passed to the objective function. A summary of the input parameters being optimized is shown in Table 8. The FC parameters have been already explained; regarding to the ξ parameter introduced in Table 8 this has been introduced to prevent the generation of unfeasible solutions by the GA during the optimization process. This parameter is a real number between 0 and 1 and correspondingly selects the eccentricity between e_{min} and e_{max} . The boundaries for the eccentricity are computed to prevent hyperbolic orbits, parabolic orbits, and orbits intersecting the earth (i.e. below some minimum height, default 250

¹ In spite of the name, the Greenwich Sidereal Time angle is always measured in radians.

2.1 Optimisation of Flower Constellations

Parameter	Description	Units
N_p	Number of petals, determines the FC orbital period	Non dimensional
F_n	Phase parameter for FCs	Non dimensional
F_h	Inter-plane phase parameter for FCs	Non dimensional
i	orbital inclination	degrees
ω	argument of perigee	degrees
ξ	eccentricity selection parameter, determines orbital shape	[0..1], Real

Table 2.2: Summary of parameters being optimized by the GA.

Km).

2.1.1.1 Objective Function

The objective function takes in input a possible solution and measures the cost of such solution according to a design parameter. In the case of continuous regional coverage the desired parameter is maximization of the coverage on the area of interest. A point on the earth surface is being observed at a time t_k if there is at least one satellite whose sensor FOV-cone intersection with the earth surface contains such point. By using the previous definition we can compute a three dimensional matrix C that for each satellite, each site, and each instant in time describes the coverage of the area. More formally, C is defined as:

$$C(i, j, k) = \begin{cases} 1 & \text{if site } i \text{ can be seen by satellite } j \text{ at time } t_k \\ 0 & \text{otherwise} \end{cases}$$

$$i = 1..N_{sites}, j = 1..N_s, k = 1..N_k,$$

where:

N_s is the number of satellites

N_{sites} is the number of points in the region

N_k is the number of time intervals

In order to compute such matrix the objective function needs the position of all the satellites for the entire simulation, therefore given the input parameters passed to the cost function, both user parameters and optimization parameters, the corresponding FC is generated and the satellite orbit is propagated in the ECEF coordinate frame of reference for the simulation duration.

2.1 Optimisation of Flower Constellations

The orbit propagation is done using a simple propagator that takes into account the secular terms of perturbation due to the J_2 coefficient in the spherical harmonic expansion of the earth gravitational field that takes into account earth oblateness².

The starting date of the simulation is also needed by the cost function for the transformation between ECI and ECEF coordinate frames.

The objective function then computes the coverage of the specified area for the simulation duration using the function *coverage.m* which computes the coverage matrix C . Since the GA implementation provided with Matlab is trying to minimize a function the objective function is actually designed to minimize the duration of the gaps in the coverage rather than the coverage itself³. The final cost returned by the function is computed according to the following pseudo-algorithm:

```
% Initial cost J
J = 0; for i = 1:nsites
% compute the visibility matrix v for each site
    for j = 1:Ns
        % if any satellite can see the site, then site is visible
        v(i, :) = v(i, :) | cov(i,j,:);
    end
% summarize data: ng is number of gaps
% Ig is a matrix of gap intervals
[ng, Ig] = gapcount(v(i,:));
% sum the total time of gap intervals
J = J + sumcoverage(t, Ig);
end
```

In the pseudo-algorithm above the colon is utilized, according to Matlab notation, to specify a vector operation over the missing index. For more details refer to: *gapcount.m* and *sumcoverage.m* functions.

² This is functionally equivalent to the J_2 propagator used by AGI satellite toolkit (STK).

³ In alternative, one can simply change sign to the returned value of the cost function.

2.1 Optimisation of Flower Constellations

The correctness of the results provided by the `coverage.m` routine has been validated using a test problem. The results obtained have been compared to the results given by AGI STK® on the same problem and the agreement of the two results is about ± 30 seconds for each access (or gap) interval with a simulation time step of 60seconds, over one day. This difference is due to the discretized approach taken in the Matlab routine. It is possible to improve the results by using a refining process at the boundaries of the intervals but the total discrepancy is of only few minutes over several hours of total coverage and does not change the nature of the solution; an improved solution on the other hand would impose an increased computational burden for each individual in a generation of the evolving population.

According to this definition of the coverage, no further improvement is possible when a 100% coverage (i.e. 0% gaps) solution is found; in such case the GA is set to stop.

2.1.1.2 Optimisation process

The optimisation process is carried out in three steps, as shown in Figure 2.3; firstly the input parameter are specified by the user, then the driver script prepares the environment for the execution of the GA and starts the optimization. The GA parameters specified in the driver script are of paramount importance to the final solution; the final solution, and the time required to find it, strongly depends on how the generations are evolved, on the size of the population and on the GA operators parameters (crossover frequency, mutation probability, use of elitism, to name a few). Given the limited computing resources available for this study the population size and the maximum number of generations have been chosen to be relatively small. The number of sites and the number of satellites utilized has been also kept as small as possible. Examples of the FC optimizations are provided in the following.

2.1 Optimisation of Flower Constellations

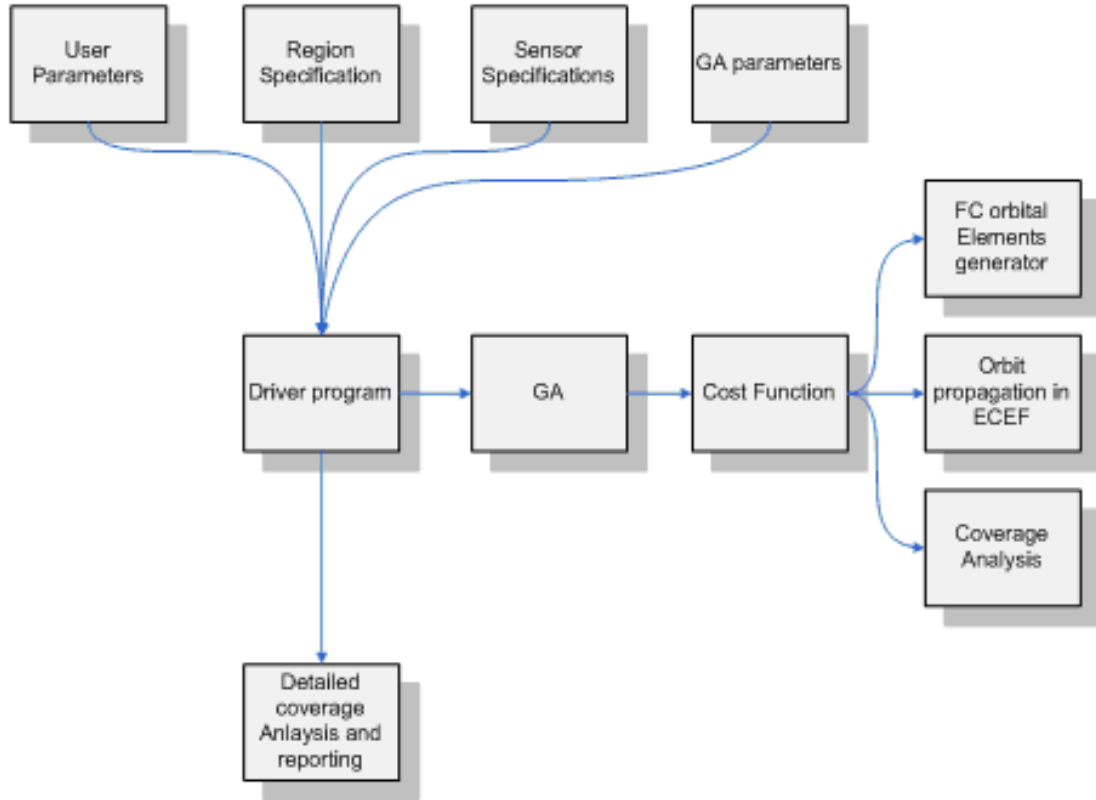


Figure 2.3: Optimisation process diagram.

Examples

The examples concerns regions in the U.S.A. simply because Matlab provides political boundaries of the states within the U.S.A. and thus the regions are easier to specify, but there is no loss of generality for the method.

Example 1

This example provides a solution to the observation of Alaska, an oil rich region. The GA has been set to stop as soon as it found a 100% coverage solution. Matlab output is provided below:

Region selected: Alaska $N_s = 8$, $N_d = 1$, $F_d = 16$, $T_{\min} = 2$ h,
 $T_{\max} = 8$ h $a_{\min} = 8059.0$ [Km], $a_{\max} = 20307.4$ [Km] ($N_{p_{\min}}$,
 $N_{p_{\max}} = (3, 11)$ Sensor FOV: 30 [deg] N. of points: 6

2.1 Optimisation of Flower Constellations

Output: Optimization terminated: minimum fitness limit reached.
Optimization time: 79.4 [s] fval = 0.0 Np = 3, Nd = 1, Ns = 8, Fn
= 7, Fd = 16, Fh = 0 inc = 61.27 [deg], w = 0.00 [deg], e = 0.488
a = 20270.4 [Km], e = 0.49, T = 0.332 [days]

Average coverage: 100.00 %

Average gap: 0.00 %

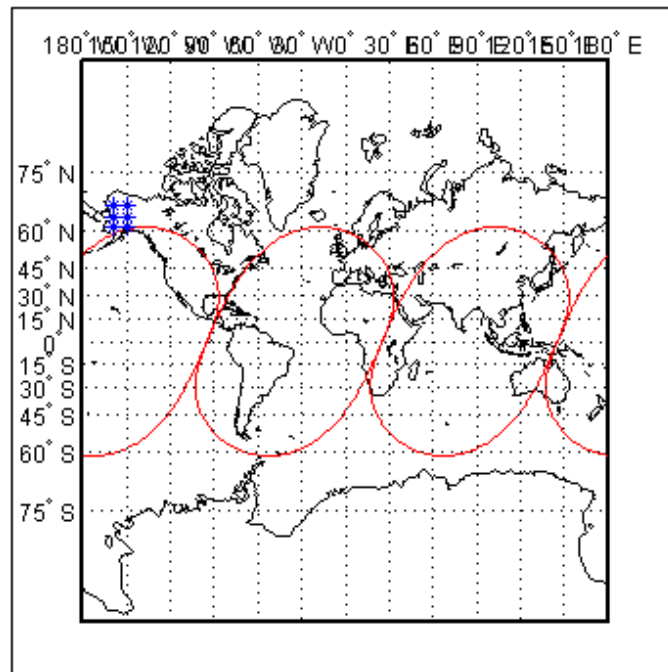


Figure 2.4: Ground track plot for Example 1

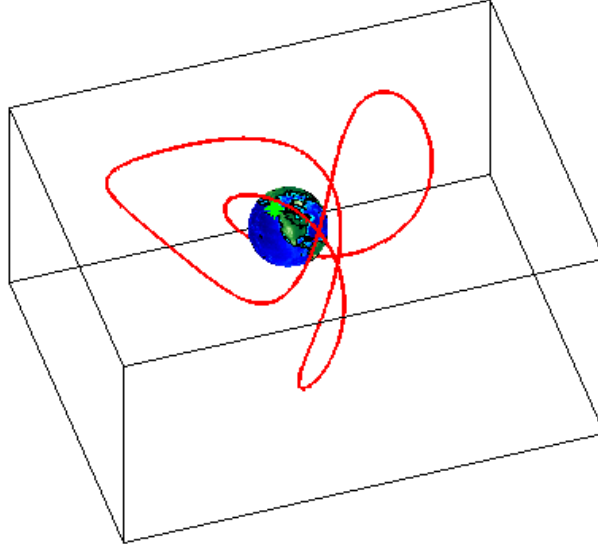


Figure 2.5: Three-dimensional relative path in ECEF coordinates for Example 1.

Example 2

In this case the region of interest is Texas, using 23 points to approximate the region. The GA finds an optimal solution using 6 satellites, that achieve continuous coverage of the region.

N. of points: 23 Selected region: Texas $N_s = 6$, $N_d = 1$, $F_d = 18$,
 $T_{\min} = 2.0$ [h], $T_{\max} = 15.0$ [h] $a_{\min} = 8059.0$ [Km], $a_{\max} =$
 30878.4 [Km] --> $(N_{p_{\min}}, N_{p_{\max}}) = (2, 11)$ Sensor FOV = 30.0
[deg]

Output: Optimization terminated: minimum fitness limit reached.
Optimization time: 310.2 [s] $f_{val} = 0.0$ $N_p = 2$, $N_d = 1$, $N_s = 6$, F_n
 $= 5$, $F_d = 18$, $F_h = 0$ $inc = 27.36$ [deg], $w = 0.00$ [deg], $e = 0.750$
 $a = 26561.7$ [Km], $e = 0.75$, $T = 0.499$ [days]

Average coverage: 100.00 %

Average gap: 0.00 %

2.1 Optimisation of Flower Constellations

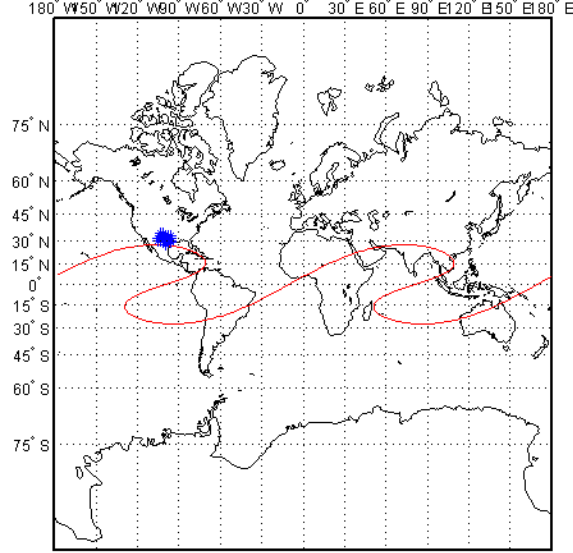


Figure 2.6: Solution for continuous coverage of Texas with 6 satellites.

Example 3

In this example only 6 satellites are allowed, in MEO orbit. In this example we are trying to achieve continuous coverage with a lower orbit. The solution found is not 100% coverage but still very close, as it is show in Figure 2.8. Four points on the Florida region are considered. An plot that shows how the GA converges toward better solutions is shown in Figure 2.9.

N. of points: 4 Input parameters: Selected region: Florida
Simulation start date: 10/1/2006 12.0 Ns = 6, Nd = 1, Fd = 18,
Tmin = 2.0 [h], Tmax=6.5 [h] $a_{\min} = 8059.0$ [Km], $a_{\max} = 17682.2$ [Km] -->(Np_min, Np_max) = (4, 11) Sensor FOV = 30.0 [deg]

Output: Optimization terminated: maximum number of generations exceeded. Optimization time: 2012.9 [s] fval = 27117.2 Np = 4, Nd = 1, Ns = 6, Fn = 1, Fd = 18, Fh = 0, inc = 45.03 [deg], w = 3.83 [deg], e = 0.074 a = 16732.9 [Km], e = 0.07, T = 0.249 [days]

Average coverage: 91.35 %

2.1 Optimisation of Flower Constellations

Average gap: 8.25 %

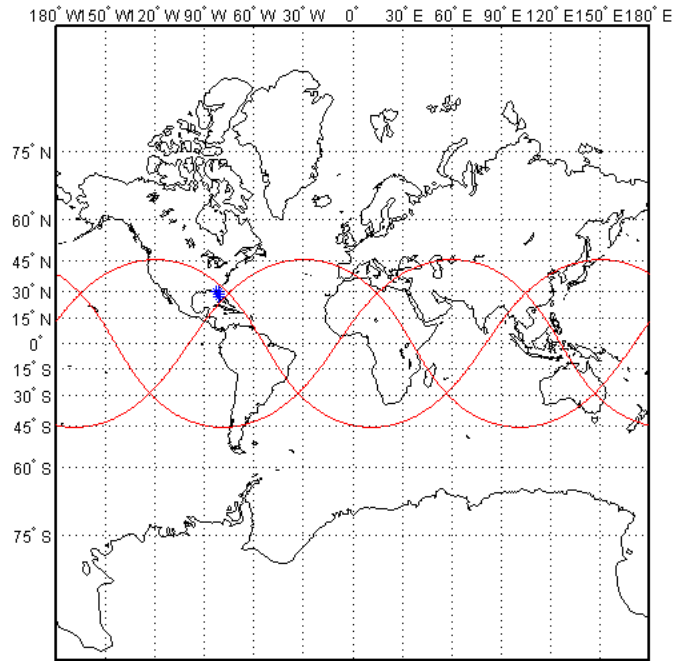


Figure 2.7: Ground track plot of best solution found in Example 3.

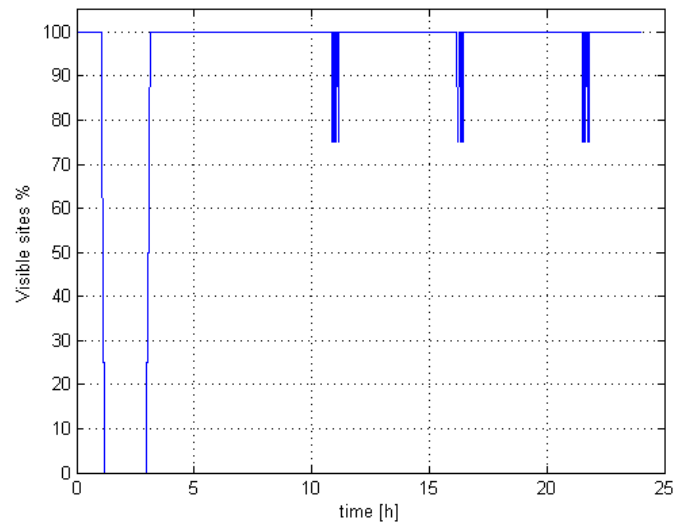


Figure 2.8: Percentage of visible sites as function of time for the solution found in Example 3.

2.1 Optimisation of Flower Constellations

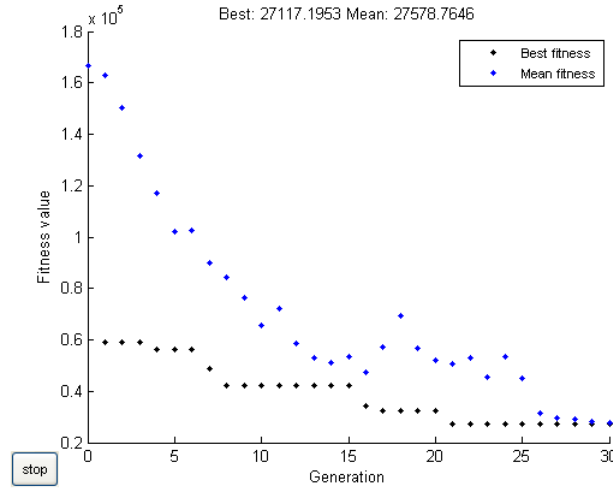


Figure 2.9: Best and mean population fitness during GA optimization for example 3.

Example 4

Another run on Florida, but the desired orbits should have a period between 3 and 4 hours, thus more satellites are needed to achieve satisfactory coverage.

N. of points: 4 Optimization terminated: maximum number of generations exceeded. Optimization time: 701.5 [s]

Input parameters: Selected region: Florida Simulation start date: 10/1/2006 12.0 Ns = 12, Nd = 2, Fd = 48, T_min = 3.0 [h], T_max=4.0 [h] a_min = 10560.3 [Km], a_max = 12792.9 [Km] --> (Np_min, Np_max) = (12, 15) Sensor FOV = 30.0 [deg]

Output: fval = 89717.5 Np = 13, Nd = 2, Ns = 12, Fn = 1, Fd = 48, Fh = 0, inc = 34.29 [deg], w = 0.00 [deg], e = 0.304 a = 12106.0 [Km], e = 0.30, T = 0.153 [days]

Average coverage: 86.37 %

Average gap: 13.41 %

2.1 Optimisation of Flower Constellations

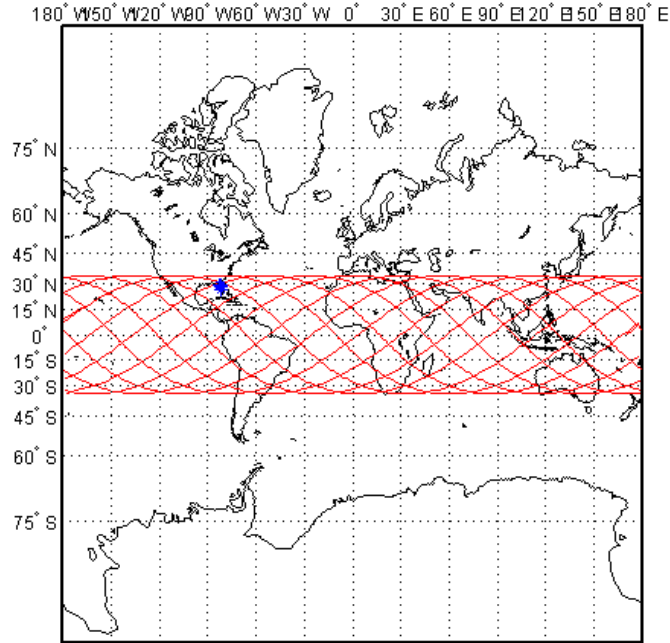


Figure 2.10: Ground track plot of best solution found in Example 4.

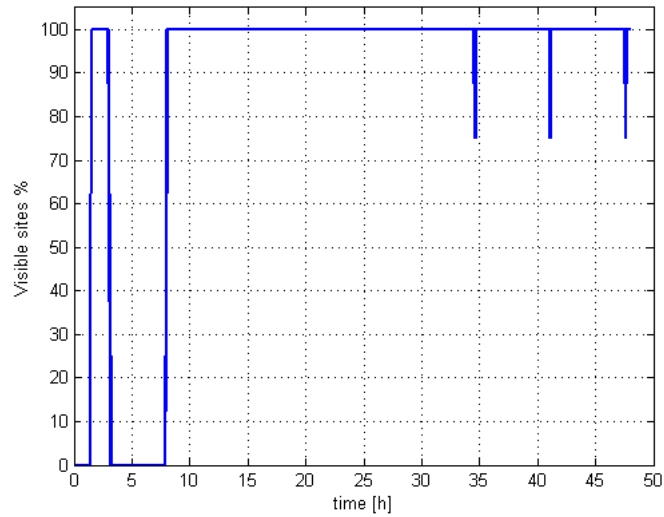


Figure 2.11: Ground track plot of best solution found in Example 4.

Examples 1-4 are shown to validate the feasibility of the approach and the correctness of the Matlab code. The examples show expected trends: if higher orbits are allowed the preferred solutions tend towards highly eccentric orbits

2.1 Optimisation of Flower Constellations

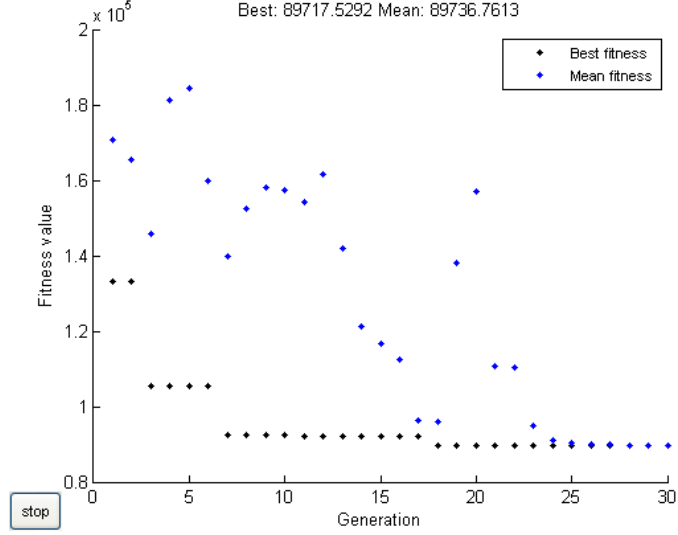


Figure 2.12: Ground track plot of best solution found in Example 3.

with high apogees above the regions of interest (example 1 and 2), thus achieving continuous coverage with a limited number of satellites. On the other end, if the height-range of allowed orbit is reduced, more satellites are needed to achieve the continuous coverage requirement, as expected.

In Figure 2.9, 2.12 the convergence history of the Genetic algorithm is shown. Blue dots represent the average fitness in the population, whereas black dots represent the history of the best solution. The plot shows that the average converges toward the best found solution, and there is also an improvement of the best individuals with the progression of generations. Some important GA parameters are shown and described in Table 2.3; for further details refer to Matlab help documents on the GA optimisation toolbox.

BIBLIOGRAPHY

Parameter	Description	Value
<i>Population Size</i>	Number of individuals in the population	30
<i>Crossover Fraction</i>	Fraction of the population in the next generation that is created using the cross over operator.	90%
<i>Generations</i>	Maximum number of generations before halt.	30
<i>Stall time limit</i>	Maximum time allowed during runtime without an improvement in the best individual.	10 minutes
<i>Fitness Limit</i>	If this value is reached, no further optimisation is possible.	0

Table 2.3: GA parameters

References

- [1] J. R. Wertz, *Mission Geometry; Orbit and Constellation Design and Management*, Microcosm Press, 2001. [2.1](#)

Chapter 3

Applications and Benefit Analysis

FCs have been designed in the past for Earth's global navigation, giving much better navigation performance (in terms of GDOP, ADOP, and coverage) than the existing Global Positioning System (GPS), Global Navigation Satellite System (GLONASS), and GALILEO constellations, using the same number of spacecraft or achieving the same performance using fewer satellites [1] [2].

3.1 Telemedicine

In this Section, we deal with telemedicine applications which are a particular type of telecommunication service which can exploit real-time and/or store-and-forward applications. For this type of service we can identify a specific number of locations involved in providing and accessing to the service. There are several telemedicine providers which exploit existing satellite systems for the provision of this telecommunication service. Most of the sites interested in accessing telemedicine services are located in rural areas and, hence, satellite systems are the most suitable choice for the platform service. However, none of these satellite systems are specifically designed for telemedicine services. Furthermore they do not provide a direct connection between the service suppliers and the service customers. In this work we design a specific FC for the provision of telemedicine services with the following features:

- near continuous coverage of a list of targets interested in providing and accessing the service;
- direct connection of service suppliers and service customers via satellites and Inter Satellite Links (ISLs);
- maximum Round Trip Time (RTT) of 200 ms.

3.1.1 Telemedicine Services

Telemedicine services enable the communication and sharing of medical information in electronic form, and thus facilitate access to remote expertise. This type of service is important for large and scarcely populated countries where there is a lack of health care facilities. Immobile patients should not be required to travel long distances to receive diagnosis and medical assistance. The objective of this work is to build up a satellite constellation able to provide medical consultancies from advanced hospitals located in Europe or USA (service suppliers) to rural and/or remote areas in Africa or Asia (service customers) via a pure satellite communication network; hereafter service suppliers and customers will be referred as "targets" for the satellite constellations. The identification of the service customer targets on Earth has been performed with respect to high demographic density and lack of medical infrastructures and terrestrial communications networks. Most of the service customers are located in rural areas while service suppliers are located in metropolitan areas. In Table 3.1 all the identified targets are listed. We should highlight that such targets are only a sample of possible locations that could be interested to such service. We assume that the service customers are provided with fixed or portable terminals that are used by medical/emergency teams wanting to connect to the service suppliers in order to request any of the several services that are listed in the following:

- qualified medical assistance by using teleconference or instant messaging;
- analysis of clinical data (electrocardiogram, radiological data, etc.);
- monitoring of vital parameters (blood pressure, pulse, oximetry, respiration, etc.);

3.1 Telemedicine

- access to medical information from digital libraries;
- follow a continuing education course (tele-medicine learning).

Table 3.1: Telemedicine service Earth targets.

Service Supplier	Latitude (deg)	Longitude (deg)
Fucino	42.80	13.13
New York	40.71	-74.00
Houston	29.76	-95.30
Seattle	47.60	-122.33
Los Angeles	34.05	-118.24
Service Customer	Latitude (deg)	Longitude (deg)
Lanzhou (China)	35.96	104.89
Lusambo (Congo)	-5.69	23.73
Baliuag (Philippines)	14.62	120.97
Mekar (Indonesia)	-6.18	106.63
Beroga (Malaysia)	3.16	101.71
Musawa (Nigeria)	12.00	8.31
Youngsfield (South Africa)	-33.93	18.46

In order to allow such services being provided, the satellite constellation must be designed for real-time applications and store-and-forward applications.

After the identification of several service suppliers and service customers, the satellite constellations will be designed with the objective to meet the following requirements:

- Near-continuous coverage of all the service customers.
- Interconnection via Inter Satellite Links (ISLs) of all the service customers and at least one service suppliers.
- Round Trip Time (RTT) lower than 200 ms in order to allow interactive applications.

- Total number of satellites lower than 10, in order to keep system cost low.

3.1.2 Constellation Design for Telemedicine

3.1.2.1 Flower Constellation Design

Once that a list of service suppliers and service customers has been defined, by using an optimization process based on a Genetic Algorithm (GA) a FC has been designed. The problem has been decomposed in two steps: the first is finding an orbit with a ground track that allow the observation of all the sites, the second is to find a distribution of satellites along the track that provides a good time access to the ground targets. The first step has been approached using a GA for a single satellite track, whereas for the second FCs have been utilized to extend the solution achieved in the first step to a FC of 8 satellites.

The cost function utilized to guide the GA optimization process is designed to maximize the dwell time over each target. Since the computational load to evaluate the correct dwell time is too demanding, the dwell time is here maximized by minimizing the satellite ground relative velocity. In order to provide a preference for satellites passing over the site, the relative velocity is weighted by the ratio of the angular displacement of the target site from the sub-satellite point direction (λ) with respect to the antenna field of view. These considerations yield to the following penalty function:

$$J_{obs} = \sum_{k=1}^N \left(1 + \frac{\lambda_k}{\theta_{FOV}} \right) |v_{rel}| \quad (3.1)$$

where α_k is the relative weight of the k -th site with respect to the other target sites. Therefore, by keeping the ground track spacecraft velocity v_{rel} as low as possible above target site we indirectly increase the dwell time over the site itself. The angle θ_{FOV} is the half field of view of the on board antenna, assumed to be pointed at nadir, and α_k is the weight of the k -th site, with $k = 1, 2, \dots, N$, with N being the number of target sites.

In order to run the GA, the design space (i.e. the chromosome) must be defined. The following parameters have been encoded in the chromosome string:

$$h_p \in (1500, 3000), i \in [0, \pi], \omega_p \in [0, 2\pi]$$

$$\Omega_0 \in [0, 2\pi], M_0 \in [0, 2\pi], t(k) \in [0, t_f], k = 1, 2, \dots, N$$

The semi-major axis of the desired orbit is chosen by the designer. The times $t(k)$ represent the instants in time in which the k -th site is accessed by the spacecraft and t_f is the final time of the simulation. The extension of the design space caused by the introduction of these time array seems counterintuitive at first. It is however justified by the need of keeping the computation time manageable: while propagating the orbit and compute these access times analytically seems to be the obvious and correct solution, this latter approach requires propagation of the orbit and a search process that slows down each GA iteration considerably. The introduction of the access times array in the design space instead allows for a quick evaluation of the cost function during each GA iterations, thus allowing a bigger population and more evaluations to be completed to achieve an improved solution. The coarse solution obtained through the GA is then refined using a gradient method search. Some of the design variable can be kept fixed as, for instance, was done with the inclination that was kept fixed at the critical value of 63.4° . The critical inclination has been chosen in order to release the need to control the drift of the perigee due to the perturbations. Once the optimization process has been completed a FC with the parameters listed in Table 3.2 has been created matching the FC parameters to the ground track resulted from the optimization.

The repeating ground track of this FC is shown in Figure 3.1, while the relative orbit in a ECEF (Earth Centered Earth Fixed) system is shown in Figure 3.2 and Figure 3.3. It can be noticed that six equally-spaced petals are placed above the locations of service providers and suppliers.

3.1.2.2 Walker Constellation Design

The Walker constellation is not designed to show repeating ground track. This means that the satellites belonging to a Walker constellation covers all the longitudes with the passing of time. On the other hand, the latitudinal coverage can

Table 3.2: Flower constellations parameters.

Number of Petals (N_p)	6
Number of Days (N_d)	1
Number of Satellites (N_s)	8
Phase Numerator (F_n)	1
Phase Denominator (F_d)	8
Phase Step (F_h)	0
Inclination (i)	116.6^0
Perigee Height (h_p)	3087 km
Argument of Perigee (ω_p)	187.07^0
$RAAN_0$	243.77^0
TA_0	172.92^0

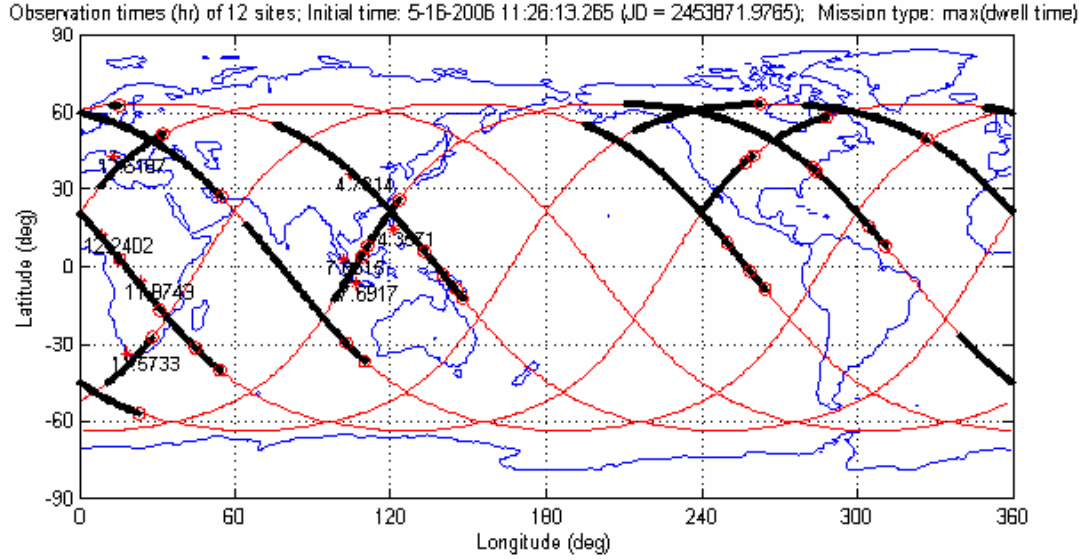


Figure 3.1: Repeating ground track of the FC for telemedicine.

be restricted to the equatorial regions by lowering the inclination. After the identification of the target with the highest latitude we have set the orbital inclination

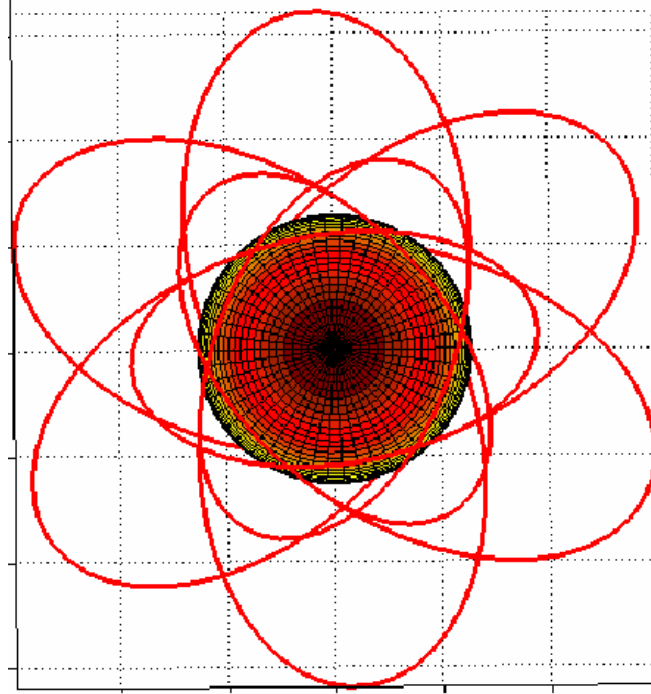


Figure 3.2: Relative orbit of the FC for telemedicine (view from the pole).

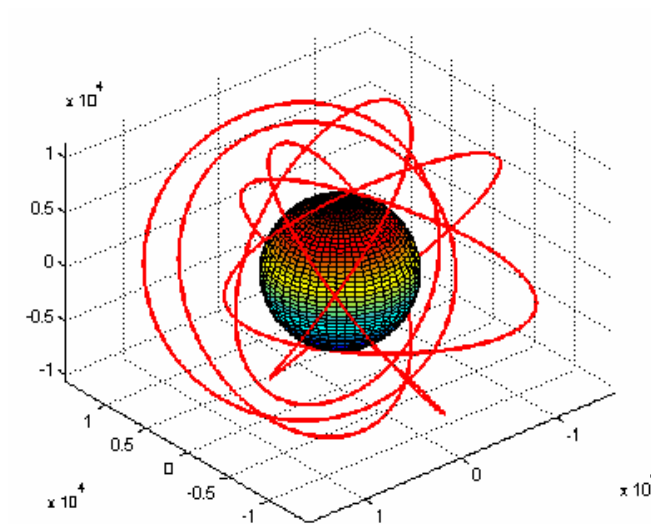


Figure 3.3: Relative orbit of the FC for telemedicine (orthographic view).

to 45^0 . The number of satellites has been set to 8 as it is for the FC, while we have set the orbit altitude to 6,841 km in order to compare an elliptic orbit constellation (the FC) and a circular orbit constellation (the Walker constellation) with the same average satellite altitude. Furthermore, we had three choices on the number p of orbital planes (8, 4 and 2) and we will show the results achieved with the best configuration. Performing several evaluation of the coverage for different $RAAN_{spread}$, we have also found that a $RAAN_{spread} = 180^0$ is the best choice. The parameters of the Walker constellation are listed in Table 3.3.

Table 3.3: Walker constellations parameters.

Number of Satellites (t)	8
Number of Planes (p)	4
Satellites per Plane ($s = t/p$)	2
Inter Plane Spacing (f)	1
$RAAN_{spread}$	180^0
Inclination (i)	45^0
Orbit Height (h)	6.841 km

3.1.3 Performance Comparison

We are going to compare the FC and the Walker constellation in terms of the following performance metrics:

- access time (%) between service providers and customers;
- mean access time between service providers and customers.

As previously described targets have been selected in order to model service providers and service customers. Telecommunications chains (using only the satellite constellation network) between all service providers and customers have been created, selecting all useful links (using 1, or none-ISL); afterwards for every

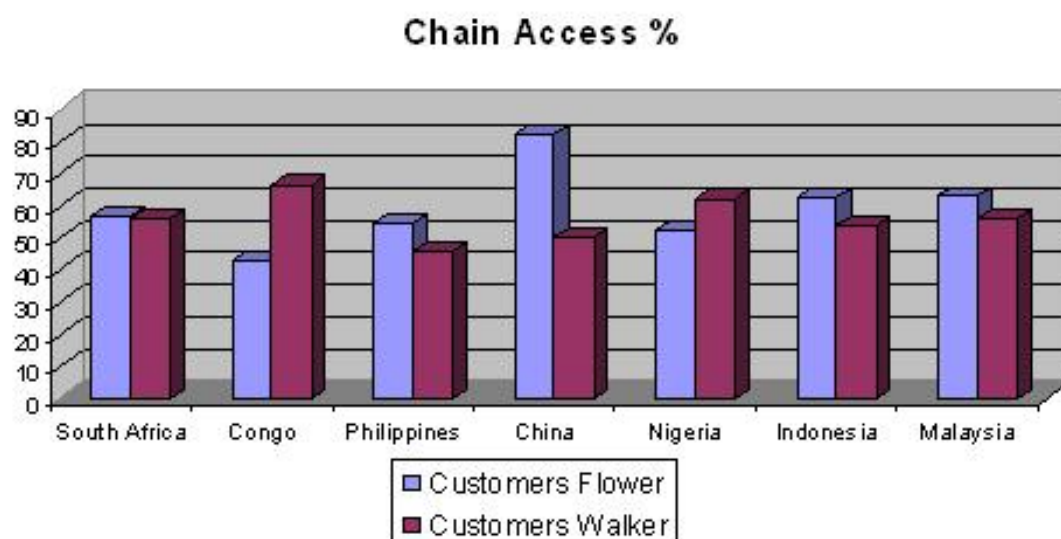


Figure 3.4: Chain access availability percentage performance comparison for all service customers.

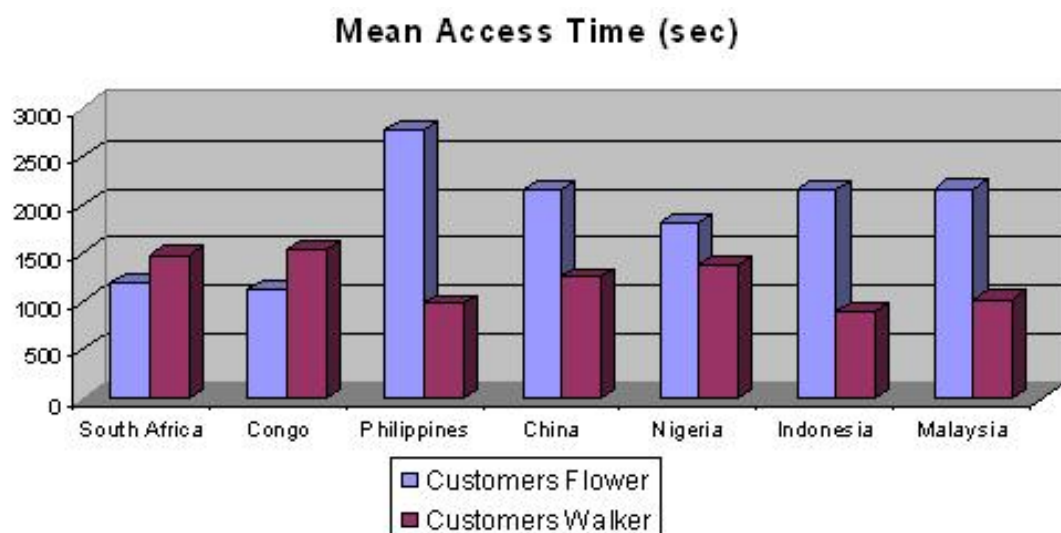


Figure 3.5: Mean access time performance comparison for all service customers.

chain time access periods have been evaluated and overlapped (in time) in order to establish the complete time-continuous coverage. The temporal coverage, evaluated in terms of percentage of the propagation time is shown in Figure 3.4.

The propagation time for the FC is set to one day ($N_d = 1$) while the propagation time for the Walker constellation is set to one month. With respect to this performance metric the bar chart in Figure 3.4 shows that the FC provides better performance for five customers by seven, giving an overall chain access of 59% versus 55% provided by the Walker constellation. The mean chains access time which is the second performance evaluation metric is shown in Figure 3.5; it can be observed that, for most of the customers (five), the FC provides better results compared with the ones offered by the Walker constellation. As a matter of fact the Walker constellation provides fractioned accesses with a mean time duration of 1220 sec. with respect to the mean time duration of 1912 sec. offered by the FC; this results means very frequent handovers for the service provided by the Walker constellation. From this analysis it can be deduced that a FC provides better performance for telemedicine services in terms of availability and quality.

3.1.4 Conclusion

In this work we designed a FC which is optimized to cover a set of targets interested in providing and accessing telemedicine services. However, the proposed optimized design can be used for a more general class of communication services and a different set of targets. It has been found that the features of the FC allow a specialised coverage of a list of targets thus providing better performance in terms of access availability with respect to a classical Walker constellation, at the expenses of a more complex design.

3.2 Martian Constellation of Orbiters

The deployment of a constellation of satellites instead of the deployment of a single satellite provides larger coverage areas (localized or even global), while increasing the design complexity and the cost. However in some situations the need to cover large areas justifies the exploitation of satellite constellations. Currently there are several applications that can get benefit from the exploitation of satellite

3.2 Martian Constellation of Orbiters

constellations, such as telecommunications, navigation and Earth observation. In this paper, a novel constellation of orbiters to be used for the so-called Interplanetary Internet, which is defined as the network of planetary networks which interconnects orbiters, landers, rovers, planetary stations, and relay satellites, is presented. In particular, we focus on the interconnection of landers, rovers and probes over Mars [3]-citemars-4. Areas of interest over the Mars surface are the north and south poles and the equator (i.e. between -15 and $+15$ degrees in latitude) [3]. Each orbiter is equipped with a medium-range radio transceiver for the communications with landed elements and a long range radio transceiver for relaying information back to Earth. Several constellations of orbiters have been proposed in order to provide communication between landers and orbiters over Mars. One of the most important constellations has been proposed by the Jet Propulsion Laboratory (JPL), named 4retro111 [3]. This constellation has been optimized to cover the equatorial and the polar regions. This objective has been fulfilled by splitting the overall constellation into two sub-constellations that can be classified as Walker constellations: the first sub-constellation is optimized to cover the equatorial region, while the second one is optimized to cover the polar areas. In this paper we are going to exploit the capabilities of the Flower Constellations (FCs) in order to provide better performance in terms of maximum gap time, availability of Inter Satellite Links (ISLs) and visibility of the Earth, with respect to the constellation 4retro111. The performance metrics are going to be optimized taking into account some constraints such as: maximum number of satellites, orbit inclination and perigee/apogee height.

Our approach to the optimization follows the approach of the 4retro111, that is, we are designing two Flower sub-constellations: the first sub-constellation is optimized to cover the equatorial region, while the second sub-constellation is optimized to cover the polar areas. The optimization process will make use of genetic algorithms and the final paper will compare the proposed FC with the already developed 4retro111.

3.2.1 Interplanetary Internet And Martian Missions

3.2.1.1 Mission Needs

Interplanetary Internet is defined as the network of planetary networks which interconnects landers, orbiters, rovers, planetary stations, and relay satellites. It encompasses both UpLinks/DownLinks (ULs/DLs), Inter-Satellite Links (ISLs), and Inter-Planetary Links (IPLs). At present, Mars is the focus of Interplanetary Internet. Actually, since the last few years, the space community has shown an increased interest in the Solar System exploration, especially for Mars. This trend is also confirmed for the next ten/twenty years. The fourth planet will be the key target of orbiters, landers and rovers, designed by the main space agencies, firstly NASA and ESA. The main scope of these efforts is to gather more and more scientific data about the red planet in order to characterize in detail the martian geology and meteorology, as well as the search of the water ice. Final objective is to define and to design manned missions to Mars, identifying possible landing sites. In references [4] [5], the authors showed some future trends for missions into deep space, especially growing data richness and more data-intensive instruments. This evolution requires an increase in returned data volumes and higher data rates, envisaging the need of data relay nodes in space. The future scenario foresees spacecraft fleet in orbit around Mars, providing telecommunications, navigation and observation services. They will exchange data with rovers, landers and probes on the surface and with the Earth, creating an infrastructure that will have to answer to the needs of flexibility and reliability over time in order to support this effort. At present, a NASA/ASI mission, the Mars Reconnaissance Orbiter (MRO), is the last one arrived at Mars in order to characterize the surface, subsurface, and atmosphere of the red planet. Its objective is also to identify potential landing sites for future missions. This orbiter hosts some telecommunications systems that will establish a fundamental support for future spacecrafts, becoming the first link in a communications bridge back to Earth, an “Interplanetary Internet”. It will help the communications of the international spacecraft fleets in coming years.

Selection of landing sites for Mars exploration missions require an intensive study. The criteria are defined as:

- safe landing;
- scientific interest (areas of geological and/or meteorological interest, possible presence of water ice, etc.);
- local environmental conditions (surface characteristics, lighting status, temperatures and so on).

We have analyzed the areas of interest for communication and navigation (Doppler based) services over the Mars ground for past, current and future missions and have defined the following targets [3]:

1. spot coverage: four sites of interest have been identified:
 - Spirit Rover: lat=-14.5deg, lon=175.3deg;
 - Opportunity Rover: lat=-1.9deg, lon=-5.9deg;
 - Mars Polar Lander: lat=-76.1deg, lon=164.7deg;
 - Phoenix Lander: lat=65deg, lon=-120deg;
2. regional coverage: the regions of interest are North polar region ($\text{lat} > 80^\circ$), South polar region ($\text{lat} < -80^\circ$), Equatorial region ($-15^\circ < \text{lat} < 15^\circ$).

Rovers, landers and probes on the surface of Mars require relay contacts at the same times every day so that they can design their missions and their operations based on invariant communications patterns. This requirement can be satisfied by designing constellations of orbiters with repeating ground tracks as is provided by FCs.

3.2.2 Communication Architecture

The task of the Interplanetary Internet is to develop a communication system architecture able to connect landers, rovers and orbiters with Earth facilities. Each orbiter is equipped with a medium range radio transceiver for communicating with landed elements and a long range radio transceiver for relaying information back to Earth.

Scientific missions require:

3.2 Martian Constellation of Orbiters

- time insensitive transfer of large size data (images and videos) from planets towards the Earth;
- time sensitive live video streaming for the control of rovers;
- telemetry, tracking and command of landed elements and orbiters.

Several issues have to be taken into account. The most important are:

1. large propagation delay;
2. limited quantity of energy;
3. discontinuity of the links.

A solution to the first issue is to develop space communication protocols optimized for long Round Trip Time (RTT), while the second issue requires the exploitation of large solar panels. In this paper, a constellation of orbiters of Mars, optimized to cover the areas of interest for most of the time, is developed. The areas of interest over the Mars surface are the equatorial belt and the poles, where most of the landing elements are expected to be placed.

3.2.3 FC Optimization

In Section 3.2.1.1, it has been stated that the objective of the present study is to develop an optimized Flower Constellation of orbiters for:

1. spot coverage;
2. regional coverage.

We are going to find a solution to our optimization problem that is at least nearly optimal. The optimization problem has been decomposed in two steps. The first step consists in finding an orbit with a repeating ground/space track that allows the observation of all the sites/regions with an access duration of each site as long as possible. The second step consists in finding a distribution of satellites along the repeating space track that provides an average gap time duration to the ground sites/regions as short as possible. The first step of the

3.2 Martian Constellation of Orbiters

optimization process has been approached by using a genetic algorithm for a single satellite track [11]. The FC parameters that are optimized during the first phase are: $N_p, N_d, h_p, i, \omega_p, \Omega_0, M_0$. Since the genetic algorithm methodology is well known and has been extensively studied, its theory will not be reviewed here; the interested reader can refer to [11]. While the first step of the optimization process is complex and has to be carefully performed on the basis of the number of ground sites (see next two subsections), the second step of the optimization process is very easy thanks to the particular properties of a FC. In fact, since the objective of the second step is to minimize the average coverage gap duration, the satellites have to be evenly spaced on the repeating space track. This task can be accomplished by setting $F_n F_d = N_s$, where $N_s=6$ as it is for the reference constellation and choosing $F_n = 1, F_h = 0$. We did not optimize any Walker constellation for our purposes, but we used the already developed 4retro111 as a reference constellation. However, it is worth noting that the optimization of a Walker constellation is more time consuming with respect to the optimization of a FC for the following reasons:

- for the optimization of a Walker constellation each satellite of the constellation has to be propagated, while in a FC it is necessary to propagate only one satellite, since every satellite follow the same repeating space track;
- for the optimization of a Walker constellation each satellite of the constellation has to be propagated for many days (at least 30 days), while in a FC it is necessary to propagate the constellation for exactly N_d days (which is usually 1 or 2 days).

Furthermore, the performance of a FC repeats every N_d days. Hence, the distribution of the accesses is more uniform with respect to a Walker constellation that does not have a repeating period. In the next two subsections we define the optimization metric of the first optimization step.

In this work we compare the performance of the designed FC with the constellation named 4retro111 proposed by JPL. Orbital parameters of the 4retro111 constellation are listed in Table 3.4. Two sub-constellation (Walker type) are designed. The first sub-constellation is composed by satellites no. 1 and 2 and

3.2 Martian Constellation of Orbiters

it is designed to provide communication services to near equatorial landed elements. The design parameters of the first sub-constellation are: $t = 2, p = 2, f = 0, RAAN_{spread} = 360^0, a = 4189.92 \text{ km}, i = 172^0$. The second sub-constellation is composed by satellites no. 3,4,5 and 6. The design parameters of the second sub-constellation are: $t = 4, p = 4, f = 1, RAAN_{spread} = 360^0, a = 4189.92 \text{ km}, i = 111^0$.

Table 3.4: Orbital elements for the 4retro111 constellation

Sat no.	h_p (km)	e	i (deg)	ω_p (deg)	$RAAN$ (deg)	M (deg)
1	800	0	172	0	0	0
2	800	0	172	0	180	0
3	800	0	111	0	0	0
4	800	0	111	0	90	90
5	800	0	111	0	180	180
6	800	0	111	0	270	270

3.2.3.1 Spot Coverage

The cost function utilized to guide the GA optimization process is designed to maximize the dwell time over each target. For the exact computation of the dwell time, the cost function should be designed such that the satellite has to be propagated for N_d days and the access of the satellite from a given ground site is computed on the basis of a given minimum elevation angle θ_m (where θ_m has been set to 20^0). This optimization process is time consuming even if the number of ground sites is low. To this respect we defined the following cost function:

$$f_{cost} = \prod_{j=1}^L \alpha_j \left(\theta(t_j) - \theta_m \right) d(t_j) \quad (3.2)$$

where α_j is the relative weight of the j -th site with respect to the other target sites, t_j is the instant of access of the satellite to the j -th site, $\theta(t_j)$ is the elevation angle at time t_j , $d(t_j)$ is the slant range at time t_j and L is the number of sites.

3.2 Martian Constellation of Orbiters

The cost function computed for a series of instants t_j , increases with the increase of the elevation angle and the slant range. For a large slant range the satellite moves slowly; hence, it remains in view for a long time. On the other hand, a large elevation angle (about 90°) means that the satellite passes over the site with a ground track as centered as possible to the site. As it is intuitive, this cost function increases with the increase of the dwell time; hence, it is a good heuristic cost function. In order to run the GA, the design space (i.e. the chromosome) must be defined. The following parameters have been encoded in the chromosome string:

$$h_p \in (100, 800), i \in [0, \pi], \omega_p \in [0, 2\pi]$$

$$\Omega_0 \in [0, 2\pi], M_0 \in [0, 2\pi], t_j \in [0, N_d], j = 1, 2, \dots, L$$

It is less intuitive to think that it is convenient, from the simulation time point of view, to increase the size of the design space of the genetic algorithm instead of performing a propagation of the satellite. In this case, the optimization metric has been computed for the 4 sites defined in Section 3.2.1.1, where each site has a weight equal to 1.

3.2.3.2 Regional Coverage

For the regional optimization we have evenly distributed a large number of sites within the regions of interest and we have optimized the dwell time for each site. When the number of sites is large, as it is the case of regional coverage, it is no longer convenient to use the previous approach for the optimization of the repeating space track and, hence, we have performed the satellite orbit propagation and then we have computed the exact dwell time. In this case, the optimization metric defined as the dwell time has been computed for a large number of ground sites evenly distributed on the Equator and the North and South Pole as it was defined in Section 3.2.1.1, where each site has a weight equal to 1.

3.2.3.3 Performance Evaluation and Comparison

In this Section we provide the design parameters of the FCs optimized by using the previously described methodologies. When there are several sites or regions widely spaced from each other, a single optimization is not the most suitable mean of performing an optimization. In our case, we can identify two regions (or group of sites), and then we can optimize a FC for each region: the polar region/sites and the equatorial region/sites. In the following subsections we present the optimization results showing FC parameters, and we compare the performance of the single FC (obtained by a single optimization process) and the double FC (obtained by a double optimization process) with the reference constellation 4retro111.

3.2.3.4 Spot Coverage - Single FC parameters

The design parameters of the single FC for spot coverage (named FC-MARS-single) are provided in Table 3.5. These design parameters generate the orbital parameters listed in Table 3.6. In order to visually show the suitability of the designed FC, the ground track and the ground sites are shown in Figure 1.

Table 3.5: Design parameters of the FC-MARS-single.

N_p	11
N_d	1
N_s	6
F_n	1
F_d	6
F_h	0
h_p	102 km
i	86.9^0
ω_p	17.7^0
Ω_0	216.6^0
M_0	289.7^0

3.2 Martian Constellation of Orbiters

Table 3.6: Orbital parameters of the FC-MARS-single.

Sat no.	a (km)	e	i (deg)	ω_p (deg)	$RAAN$ (deg)	TA (deg)
1	4130	0.154	86.9	17.7	216.6	272.1
2	4130	0.154	86.9	17.7	276.6	345.8
3	4130	0.154	86.9	17.7	336.6	64.9
4	4130	0.154	86.9	17.7	36.6	125.1
5	4130	0.154	86.9	17.7	96.6	172.3
6	4130	0.154	86.9	17.7	156.6	217.7

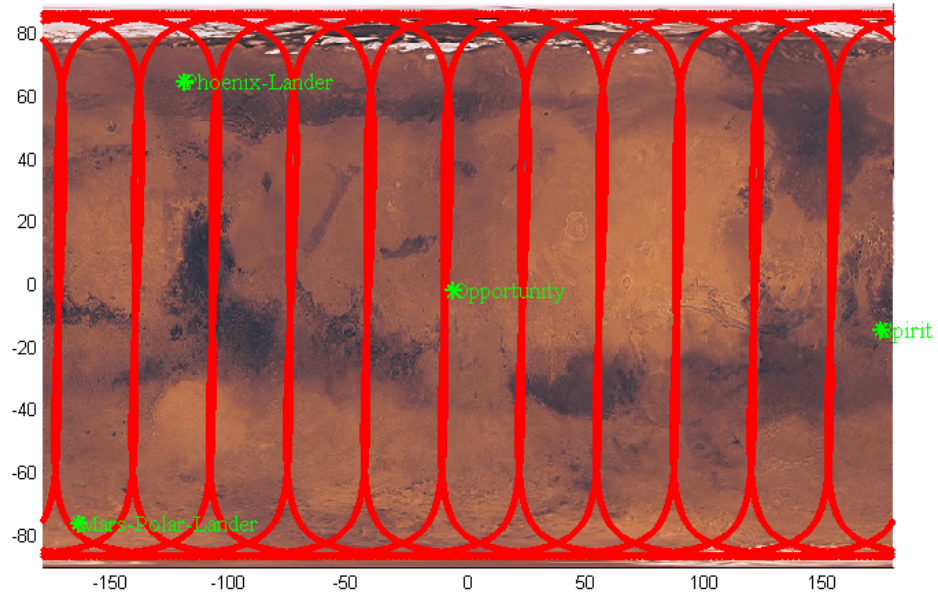


Figure 3.6: Ground track of the FC-MARS-single.

3.2.3.5 Spot Coverage - Double FC parameters

The double FC for spot coverage has been named FC-MARS-double. The design parameters of the first Flower sub-constellation are provided in Table 3.7, while the design parameters of the second Flower sub-constellation are provided in Table 3.8. These design parameters generate the orbital parameters listed in Table 3.9. The ground track and the ground sites are shown in Figure 3.7.

Table 3.7: Design parameters for the first sub-constellation of the FC-MARS-double.

N_p	11
N_d	1
N_s	4
F_n	1
F_d	4
F_h	0
h_p	677 km
i	85.8^0
ω_p	303.4^0
Ω_0	334.8^0
M_0	210.7^0

3.2.3.6 Regional Coverage - Single FC parameters

The design parameters of the single FC for regional coverage (named FC-MARS-singleR) are provided in Table 3.10. These design parameters generate the orbital parameters listed in Table 3.11. The ground track and the ground sites are shown in Figure 3.8.

3.2.3.7 Regional Coverage - Double FC parameters

The designed double FC for regional coverage has been named FC-MARS-singleR. The design parameters of the first Flower sub-constellation, optimized for the

3.2 Martian Constellation of Orbiters

Table 3.8: Design parameters for the second sub-constellation of the FC-MARS-double.

N_p	11
N_d	1
N_s	2
F_n	1
F_d	2
F_h	0
h_p	100 km
i	22^0
ω_p	164.5^0
Ω_0	94.4^0
M_0	314^0

Table 3.9: Orbital parameters of the FC-MARS-double.

Sat no.	a (km)	e	i (deg)	ω_p (deg)	$RAAN$ (deg)	TA (deg)
1	4130	0.015	85.8	303.4	334.8	209.8
2	4130	0.015	85.8	303.4	64.8	299.2
3	4130	0.015	85.8	303.4	154.8	31.6
4	4130	0.015	85.8	303.4	244.8	122.2
5	4130	0.154	22	164.5	94.4	299.45
6	4130	0.154	22	164.5	274.4	145.2

coverage of the polar regions, are provided in Table 3.12. The first step of the optimization process for the equatorial region resulted in a satellite with an inclination close to 0^0 . The design of a FC of two satellites with an inclination close to 0^0 results in a couple of satellites positioned always close to each other, and hence, with an overlapping of coverage that is not needed. Thus, we have chosen to space the satellites of 180^0 . In conclusion, the second sub-constellation is not

3.2 Martian Constellation of Orbiters

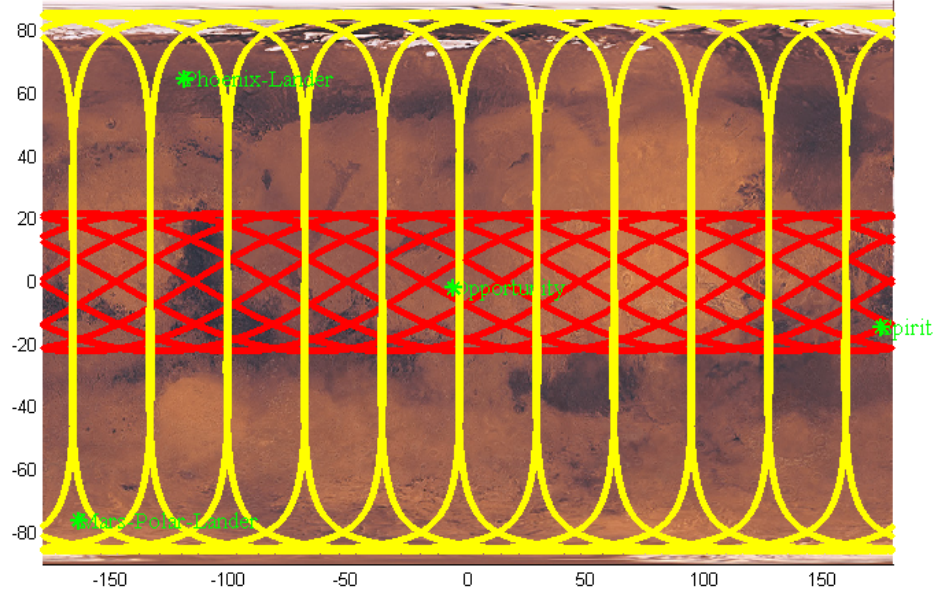


Figure 3.7: Ground track of the FC-MARS-double.

Table 3.10: Design parameters of the FC-MARS-singleR.

N_p	11
N_d	1
N_s	6
F_n	1
F_d	6
F_h	0
h_p	431 km
i	91°
ω_p	171.1°
Ω_0	159.9°
M_0	190.2°

3.2 Martian Constellation of Orbiters

Table 3.11: Orbital parameters of the FC-MARS-singleR.

Sat no.	a (km)	e	i (deg)	ω_p (deg)	$RAAN$ (deg)	TA (deg)
1	4130	0.07	91	171.1	159.9	188.8
2	4130	0.07	91	171.1	219.9	242.4
3	4130	0.07	91	171.1	279.9	303.2
4	4130	0.07	91	171.1	339.9	11.8
5	4130	0.07	91	171.1	38.9	78.5
6	4130	0.07	91	171.1	98.9	136.3

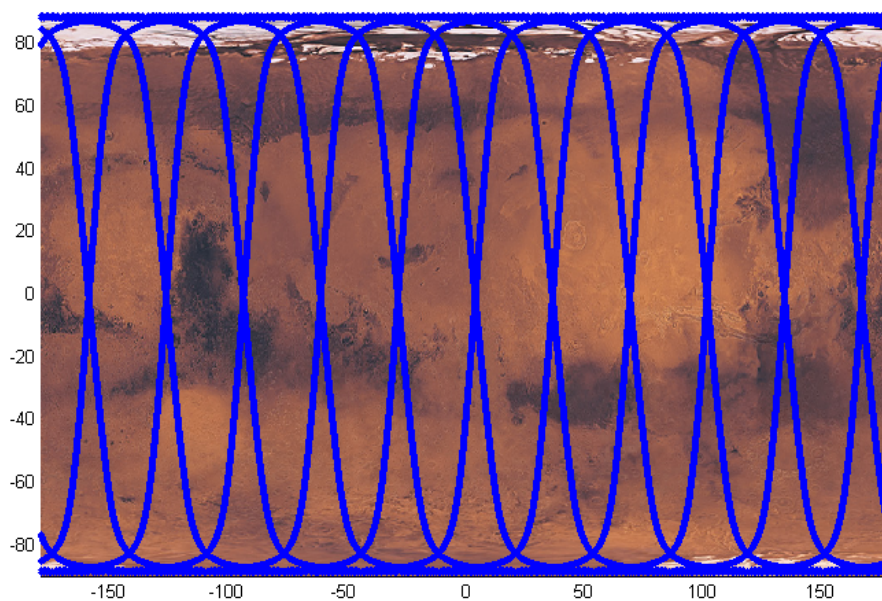


Figure 3.8: Ground track of the FC-MARS-singleR.

exactly an FC, but a constellation of two satellites with repeating ground of the same period N_d . All the parameters of these two satellites are the same, while the RAAN is opposite. The orbital parameters of the final constellation are listed

3.2 Martian Constellation of Orbiters

in Table 3.13. The ground track and the ground sites are shown in Figure 3.9.

Table 3.12: Design parameters for the first sub-constellation of the FC-MARS-doubleR.

N_p	11
N_d	1
N_s	4
F_n	1
F_d	4
F_h	0
h_p	661.5 km
i	88.1^0
ω_p	313.7^0
Ω_0	342^0
M_0	128.5^0

Table 3.13: Orbital parameters of the FC-MARS-doubleR.

Sat no.	a (km)	e	i (deg)	ω_p (deg)	$RAAN$ (deg)	TA (deg)
1	4130	0.017	88.1	313.7	342	130
2	4130	0.017	88.1	313.7	72	217
3	4130	0.017	88.1	313.7	162	306
4	4130	0.017	88.1	313.7	252	39
5	4130	0.017	49.2	49.2	235.1	330.8
6	4130	0.017	49.2	49.2	55.1	330.8

3.2.4 Performance Comparison

In Table 11, the performance comparison results for spot coverage are summarized.

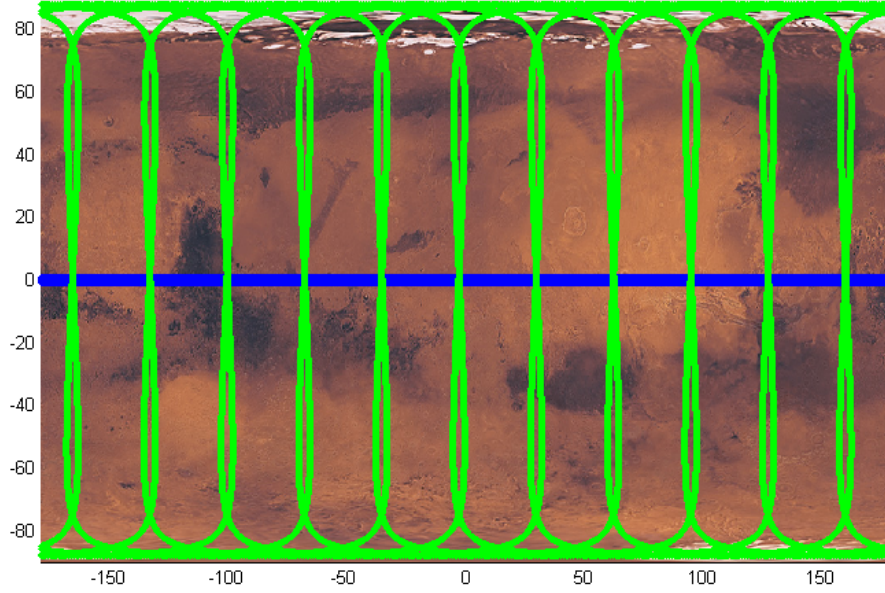


Figure 3.9: Ground track of the FC-MARS-doubleR.

With respect to the coverage percentage metric, the best performance for Opportunity site is achieved with the 4retro111 constellation even if for all the other sites FC constellations provide better results. In particular the FC-MARS-single is the best choice for Polar Lander site, while FC-MARS-double is the best one for both Phoenix Lander and Spirit sites. When looking at the overall mean access time performance, it can be stated that the best performance is achieved with FC-MARS-single and FC-MARS-double constellations, giving a mean value of 846 and 758 seconds respectively, while 4retro111 has a mean value of 548 seconds. Considering the third metric, average gap time, the Table shows that the best global performance is provided by FC-MARS-double, having a mean value of 3623 seconds; while 4retro111 and FC-MARS-single have a mean value of 4394 and 4812 seconds (even if the low performance of this last FC is caused by the high average gap time experienced by the Opportunity site). In Table 3.15, the performance comparison results obtained for regional coverage are shown.

3.2 Martian Constellation of Orbiters

Table 3.14: Performance comparison of the proposed constellation for spot coverage.

Constellation	Site	Coverage	Mean Access Time (s)	Average Gap Time (s)
4retro111	Opportunity	19.4	566	2365
	Phoenix L.	13.7	629	4746
	Polar L.	9.3	515	5485
	Spirit	11.3	482	4982
FC-MARS-single	Opportunity	9.6	759	11895
	Phoenix L.	16.3	485.5	2283
	Polar L.	68.65	907	165
	Spirit	18	1296	4908
FC-MARS-double	Opportunity	16.9	993	7299
	Phoenix L.	22.3	689	2116
	Polar L.	33.2	662	922
	Spirit	21.6	691	4156

For what concerns regional coverage, the best coverage percentage are given by FCs, in particular FC-MARS-singleR provides the higher coverage for polar areas, while FC-MARS-doubleR provides the best performance for the equatorial belt and also high performance for polar sites. Also considering mean access time, performance of FCs are higher with respect to 4retro111 for both polar and equatorial regions. Regarding average gap time 4retro111 and FC-MARS-doubleR provide comparable performance for equatorial region, while FC-MARS-singleR one is not quite as good; even if for polar regions this last FC offers the lowest values of gap time. Considering overall performance metrics, FC-MARS-doubleR is certainly the best choice.

3.2.5 Conclusions

The paper analyzed and proposed a constellation of martian orbiters aimed to communication services to landed elements (e.g. rovers, landers, probes) located

3.3 Interferometric Imaging

Table 3.15: Performance comparison of the proposed constellation for regional coverage.

Constellation	Site	Coverage	Mean Access Time (s)	Average Gap Time (s)
4retro111	Equator	19.7	726	2887
	North Pole	15.8	633	3961
	South Pole	15.8	633	3961
FC-MARS-singleR	Equator	10.8	780	8598
	North Pole	56.5	805	242
	South Pole	64.6	805	242
FC-MARS-doubleR	Equator	20.6	749	2762
	North Pole	43.9	807	731
	South Pole	38	807	731

on areas with scientific interest. We designed optimized FCs providing high access duration and low gap duration. The optimization of the FCs has been performed for spot coverage and regional coverage. It has been found that our proposed FCs provide better performance with respect to the reference constellation 4retro111 in terms of coverage %, mean access time and average gap duration.

3.3 Interferometric Imaging

3.3.1 Introduction

Nowadays the search of planets in other solar systems is still at a beginning stage. The first celestial body with a mass comparable with the Jupiter's one was founded in 1995 by Mayor and Queloz, and from that time many space missions have been planned to detect stars with Earth-like orbiting planets.

The possibility of using multiple satellites for interferometric imaging systems has gained interest in the last years. There are many projects based on space-based interferometry imaging technology, but they are still at the preliminary design phase. Among these we can mention:

- *SIM* (NASA): Space Interferometry Mission.

This is the only space project at advanced stage progress. It is planned to observe far stars with a resolution of micro-arcsecond in order to find extra-solar planets.

- *TPF* (NASA): Terrestrial Planet Finder.

Its primary science driver is imaging terrestrial planets involving visible light coronagraph and an infrared large-baseline interferometer with 5 satellites, rigidly connected. This mission will study all aspects of planets outside our solar system.

- *IRSI-Darwin* (ESA): Infra-Red Space Interferometer.

This is the European version of the TPF mission. It is planned to have free-flyer architecture, with separate spacecraft for every telescope.

3.3.2 Optical Interferometric Imaging

The resolution of a telescope depends on the diameter of its mirror. The larger the mirror, the better resolution one can achieve. But the idea to build a telescope larger than few kilometers is impracticable. Progress in high angular resolution astronomy can be obtained using different small telescopes to produce a resolution equal to that provided by one with the diameter equal to the maximum inter-telescopes distance. This can be obtained working with interferometry. Interferometry measures the interference of an electromagnetic field. Optical interferometry collects two or more light beams arriving from different observation points and then coherently combines them to make an interference pattern. It is limited to visible and infrared wavelengths. The physics is the same regarding the Young's double slit experiment where the star is the light source, the telescopes are the slits and the separation of the slits is the baseline.

If the telescopes are spread out over a large area it is possible to measure very small objects. For imaging planets in other solar systems, the distance between satellites has to be in the order of thousands of kilometers. For an Earth-ground based interferometric system, the atmosphere perturbation represents one of the major issue for interferometry imaging. The atmosphere presence causes losing

3.3 Interferometric Imaging

in light coherence and consequently it limits the brightness the objects can be observed. For this reason space is an ideal place for interferometry.

Images of planetary systems are reconstructed through different measurements taken in successive instants time. While moving relative to each other, the spacecrafts' configuration changes with time and this creates different projections of the baseline onto a plane perpendicular to the line of sight to the star. Measurements are collected, transmitted, and then Fourier transformed in a two dimensional plane of spatial frequencies called the Fourier plane or the “ $u-v$ ” plane. For every point in this plane there is a symmetrical one respect to the origin. The challenge is to obtain a wide variety of baseline's lengths and orientations for covering the “ $u-v$ ” plane in an optimal way.

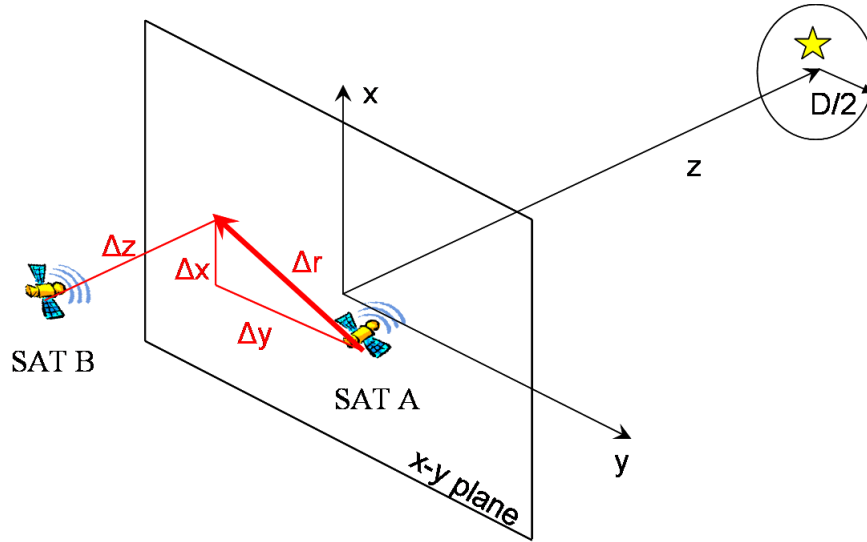


Figure 3.10: Spatial physical plane

Referring to Fig. 3.10 let Δr be the projection of the baseline between satellites A and B onto a “ $x-y$ ” plane that is perpendicular to the line of sight of the star, and Δx and Δy , be the components of Δr on the observation plane. Let \vec{z} be the distance from the image plane to the observation plane. Finally, let D be the diameter of the region to observe, defined as

$$D = 1.22 \frac{\lambda z}{a} \quad (3.3)$$

3.3 Interferometric Imaging

where λ is the wavelength and a is the resolution desired.

The scaled projection of the baseline in the plane perpendicular to the observation direction gives the information on the frequency

$$\left(\frac{\Delta x}{\lambda z}, \frac{\Delta y}{\lambda z} \right) = (\Delta u, \Delta v) \quad (3.4)$$

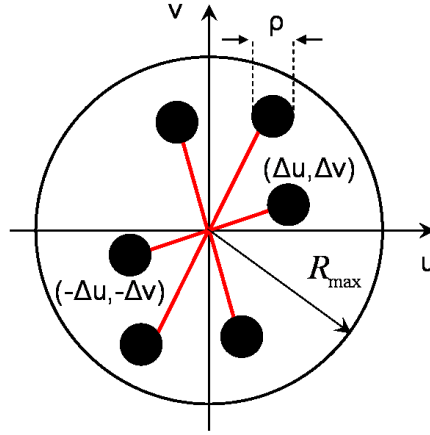


Figure 3.11: Spatial frequency plane

Figure 3.11 shows the spatial frequency plane and how it is covered. The maximum radius of the resolution disk is defined as

$$R_{max} = \frac{1.22}{a} \quad (3.5)$$

and every point covers the Fourier plane with a sphere of diameter

$$\rho = \frac{2R_{max}}{N} \quad (3.6)$$

where N is the number of pixels desired.

The interferometric measurements are made between pair of telescopes and so more satellites are used, more measurements are collected simultaneously. We desired only the set of measurements $(u, v) : \sqrt{u^2 + v^2} \leq R_{max}$. For an optimal coverage we are interested in having the resolution disk completely painted by the balls with the smaller number of spacecrafts. Every point covered in the Fourier plane can then be related to a pixel. The filled fraction of the pixels plane indicates the quality of the resulting image.

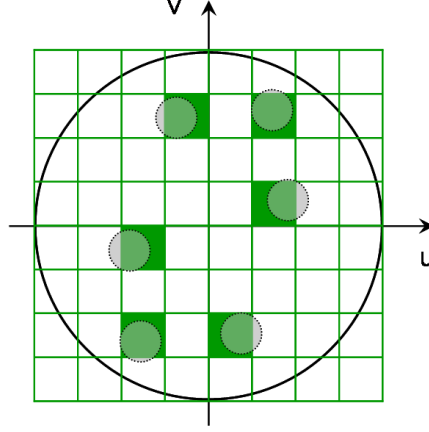


Figure 3.12: Pixels plane

3.3.3 Flower Constellations for Interferometry

This work contains a preliminary study on how to design Flower Constellations to interferometric imaging missions. Imaging far stars can require baseline like the Earth diameter, so a wide formation of satellites, instead of a Formation Flying, can be a right choice. Referring to the NASA TPF mission we consider 5 satellites but free-flying. The Flower Constellation design parameters are:

- Orbital period: $90 \text{ min} \leq T \leq 300 \text{ min}$
from T we can choose N_d and N_p relative prime
- Perigee altitude: $300 \text{ km} \leq h_p \leq h_{p_{circular}}$
from T we can compute the semi-major axis and the maximum h_p related to a circular orbit
- Phasing numerator: $F_n \leq N_d$
- Phasing denominator: $1 \leq F_d \leq 100$
- Phasing step: $0 \leq F_n \leq N_d - 1$
- Orbital inclination: $0 \leq i \leq \pi$
- Perigee argument: $0 \leq \omega \leq 2\pi$

- Constellation colatitude: $0 \leq \lambda \leq \pi$
- Constellation azimuth: $0 \leq \psi \leq 2\pi$

3.3.4 Numerical Optimization Results

The goal of this section is to find the Flower Constellation parameters for the optimal coverage of the “ u - v ” plane. Consider to observe a star distant 30 parsec from the Earth, at the wavelength of $\lambda = 500$ nm (visible light), with a resolution of $a = 800$ km, with two different pixels value of 10×10 pixels first and 12×12 pixels later. The following subsections provide the results obtained using two different optimization algorithms, namely, the *Genetic Algorithm* and the *Particle Swarm Optimization*.

FC Parameters	GA, $N = 10$	PSO, $N = 10$	GA, $N = 12$	PSO, $N = 12$
N_p	32	95	65	41
N_d	3	12	6	4
F_n	2	1	1	7
F_d	63	50	33	95
F_h	2	10	4	1
i	7.3°	64.3°	78.6°	66.7°
ω	174.8°	307.1°	268.4°	212.1°
λ	21.5°	25.8°	60.9°	55.9°
ψ	332°	301.3°	38.2°	114.2°

Table 3.16: FC parameters

Both the optimization algorithms have reached very good solutions with a coverage percentage of almost 100% with different Flower Constellation parameters.

From the 12×12 pixel test case results it is clear that the coverage percentage decreases by increasing the number of pixels, while maintaining the same number of satellites. In this case the Genetic Algorithm seems to provide better results than the Particle Swarm Optimization. In fact the resolution disk is covered at 87.87% with the GA and at 83.33% with the PSO.

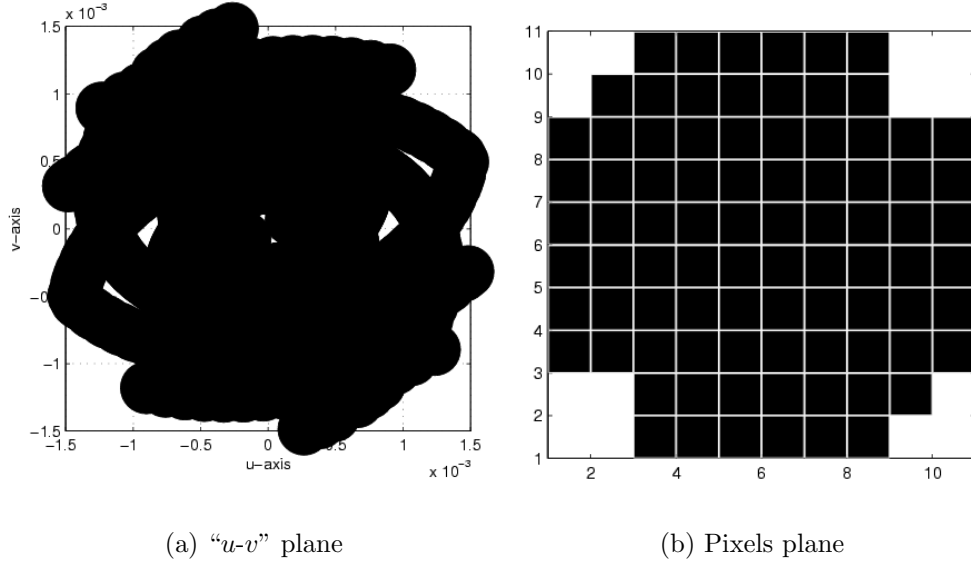


Figure 3.13: Genetic Algorithm for 10×10 pixels: Coverage = 97.72%

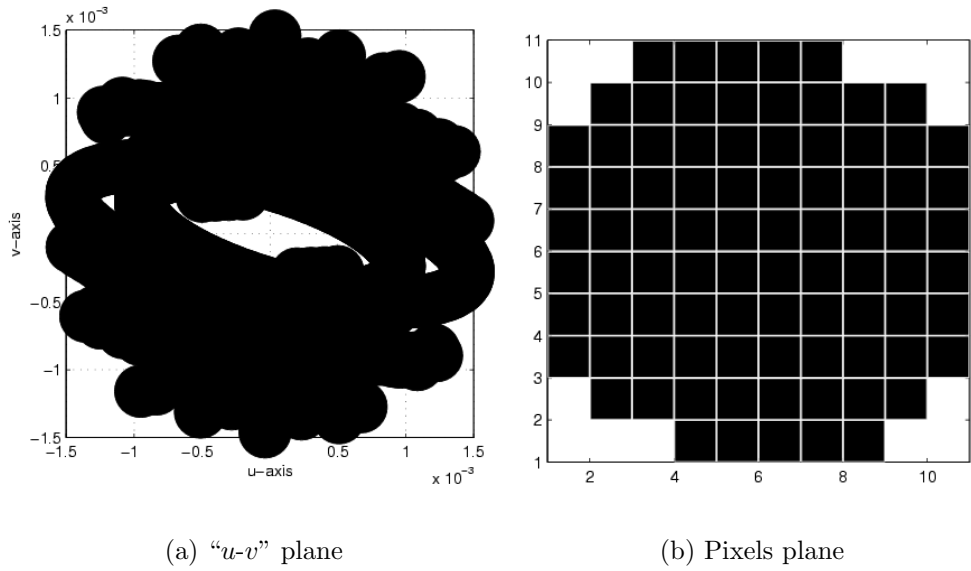


Figure 3.14: Particle Swarm Optimization for 10×10 pixels: Coverage = 97.72%

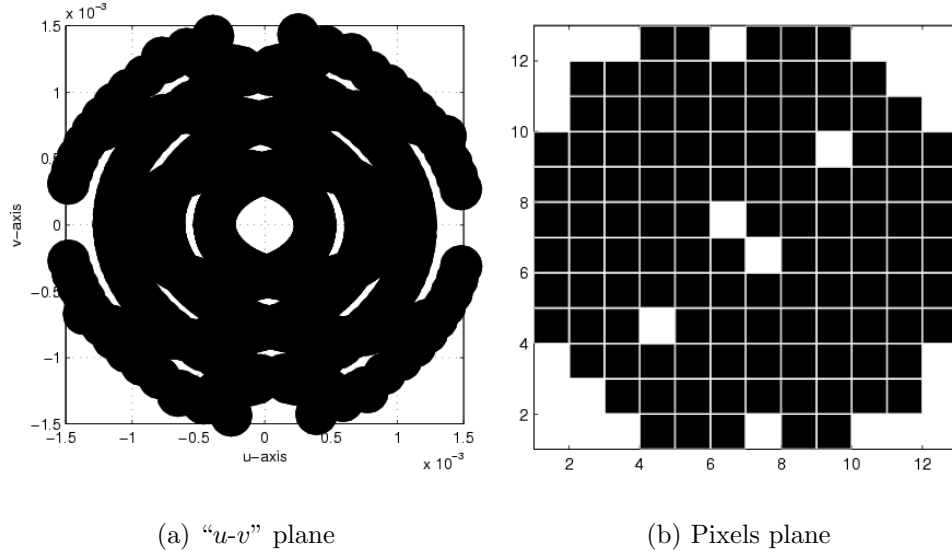


Figure 3.15: Genetic Algorithm for 12×12 pixels: Coverage = 87.87%

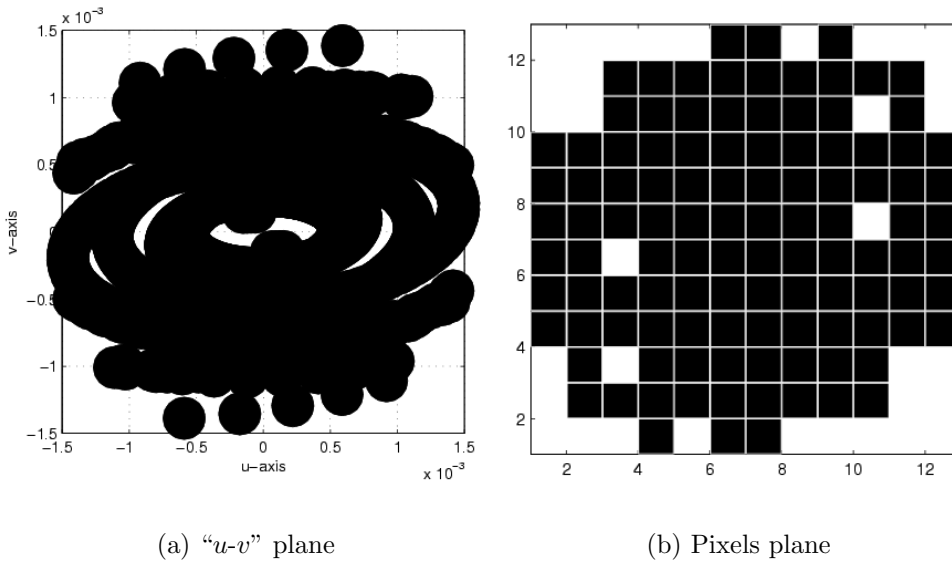


Figure 3.16: Particle Swarm Optimization for 12×12 pixels: Coverage = 83.33%

3.4 Global Navigation Services

The GalileoSat constellation of the European Commission (EC) and the European Space Agency (ESA) will place 27 satellites in 3 circular orbit planes. For navigation purposes, at least 4 satellites should be in view at any time and place on the Earth. However, the effect of trees, mountains, and buildings require more satellites in view. Furthermore, 4 satellites may not be sufficient for the optimal navigation information since the geometry of the sightlines affects the navigation performance. The current constellation method such as Walker delta pattern and its modified versions may not satisfy all these requirements.

In [2], new constellations for global navigation system are developed by combining FC design schemes and genetic algorithms. A new constellation was called Global Navigation Flower Constellation (GNFC) and uses the symmetric phasing technique of the FC so that satellites in the constellation are distributed uniformly in its relative path.

In the comparisons in terms of Geometric Dilution of Precision (GDOP) between GalileoSat and GNFC constellations, the GNFC using 27 satellites shows that GDOPs are better in most regions although it shows poor values in small areas. This behaviour cannot be avoided and there will always be regions with poor GDOPs of GNFC with respect to Galileosat. However, by using proper fitness functions, the poor GDOP regions can be placed in the least required regions. This kind of approach is possible because the FC design scheme can use optimisation weights in order to locate poor GDOPs values on less important areas. Furthermore, the results using 26 satellites in the constellation show that the overall GDOPs are lower than those of GalileoSat constellation. This means that the reduction of the number of satellites in the constellation could be obtained by adding appropriate fitness functions to avoid poor GDOPs in most required regions. Therefore, cost and time effectiveness in the deployment of the GalileoSat constellation may certainly take benefit from the above results, in particular accounting for the tight strategic and commercial planning of the Galileo services.

References

- [1] K. Park, M. Wilkins, C. Bruccoleri, D. Mortari, *Uniformly Distributed Flower Constellation Design Study for Global Positioning System*, Paper AAS 04-297 of the 2004 Space Flight Mechanics Meeting Conference, Maui, Hawaii, February 9-13, 2004. [3](#)
- [2] K. Park, M. Ruggieri, D. Mortari, *Comparisons between GalileoSat and Global Navigation Flower Constellations*, 2005 IEEE Aerospace Conference, March 5-12, 2005, Big Sky, Montana. [3](#), [3.4](#)
- [3] T. A. Ely, R. L. Anderson, Y. E. Bar-Sever, D. J. Bell, J. R. Guinn, M. K. Jah, P. H. Kallemeyn, E. D. Levene, L. J. Romans, S. C. Wu, “Mars Network Constellation Design Drivers and Strategies”, AAS/AIAA Astrodynamics Specialist Conference Paper AAS 99-301, Girdwood, Alaska, August 16-18, 1999. [3.2](#), [3.2.1.1](#)
- [4] R. J. Cesarone, R. C. Hastrup, D. J. Bell, D. T. Lyons, K. G. Nelson, “Architectural Design for a Mars Communications and Navigation Orbital Infrastructure”, paper no. AAS 99-300, AAS/AIAA Astrodynamics Specialist Conference, Girdwood, Alaska, August 16-18, 1999. [3.2.1.1](#)
- [5] D. J. Bell, T. Ely, “Constellation Design of the Mars Network, A System for Communications and Navigation at Mars”, Deep Space Communications and Navigation Systems Symposium, Pasadena CA, September 21-23, 1999. [3.2.1.1](#)
- [6] R. C. Hastrup, R. J. Cesarone, D. D. Morabito, J. M. Srinivasan, “Mars Comm/Nav MicroSat Network,” 13th Annual AIMUSU Conference on Small Satellites, paper SSC 99-VII-5, Logan, Utah, August 23-26, 1999.
- [7] Mortari, D., Wilkins, M.P., and Bruccoleri, C. “The Flower Constellations”, The Journal of the Astronautical Sciences, Special Issue: The John L. Junkins Astrodynamics Symposium, Vol. 52, Nos. 1 and 2, January-June 2004, pp. 107-127.

BIBLIOGRAPHY

- [8] Wilkins, M., Bruccoleri, C., and Mortari, D. “Constellation Design Using Flower Constellations”, Paper AAS 04-208 of the 2004 Space Flight Mechanics Meeting Conference, Maui, Hawaii, February 9-13, 2004.
- [9] Mortari, D. and Wilkins, M.P. “The Flower Constellation Set Theory. Part I: Compatibility and Phasing”, Submitted to the IEEE Transactions on Aerospace and Electronic Systems.
- [10] Wilkins, M.P. and Mortari, D. “The Flower Constellation Set Theory. Part II: Secondary Paths and Equivalency”, Submitted to the IEEE Transactions on Aerospace and Electronic Systems.
- [11] D.E. Goldberg, “Genetic Algorithm in Search, Optimization and Machine Learning”, Addison Wesley, 1989. [3.2.3](#)

Chapter 4

Feasibility

4.1 Control and Maintenance

4.1.1 Orbital Perturbations

Satellite constellations represent a mandatory solution in any case in which we need to monitor and to offer a coverage spread to wide Earth regions for long periods of time. The choice of the constellation type is application dependent. Usually, the main choice is between circular and elliptical orbits, the first one being best suitable to uniform coverage and the second one to specific regional coverage.

However, whatever solution is adopted, we need to manage the complexity of a system composed of many satellites with all the problems related to, as launching of a significant number of satellites, distributing them in the right position, controlling and maintaining the set for all the lifespan, providing the disposal at the end of life and so on. Specifically, the control and the maintenance of the constellation represents a challenging item because of dealing with managing and monitoring a high number of satellites. But especially because the adopted strategy is strictly related to the overall costs of the constellation. Therefore it is particularly important to identify advantages and disadvantages of a satellite constellation with regard to the control and the maintenance in order to find out control elements of costs.

If satellites were subjected only to the gravitational field generated by a spherically symmetrical Earth, a constellation would keep its pattern for all the lifespan

without the need of intervention from the ground station. Unfortunately, our planet, even if has spherical-like shape, presents various drifts as a flattening of poles and equator and a non-uniform distribution of mass. In addition, the Earth is influenced by the gravitational field of other bodies, especially Sun and Moon; the first one because of the huge mass and the second one because of the relatively low distance. Other effects can be considered, mainly for some low altitude orbits, as the presence of atmosphere, which causes a slowing of the satellite with orbital decaying; the solar radiation pressure, which modifies the orbital eccentricity, can be also considered for higher orbits. This implies that the Kepler laws are not accurate enough in order to obtain the motion of satellites. Actually, Kepler laws allow to determine the orbit by means of the six orbital elements, time fixed (osculating elements): semimajor axis, eccentricity, inclination, right ascension of the ascending node, argument of perigee, mean anomaly.

The presence of additive effects, previously mentioned, adds perturbations to the orbital elements, causing time variations. These perturbations appear as short/long period variations (with respect to the orbital period) and secular variations (which increase or decrease with time) in the orbital elements.

When the satellites are more than one, the perturbations effect must be seriously taken into account because affect not only single satellites but also the structure and the shape of the initial constellation, causing a performance degradation with respect to the provided application.

To keep the pattern of a constellation over a long time is a difficult task and the efficiency of accomplish this is strictly related to the overall costs. Usually, control and maintenance of a constellation requires knowledge and control of each satellite but also control of each satellite with respect to the others. Specifically, constellations require a suitable control and maintenance to prevent collisions between satellites and to keep the constellation pattern over lifespan through in-track and cross-track station-keeping to overcome the perturbations effect. The station-keeping can be relative when relative positions between satellites are maintained but not their absolute positions (approach more complex and without propellant saving). Otherwise, absolute stationkeeping can be applied through fixing each satellite within a “box” rotating with the constellation pattern; it minimises the propellant usage.

Figure 4.1 shows the main cost drivers in constellation design. They include

Items	Drivers		
Satellite	Antenna size / Nr of beams	Power requirement	Nr of sat
Launch	Altitude	Orbit type	-
Gnd system	Nr of GWs	-	-
Operation costs	Constellation maintenance	Constellation management	-

Figure 4.1: Satellite constellations cost drivers.

costs related to satellites, as their number, antenna sizes/ number of beams and power requirements; to the launch, as the operative altitude (LEO, GEO, HEO, etc.) and the orbit shape; to the ground system, as the number of gateways. All these items contribute to the overall cost and with regard to this list, the launch item is particularly commanding.

However, in case of high number of satellites, the operation costs especially demand attention. Such an item foresees elements as constellation maintenance and management, which include all the phases related to the on orbit maintenance of the satellites (phasing, correction manoeuvres, station-keeping, etc.) and their management from the ground stations. To this scope, it needs to take into account the perturbations effect on the satellites in order to establish a fuel consumption budget devoted to correct them.

4.1.2 Perturbations in Flower and Walker Constellations

The study, previously described in the report, has provided two examples of Flower and Walker for the application of telemedicine. Two kind of constellations have been developed for this application. The first one is a Walker constellation and the second one is a Flower constellation. Both have been realised so that a suitable comparison were possible between them (as same number of satellites and same mean height, etc.).

The Walker constellation is a classical constellation characterised by an intrinsic symmetry due to the methodology of designing. It not provides repeating ground track but the ground track covers all the longitudes with the flowing of time. These items make a Walker suitable to offer uniform coverage. The FC is a particular type among the possible infinite FC's sets, anyway all of them are characterised by having repeating ground track. Specifically, all the satellites follow the same relative trajectory (repeating space track or compatible orbits). These relative trajectories constitute a continuous, closed-loop, symmetric pattern of flower petals.

The use of elliptical orbits allows special coverage over specific regions, however the choice of a particular FC and the properly phasing scheme permits to obtain an optimised and uniform coverage.

Usually, control and maintenance of satellites is expressed in terms of ΔV , that is the required velocity change to be applied to compensate for drifts in order to "fix" the satellite in the foreseen position (on the basis of the operation requirements). In general, a ΔV budget, sum of the velocity changes required during all the constellation lifespan, is calculated to take into account the fuel consumption due to orbit transfer, station-keeping, orbit manoeuvres, re-phasing, plane change, disposal at end of life and so on. This quantity, being directly related to fuel consumption and hence to the cost, allows to evaluate the influence of the control and maintenance over the overall cost.

The approach here used has been to evaluate how the perturbations affect both the constellations developed for the telemedicine (Flower and Walker) and to quantify their effect. The analysis carried out is illustrated in the next paragraphs.

The study is based on the Satellite Tool Kit (STK) software, the most used tool in orbital mechanics for the design and analysis of satellites and constellations. Considering the constellations designed for telemedicine (already compared in coverage performance), both have been analysed with regard to the perturbations effect. At first, only perturbations induced by the J_2 effect have been considered. Afterwards, the third-body perturbation (Sun and Moon) and the atmospheric drag have been added. In this way, we highlighted which parameters affect mostly these special Flower and Walker configuration from the point of view of control and maintenance. Considerations about general Flower and Walker constellations will be also reported.

The metrics used to compare the perturbations affection on the constellations has been the estimate of the keplerian orbital elements drift, evaluating the variation on a fixed time period (one month and one year). Obviously, the parameters of the constellations are different but expressly designed to offer the best performance for the telemedicine application. Therefore, considering the constellations from the application point of view, we want to highlight in this task which is their behaviour with respect to the perturbations effect.

The orbital parameters of Flower and Walker constellations employed for telemedicine are shown in figures 4.2 and 4.3.

Considering the altitude of satellites, changing from 3000 km at the perigee to 9700 km at the apogee for the FC and equals to 6800 km for the Walker, both constellations are affected mostly by the perturbations due to the J_2 effect, the value of which is three orders of magnitude higher than the following geopotential coefficients; it is also dominant with respect to the other effects (mentioned in previous subsection) because of the major proximity of the Earth. The J_2 effect produces secular variations in three orbital elements, the argument of perigee (ω), the right ascension of the ascending node (Ω), the mean anomaly (M):

$$\frac{d\omega}{dt} = \frac{3}{4}nJ_2 \left(\frac{R}{a}\right)^2 \frac{4 - 5\sin^2 i}{(1 - e^2)^2} \quad (4.1)$$

Orbital Elements\ # Flower Sat	a (km)	e	i (degrees)	Ω (degrees)	ω (degrees)	M (degrees)
1	12769.6	0.2588	116.6	243.77	187.07	168.00
2	12769.6	0.2588	116.6	288.77	187.07	258.00
3	12769.6	0.2588	116.6	333.77	187.07	348.00
4	12769.6	0.2588	116.6	18.77	187.07	78.00
5	12769.6	0.2588	116.6	63.77	187.07	168.00
6	12769.6	0.2588	116.6	108.77	187.07	258.00
7	12769.6	0.2588	116.6	153.77	187.07	348.00
8	12769.6	0.2588	116.6	198.77	187.07	78.00

Figure 4.2: Orbital elements of telemedicine FC.

$$\frac{d\Omega}{dt} = -\frac{3}{2}nJ_2 \left(\frac{R}{a}\right)^2 \frac{\cos i}{(1-e^2)^2} \quad (4.2)$$

$$\frac{dM}{dt} = -\frac{3}{4}nJ_2 \left(\frac{R}{a}\right)^2 \sqrt{1-e^2} \frac{3\sin^2 i - 2}{(1-e^2)^2} \quad (4.3)$$

where a , e and i define semimajor axis, eccentricity, inclination of the orbit while n , R and J_2 indicate mean motion, Earth equatorial radius and geopotential coefficient of second order (flatness).

J₂ Perturbations

First analysis has been carried out with respect to the J_2 perturbations. Both the constellations, Flower and Walker, have been propagated for one month taking into account the effects induced by J_2 . The analysis has been conducted with the software STK (Satellite ToolKit); Astrogator, a powerful tool for space missions analysis, has been used. The propagation has been done using a numerical propagator with J_2 effect and an eighth order Runge-Kutta-Verner integrator with

Orbital Elements\ # Walker Sat	a (km)	e	i (deg)	Ω (deg)	ω (deg)	M (deg)
1	13219.9	0	135.00	0	0	0
2	13219.9	0	135.00	0	0	180
3	13219.9	0	135.00	45	0	135
4	13219.9	0	135.00	45	0	315
5	13219.9	0	135.00	90	0	270
6	13219.9	0	135.00	90	0	90
7	13219.9	0	135.00	135	0	45
8	13219.9	0	135.00	135	0	225

Figure 4.3: Orbital elements of telemedicine Walker constellation.

ninth order error control.

Figures 4.2 and 4.3 show the orbital elements of the constellations.

Figure 4.4 shows the J_2 effect on the ground track of the Flower constellation after one month.

As shown in the Figure, the repeated ground track shifts in time (yellow colour) due to the J_2 effect with respect to that one without perturbations (green colour). This behavior is mainly due to RAAN drift.

Actually, the main effect of the J_2 perturbation on the identified constellations is the progression (because the inclination is higher than 90 degrees) of the right ascension of the ascending node (secular effect).

This means that each orbit plane progresses counterclockwise along the equatorial plane. The variation of RAAN ($\Delta\Omega$) and mean anomaly (ΔM) has been evaluated for both constellations over one month; each satellite of a constellation presents the same effect due to the common value of a, e, i.

Figure 4.5 shows the calculated value and Figure 4.6 the progression over one month. With respect to the chosen configuration, Walker constellation shows a faster increase in RAAN progression with a monthly $\Delta\Omega = 17.04$ degrees versus

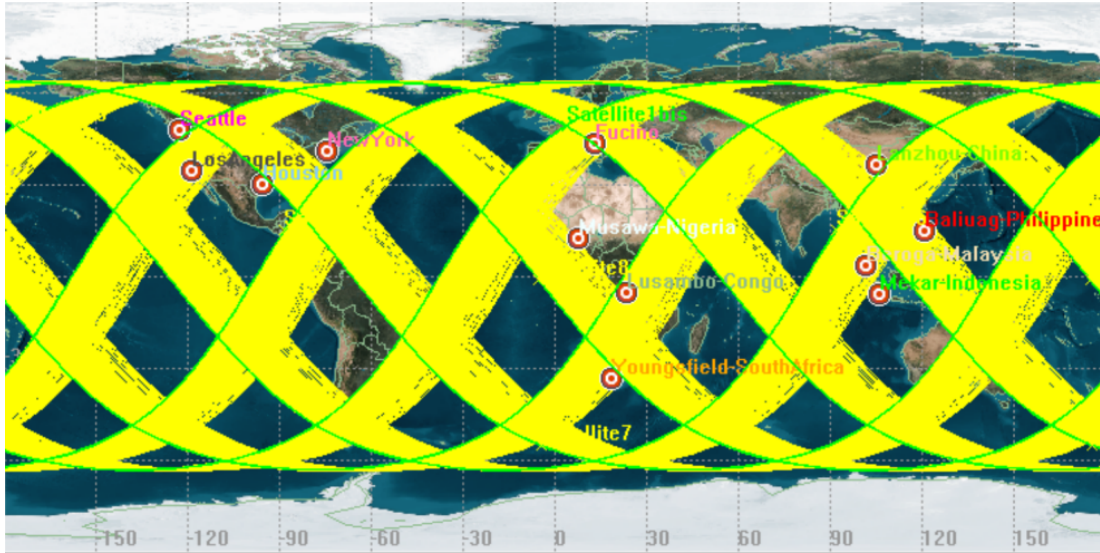


Figure 4.4: Ground track shift of the Flower Constellation over one month.

J_2 effect	$\Delta\Omega$ (deg/month)	ΔM (deg/month)
Flower	13.99	6.02
Walker	17.04	-6.01

Figure 4.5: J_2 effect on RAAN and mean anomaly.

a $\Delta\Omega = 13.99$ degrees for the Flower; however, the drift in mean anomaly is the same but with opposite direction.

Concerning the perigee argument, it is not defined for the Walker (circular orbit)

and is fixed at the critical inclination $i = 116.6$ degrees for the Flower so the drift is nulled. Slight effects are generated on a , e and i through periodic variations

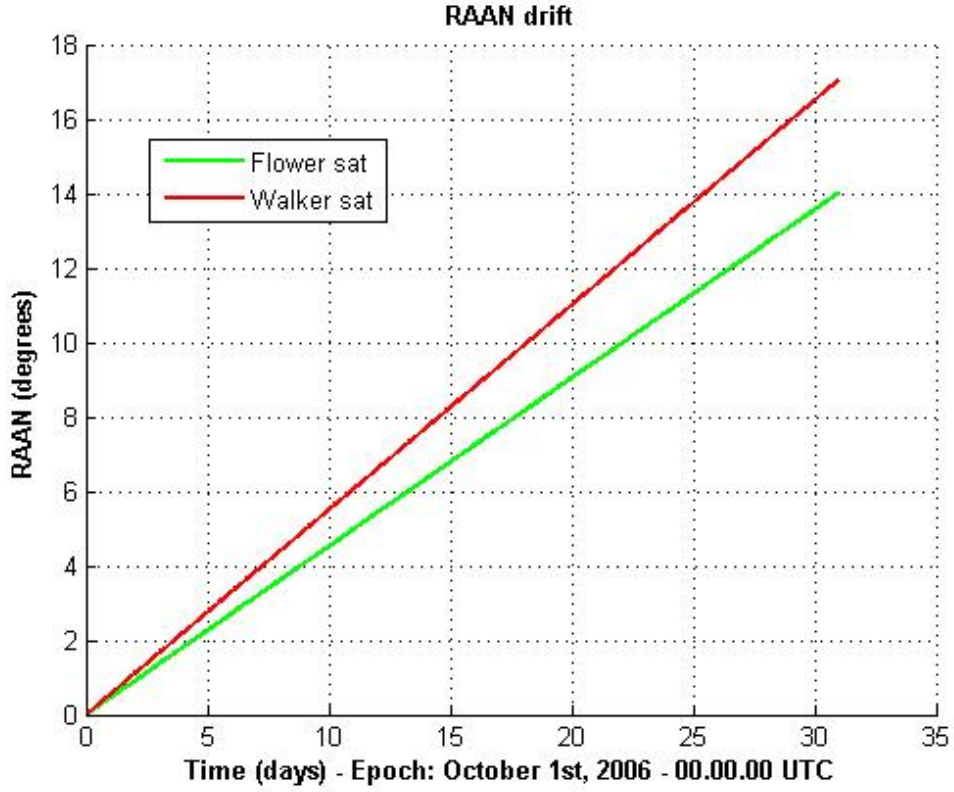


Figure 4.6: RAAN time progression for Flower and Walker constellations.

around a mean value for the Flower constellation.

The same simulation has been carried out taking into account the perturbation induced by the gravitational field of third body, specifically Sun and Moon, and also the atmospheric drag. Nonetheless, the difference with respect to the J_2 effect after a one month propagation is minimum, hence their influence has been evaluated only over long period (one year).

J_2 and 3rd body and drag effects

The following analysis focused on the study of cumulative perturbations affecting

the constellations over a one year period. In particular, gravitational geopotential (until 12^{th} order and degree), Sun and Moon gravitational field and atmospheric drag (using the 1976 Standard Atmospheric Model) have been considered. The STK's Long-term Orbit Predictor (LOP) has been used as propagator due to the fact that it allows accurate prediction of the motion of a satellite's orbit over many months or years. For each constellation the evolution of the six orbital elements has been analysed.

Next paragraphs present the results obtained. Next pages report also plots of the orbital parameters drift of a Flower and Walker constellation respectively over a one year period. Plots for only one satellite for constellation are reported; the behaviour is similar to the other satellites.

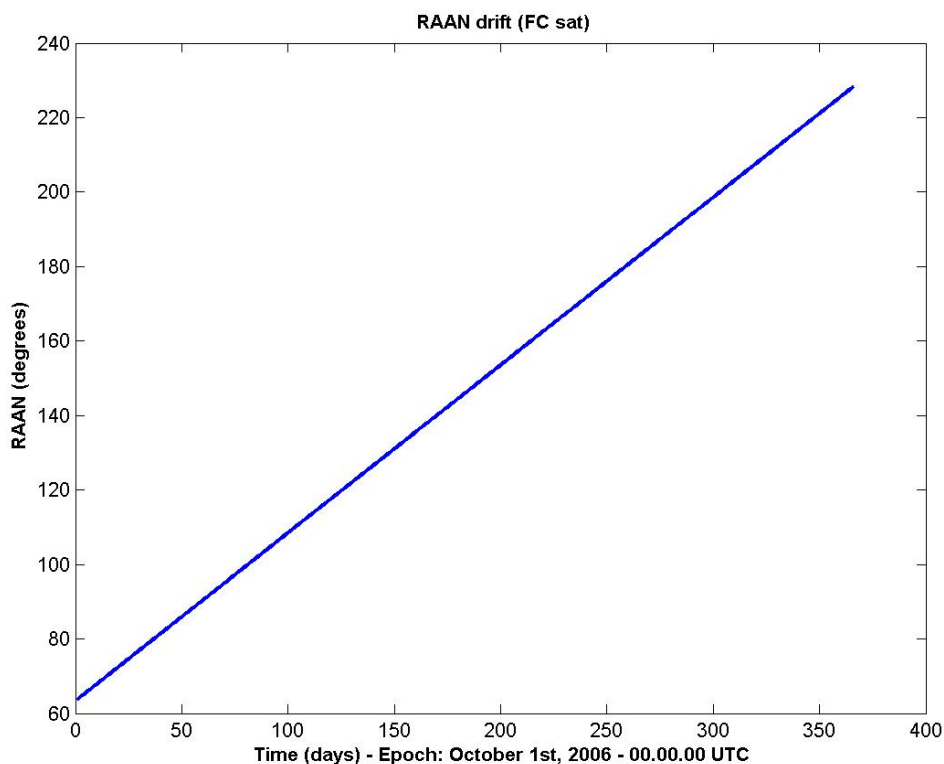


Figure 4.7: RAAN evolution for the Flower satellite.

As highlighted in those figures, the FC RAAN drift increases linearly and is

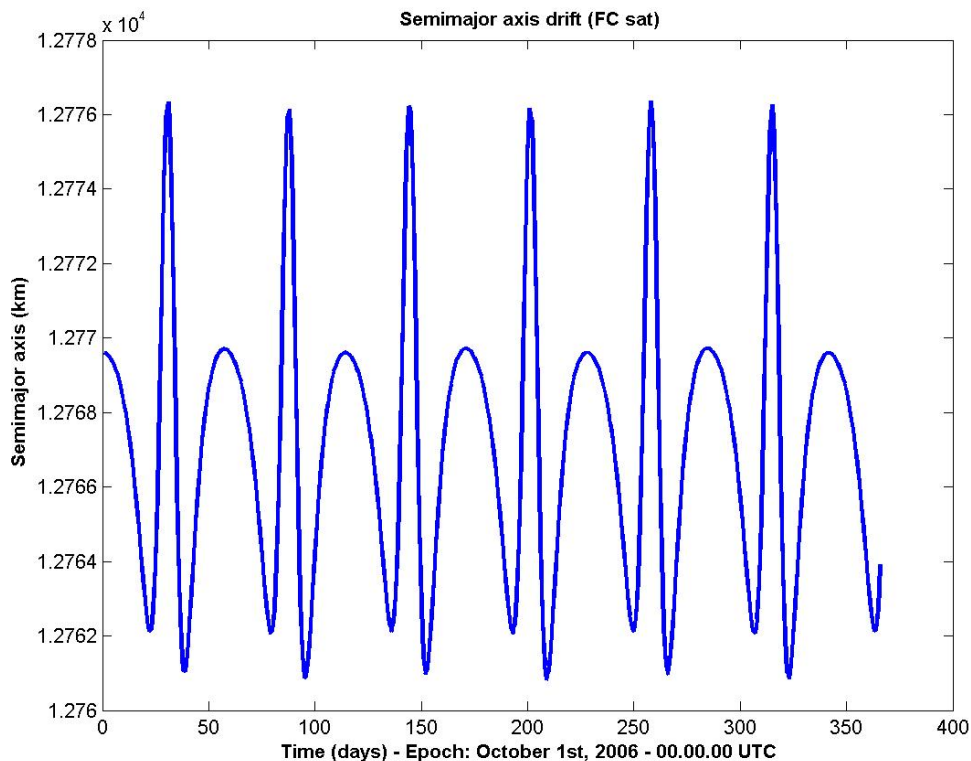


Figure 4.8: Semimajor axis evolution for the Flower satellite.

about 165 degrees for each satellite after one year of propagation. Figure 4.7 shows the drift evolution. On the opposite, the Walker constellation has a faster rise in RAAN with a maximum value of about 200 degrees for each satellite; figure 4.15 shows the drift evolution. The difference is significant and affects the most perturbed element in both the constellations. This means a significant difference in the ΔV budget required to control the constellation configuration. This control must be operated on four orbital planes for the Walker and eight for the Flower; in both cases, the control must be applied on eight satellites.

The semimajor axis (a) of the FC satellite experiences periodic fluctuations (with a period of about 75 days) around a mean value with a variation range of 15 kilometres; figure 4.8 shows the typical pattern of variation. The same element for the Walker changes more rapidly over time than Flower's but with a shorter range,

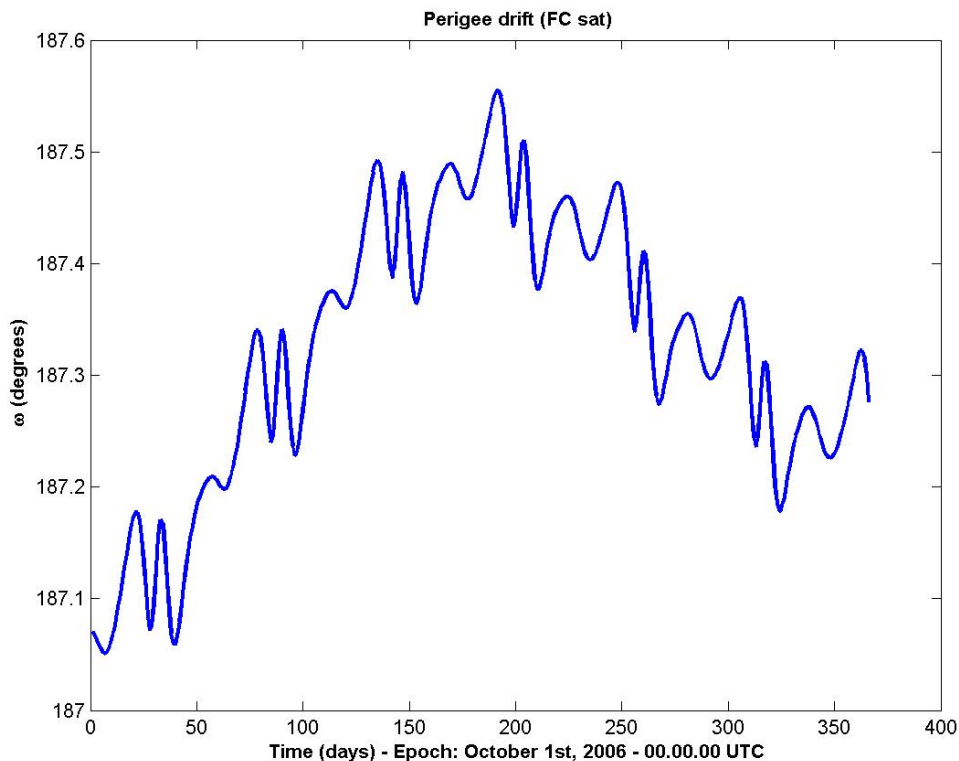


Figure 4.9: Perigee argument evolution for the Flower satellite.

about 5 kilometres (figure 4.16).

With respect to the other parameters (ω , e , i), the Flower satellites show a similar behaviour constituted by an increase or decrease over time along with periodic variations (figures 4.9, 4.10, 4.11). Walker satellites are subjected to similar trend but eccentricity and inclination undergo faster, lower amplitude, shorter-period variations than Flower's (figures 4.17 and 4.18).

For the Flower satellites, the eccentricity is slightly changing with variations of 3×10^{-3} at the peak with respect to a significant orbit eccentricity (0.25878). The inclination undergoes a maximum drift of 0.13 degrees over one year. The inclination of the Flower satellites is fixed at the critical value and hence no rotation of perigee is allowed; however a slight shift is registered because the value nulling the drift in the equation 4.1 is only approximated by 63.4 or 116.6 degrees. Any-

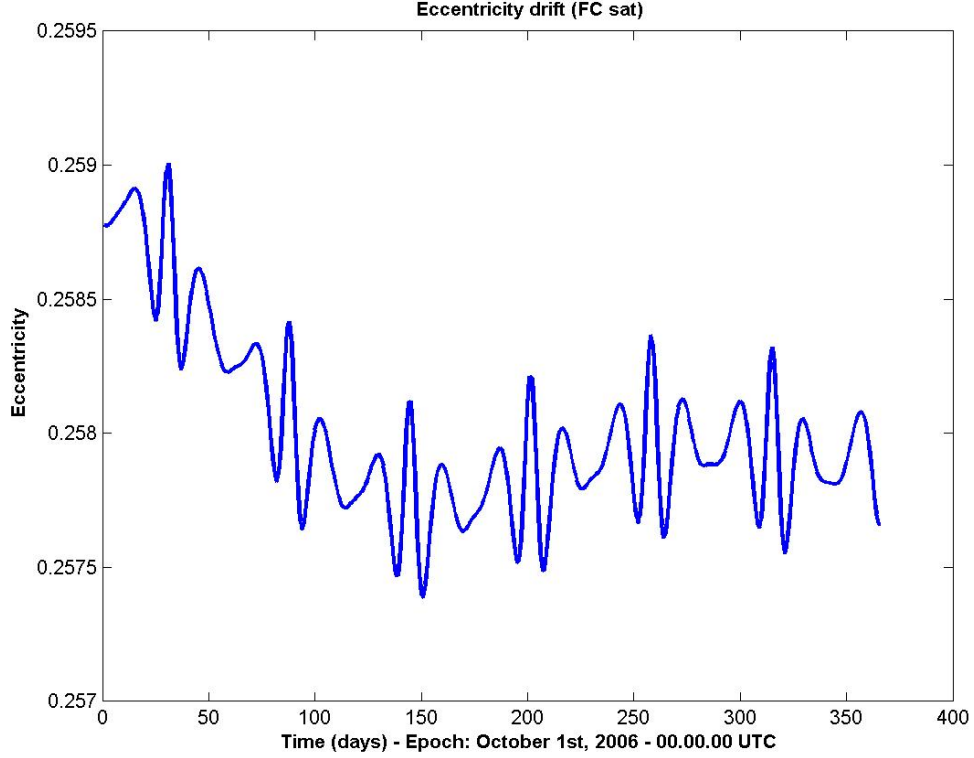


Figure 4.10: Eccentricity evolution for the Flower satellite.

way, the drift obtained is very low and ranging from a minimum of 0.5 deg/year (satellite # 6) to a maximum of 1.8 deg/year (satellite # 1). These values are negligible with respect to the constellation control in terms of ΔV budget. Figure 4.9 shows the evolution of perigee drift over one year.

For the Walker satellites, the eccentricity undergo amplitude variations of the same magnitude order than Flower's, $1 * 10^{-3}$ typically. Also the inclination presents a drift range similar to the Flower's. However, Walker constellation, having only four orbit planes, have only four different drifts because of the inclination drift depends on RAAN.

The total range of variation for each parameter and each satellite is reported in figures 4.13 and 4.14, for the Flower and Walker constellation respectively. These figures report the difference between maximum and minimum values of

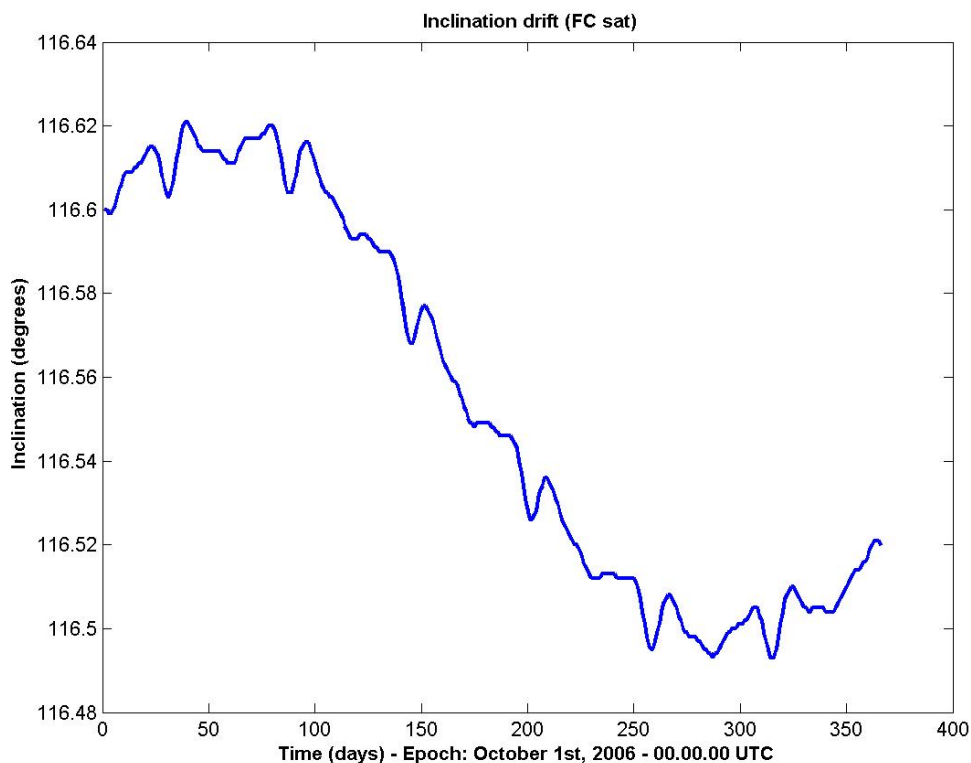


Figure 4.11: Inclination evolution for the Flower satellite.

the orbital elements over one year for the constellations. These differences allow to identify a range in which the orbital elements change over one year period. This range allows to qualitatively evaluate the entity of corrective manoeuvres mandatory for control and maintenance of the constellation configuration.

4.1.3 Control and Maintenance Solutions

The analysed Flower is a particular FC because the inclination is fixed at the critical value $i = 116.6$ degrees. However, Flower constellations generally have not critical inclination and hence it needs to consider the perigee drift. Concerning constellation control and maintenance, the maintenance of the perigee is an important item to be considered. Actually, elliptical orbits with generic inclination are affected by perigee rotation due to perturbations effect. Such a drift is

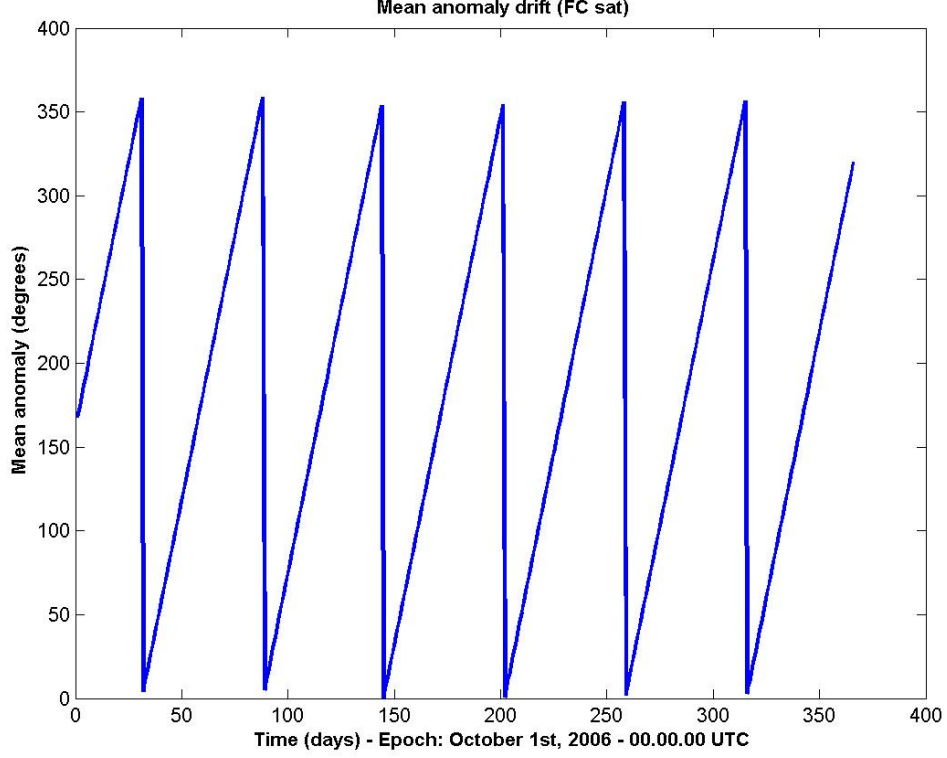


Figure 4.12: Mean anomaly evolution for the Flower satellite.

problematic for applications as telecommunications, for example, requiring the apogee fixed over a specific region of the Earth. A possible solution is to fix the perigee through the constraint of using critical inclination. Otherwise, it needs to properly compensate the drift.

With respect to this, it is possible to illustrate some elements. Equation 4.4 expresses the perigee drift in terms of radial and transverse acceleration, a_r and a_s respectively.

$$\frac{d\omega}{dt} = -\frac{\sqrt{1-e^2} \cos \phi}{nae} a_r + \frac{p \sin \phi}{eh} \left(\frac{2 + e \cos \phi}{1 + e \cos \phi} \right) a_s \quad (4.4)$$

where n, ϕ, p are, respectively, mean motion, true anomaly and $p = a(1 - e^2)$.

Orbital Elements\ # Flower Sat	Δa (km)	Δe	Δi (deg)	$\Delta \Omega$ (deg)	$\Delta \omega$ (deg)
1	15.73	0.003	0.12	165.52	1.79
2	15.72	0.002	0.10	165.10	1.66
3	15.52	0.002	0.08	165.04	1.23
4	15.62	0.002	0.09	164.21	0.48
5	15.55	0.002	0.13	164.50	0.50
6	15.63	0.002	0.07	164.54	0.51
7	15.50	0.003	0.08	165.30	0.94
8	15.80	0.003	0.11	165.11	1.30

Figure 4.13: Differences between maximum and minimum values of the orbital elements over one year for the Flower constellation.

In order to compensate the perigee drift there are two options: tangential thrust at $\phi = 90, 270$ degrees or radial thrust at $\phi = 0, 180$ degrees. In case of tangential thrust, choosing $\phi = 90, 270$ from equation 4.4, we get:

$$\frac{d\omega}{dt} = \frac{p}{eh} \sin \phi \left(\frac{2 + e \cos \phi}{1 + e \cos \phi} \right) a_s \quad (4.5)$$

and afterwards:

$$\Delta \omega_{orbit} = \left(\frac{2\pi}{eh} \right) \Delta V_{orbit} \quad (4.6)$$

Putting this expression equals to the orbit drift:

$$\Delta \omega_{orbit} = -\frac{3\pi J_2}{2} \left(\frac{R}{p} \right)^2 (5 \cos^2 i - 1) \quad (4.7)$$

we get the ΔV required to compensate the drift:

$$\Delta V_{orbit} = - \left(e \sqrt{\frac{\mu}{p}} \right) \left(\frac{3\pi J_2}{4} \right) \left(\frac{R}{p} \right)^2 (5 \cos^2 i - 1) \quad (4.8)$$

Orbital Elements\ # Walker Sat	Δa (km)	Δe	Δi (deg)	$\Delta \Omega$ (deg)*	$\Delta \omega$ (deg)
1	5.02	0.001	0.10	200.87	-
2	5.01	0.001	0.10	200.87	-
3	5.02	0.001	0.14	200.62	-
4	5.01	0.001	0.14	200.62	-
5	5.01	0.001	0.08	200.49	-
6	5.01	0.001	0.08	200.49	-
7	5.00	0.001	0.09	200.74	-
8	5.00	0.001	0.09	200.74	-

Figure 4.14: Differences between maximum and minimum values of the orbital elements over one year for the Walker constellation.

where μ is the Earth gravitational parameter. In this case, the tangential impulse allows to control the perigee with a certain ΔV but at the same time changes semimajor axis and eccentricity. In case of radial thrust, from equation 4.4, we get:

$$\Delta \omega_{orbit} = \left(\frac{1}{e} \sqrt{\frac{p}{\mu}} \right) \Delta V_{orbit} \quad (4.9)$$

then, considering the orbit drift, we get:

$$\Delta V_{orbit} = - \left(e \sqrt{\frac{\mu}{p}} \right) \left(\frac{3\pi J_2}{2} \right) \left(\frac{R}{p} \right)^2 (5 \cos^2 i - 1) \quad (4.10)$$

In this case, the ΔV required for the perigee maintenance is twice that one used for the tangential impulse (equation 4.8) but it has the advantage of not affecting semimajor axis and eccentricity.

On the basis of these considerations, it is useful to introduce a special technique

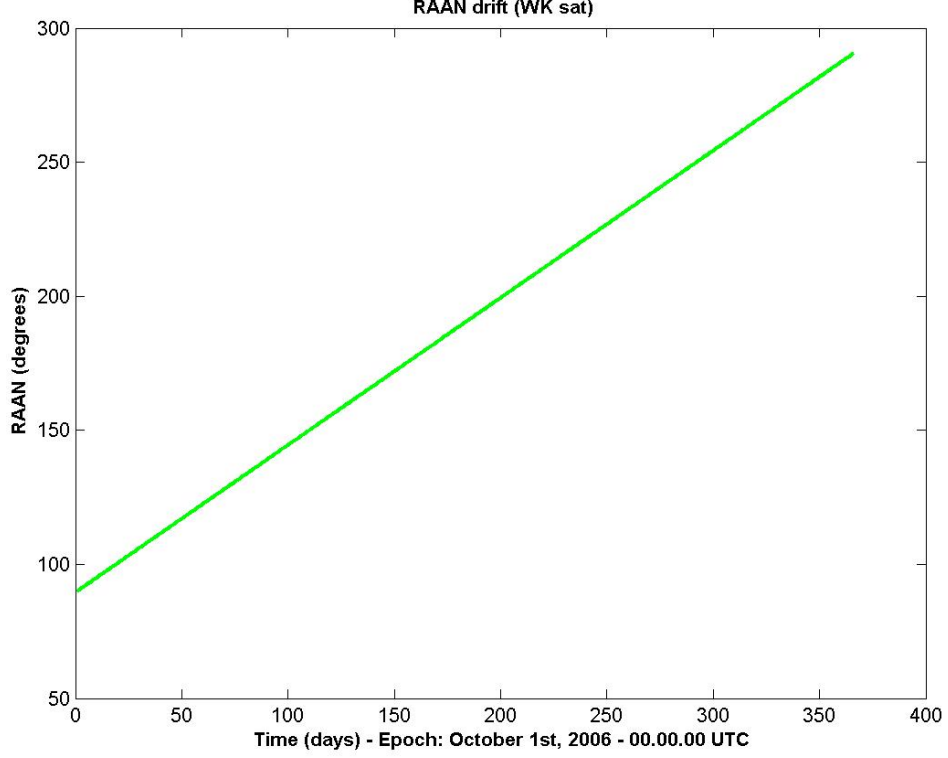


Figure 4.15: RAAN evolution for the Walker satellite.

suitable to perigee maintenance (Ref. Prof. S.R. Vadali and Prof. D. Mortari), the optimal two-impulse perigee maintenance.

The perigee drift expressed in terms of radial and transverse velocity change is (ΔV_r and ΔV_t):

$$\Delta\omega = -\frac{\cos\phi}{e}\Delta V_r + \frac{\sin\phi(2 + e\cos\phi)}{e(1 + e\cos\phi)}\Delta V_t \quad (4.11)$$

On the basis of this equation it is possible to evaluate which are the values ϕ_1 and ϕ_2 that make minimum the ΔV required to compensate a certain $\Delta\omega$. In case of correction manoeuvre, the application of a single impulse causes changes in semimajor axis and eccentricity. At the base of the perigee maintenance technique

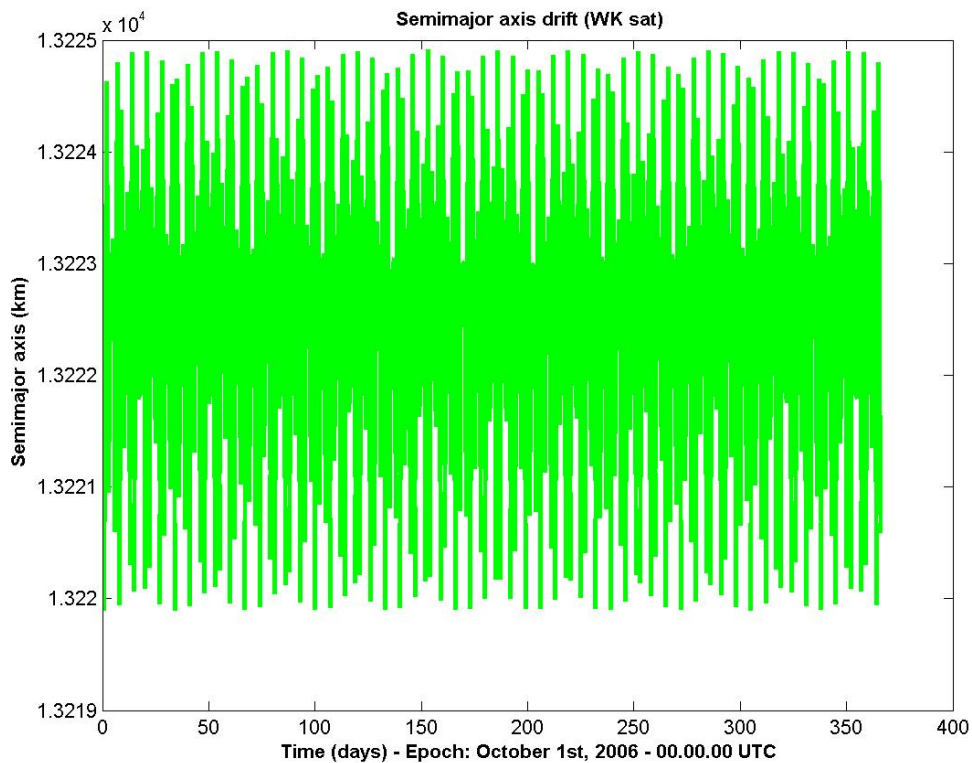


Figure 4.16: Semimajor axis evolution for the Walker satellite.

is the idea to use two impulses at ϕ_1 and ϕ_2 , each one correcting for the drift $\Delta\omega/2$, so that the respective variations in a and e are nulled:

$$\begin{aligned}\Delta a_1 + \Delta a_2 &= 0 \\ \Delta e_1 + \Delta e_2 &= 0\end{aligned}$$

The optimal velocity change is expressed by:

$$\Delta V_{opt} = \frac{1}{12}e(6 - e^2)\sqrt{\frac{\mu}{p}}\Delta\omega \quad (4.12)$$

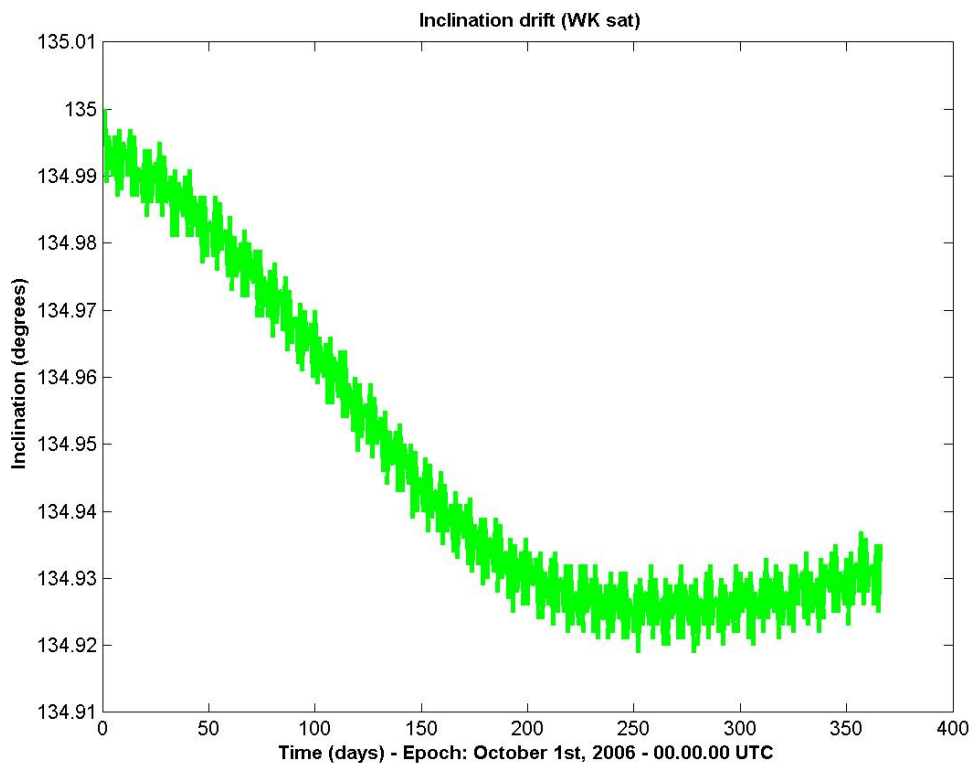


Figure 4.17: Inclination evolution for the Walker satellite.

This expression constitutes the optimal velocity change in case of perigee maintenance with minimum ΔV requirement, and could be applied for FC without critical inclination.

4.2 Constellation Positioning

The developed algorithm searches for the best trajectory of the satellites to be deployed. Satellite propagation is performed by using the Lagrange Planetary Equations (LPEs) per each time step. Regarding the time step, increasing its value the manoeuvre takes more time to be completed, but results have less precision. To determine the difference between two orbits a complex number

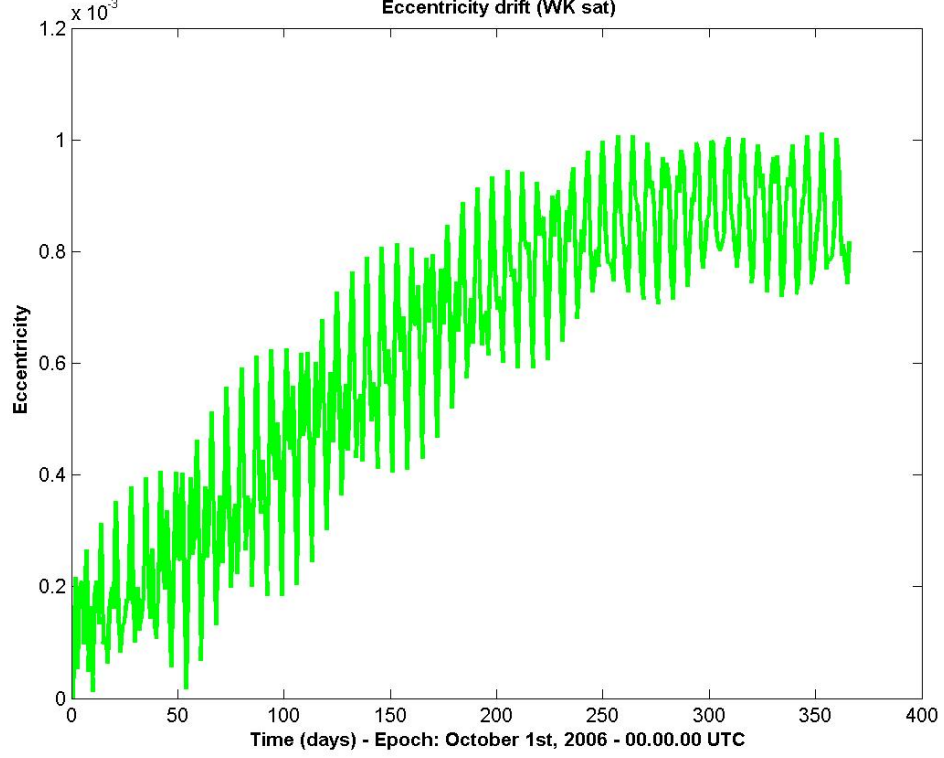


Figure 4.18: Eccentricity evolution for the Walker satellite.

defined as follows has been defined:

$$E_0(d, \delta) = (1 + d)^{-j\delta} \quad (4.13)$$

where:

$$\delta = \cos^{-1} \left(\frac{\text{trace}(T_1 T_2^T) - 1}{2} \right) \quad (4.14)$$

and:

$$\sqrt{(a_1 - a_2)^2 + (b_1 - b_2)^2} \quad (4.15)$$

T is the transformation matrix to ECI reference system (i.e. the rotation matrix for changing orbital reference system, x radial direction, z normal to the orbital

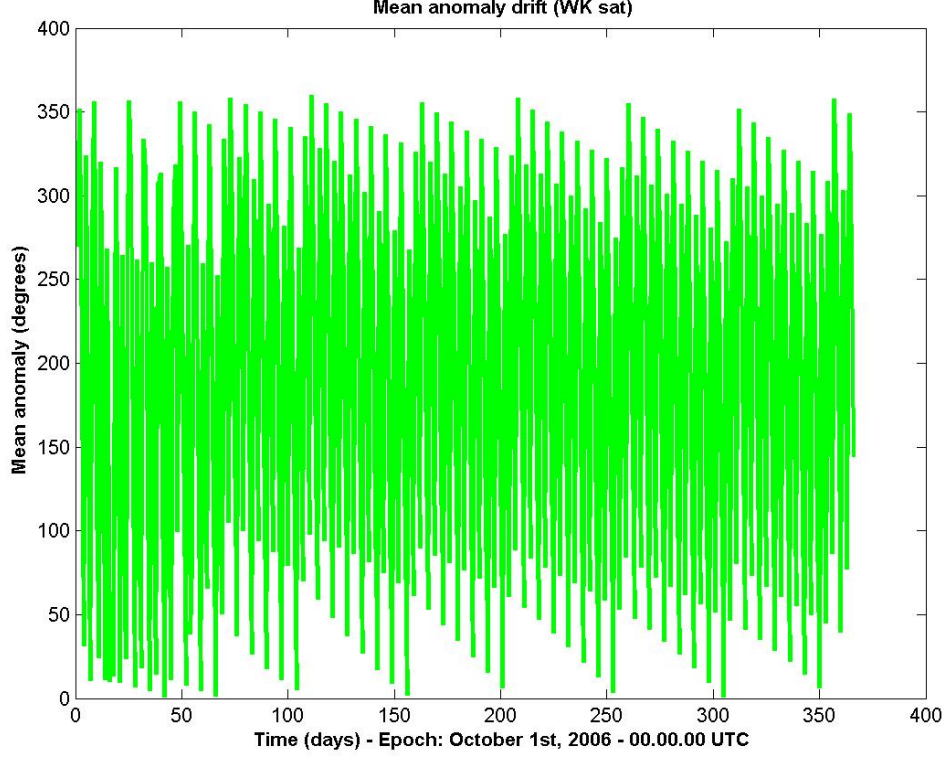


Figure 4.19: Mean anomaly evolution for the Walker satellite.

plane, y to complete), a and b are the semi-major and semi-minor axes of the orbit. Subscript index 1 refers to the parameters of the designed final orbit; the subscript index 2 refers to the parameters of the orbit that has to be compared to the other one. The module, $(1 + d)$, represents the distance of the orbits shapes, the angle δ expresses the differences in terms of orientation. To obtain a zero error comparing the two orbits, d must be zero and δ must be one, so that $EO = 1$.

If at the place of the orbit indicated by subscript 2 the sequence of orbits that satellite will go through for reaching the designed final orbit are introduced, the complex number E_O could be intended as an objective function, so that $E_0 = E_0(t)$.

In fact, maximizing the delta between two time step dt the best trajectory

between two orbits is obtained:

$$\delta = E_0(t) - E_0(t + dt) \quad (4.16)$$

By propagating this concept by induction, from the initial to the designed orbit, the transferring trajectory can be obtained. For obtaining the orbits sequence, the algorithm works on the engine firing angles: it is supposed to have an electric thruster with a given specific impulse and thrust power (on/off or variable in a set of values). The engine can be oriented in any direction of an hypothetical sphere around the satellite: this is achieved with two angles: horizontal (from 0 to 2π) and vertical (from $-\pi$ to π), the same as latitude and longitude. At every time step, algorithm finds the best direction that gives the maximum delta looking for the best couple of firing angles each in its range of values. We used a custom propagator that implement the Lagrange Planetary Equations in the Gauss form, that express in an explicit form the variations of the orbital parameters under the effect of a central body and its non-conservative perturbing forces. Thus, the gravitational field constant J_2 has been included:

$$\left\{ \begin{array}{l} \frac{da}{dt} = \frac{2a^2}{H} \left(e \sin(\theta) acc_r + \frac{p}{R_{sat}(\theta)} acc_t \right) \\ \frac{de}{dt} = \frac{1}{H} \{ p \sin(\theta) acc_r + [(p + R_{sat}(\theta)) \cos(\theta) + e R_{sat}(\theta)] acc_t \} \\ \frac{di}{dt} = \frac{R_{sat}(\theta) \cos(\theta + \omega)}{H} acc_n \\ \frac{d\Omega}{dt} = \frac{R_{sat}(\theta) \sin(\theta + \omega)}{H \sin(i)} acc_n \\ \frac{d\omega}{dt} = \frac{1}{eH} \{ -p \cos(\theta) acc_r + [(p + R_{sat}(\theta)) \sin(\theta)] acc_t \} - \frac{R_{sat}(\theta) \sin(\theta + \omega) \cos(i)}{H \sin(i)} acc_n \\ \frac{dM}{dt} = \frac{1}{na^2e} \{ [p \cos(\theta) - 2e R_{sat}(\theta)] acc_r - (p - R_{sat}(\theta)) \sin(\theta) acc_t \} \end{array} \right. \quad (4.17)$$

The following parameters have been defined:

- $a, e, i, \Omega, \omega, M$ are the six classical orbital parameters;
- θ is the true anomaly;
- $R_{sat}(\theta) = \frac{a(1-e^2)}{1+e \cos(\theta)}$ is the satellite distance from Earth centre;
- $p = \sqrt{a(1-e^2)}$ is the orbit semilatus rectum;
- n is the mean motion;

- H is the angular moment of the satellite;
- acc_r, acc_n, acc_t are the three components of an acceleration vector applied to the satellite: radial, normal and tangent to actual orbit: $acc_r = \frac{F_r}{mass_{sat}}, acc_n = \frac{F_n}{mass_{sat}}, acc_t = \frac{F_t}{mass_{sat}};$
- atg is the angle of the satellite speed at any time t , referred to perigee;
- $mass_{sat}$ is the mass of the satellite;
- $\mathbf{F}_{rtn}(lat, lon, atg) = \mathbf{M}_z(atg - \pi/2)F_{orb}(lat, lon)$
- $\mathbf{M}_z(\alpha)$ is the rotation matrix around z-axis;
- $F_{lowthrust}$ is the engine's intensity of thrust;
- $\mathbf{F}_{orb}(lat, lon)$ is the engine's vector of thrust;

Some consideration has to be made about the time step: large time steps such as 100 seconds have a bad influence on the simulation performance, because in 100 seconds the satellite goes through a big arc of the orbit and some orbital good position (e.g. the RAAN) could be missed, in spite of changing the harder reconfigurable parameters. Smaller time steps reduce at the minimum the missing of good positions for firing, but a dt smaller than 1 second need a better computing precision.

4.3 Deployment

Through the use of a software application, it is possible to study the performance of the Flower constellations in terms of staged deployment or combined deployment. It is here intended with combined deployment a deployment in which the satellites are taken from different constellations to deploy. For example, it is possible to combine the deployment of south and north cover FC choosing a subset of satellites from each one. In fact, the difference among orbits is only arguments of perigee, also if it is not the easiest parameter to change. Due to the equally spatial distribution of orbits around the Earth, for deploying a single Flower Constellation, it must be provided a manoeuvre for changing the RAANs.

4.3 Deployment

As shown in equations (3), the acceleration in the normal direction of the orbit (acc_n) modifies the RAAN, but also the inclination. For solving a n-satellites deployment problem, it has to be found the best common orbit in which launcher releases the satellites. A common orbit can be obtained computing an hypothetical back transfer for all satellites: each satellite begins the transfer from its final orbit, ending when all satellites reach the same orbit that could be assumed as the satellites release orbit of the launcher. The way to attain that strategy is to calculate, every time step of the simulation, the average of the orbital parameters of all satellites while they are changing their orbits to reach the common release orbit. Two simulations about the deployment are here presented. Due to the similarity of results using low thrusts and high thrusts, it is possible to simulate with a proportional value that multiply both engine thrust vector and specific impulse. Engine considered has a thrust vector of 0, 0.08, 0.16 and 0.24 Newton and its ISP is 4100 seconds so. Simulation have a multiply factor of 1000; time step is fixed at 10 seconds. The first simulation was carried out on three satellites belonging to a seven satellites Flower Constellation developed for Telemedicine services. The constellation orbital parameters are listed in Table 4.1:

Table 4.1: Orbital elements of the Flower Constellation for Telemedicine

Sat no.	a (km)	e	i (deg)	ω (deg)	Ω (deg)	M (deg)
1	12769	0.25932	116.6	187.07	243.77	168
2	12769	0.25932	116.6	187.07	295.19	219.42
3	12769	0.25932	116.6	187.07	346.62	270.85
4	12769	0.25932	116.6	187.07	38.05	322.28
5	12769	0.25932	116.6	187.07	89.48	13.71
6	12769	0.25932	116.6	187.07	140.91	65.14
7	12769	0.25932	116.6	187.07	192.34	116.57

Figure 4.20 shows the back transfer for each satellites; the black and the green dotted orbits are the initial orbits for satellites number 1 and 3 of the Table 4.1. Not all transfer path is here showed for simplifying the reader understanding.

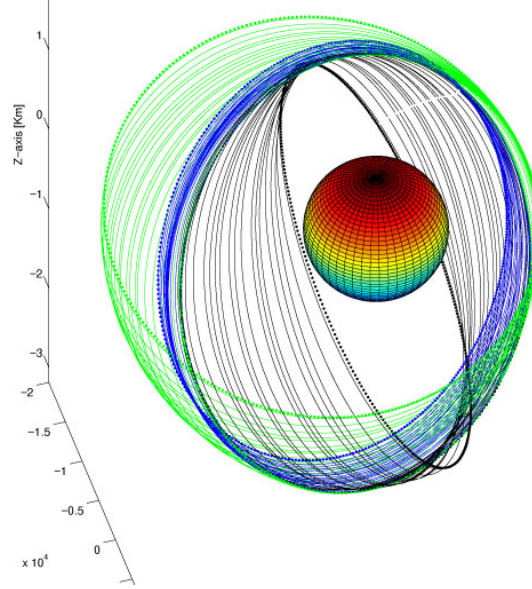


Figure 4.20: Transfer orbits for three satellites.

In Figure 4.21, shown the common orbit evolution during satellites transfers is shown. The black orbit represent the initial common orbit calculated with initial orbital parameters of the three satellites, the red orbits are the intermediate common orbits during simulation and the blue orbit is the final common release orbit.

In Figure 4.22 and 4.23, the evolution of five orbital parameters (a, e, i, ω, Ω) are represented, while the mean anomaly is not considered.

The first simulation is completed in 7.900.000 seconds (2217.1hours, 92.3787 days) and parameters of the final common release orbit are listed in Table 4.2:

Table 4.2: Common release orbit parameters.

a (km)	e	i (deg)	ω (deg)	Ω (deg)	M (deg)
12968	0.22571	120.87	145.47	296.17	269.72

Differences with the three initial orbits are:

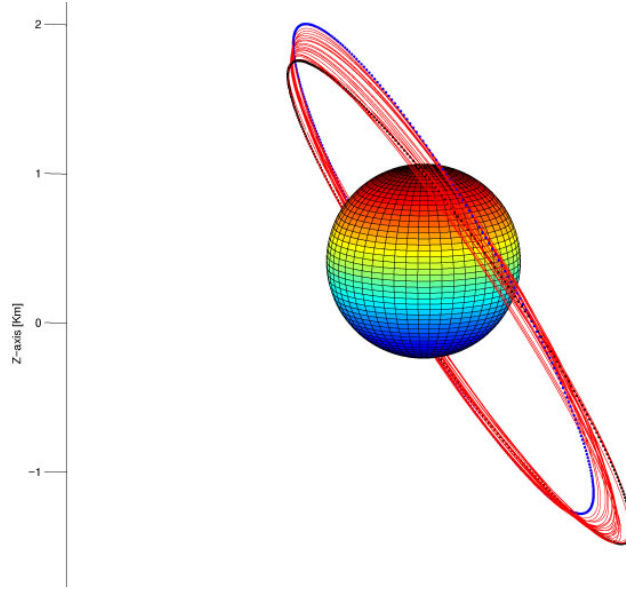


Figure 4.21: Common orbit forming (starting from blue, through reds until the black is reached).

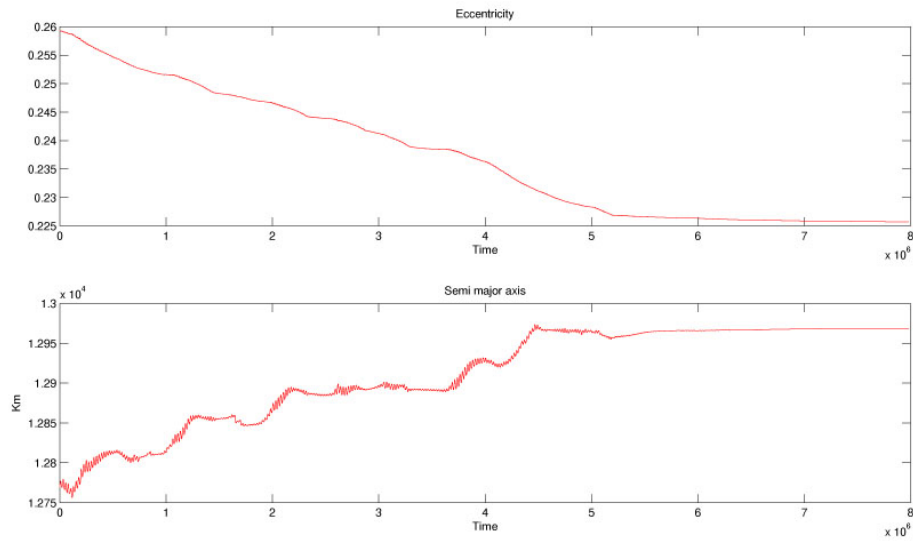


Figure 4.22: Common orbit Eccentricity and Semi major axis evolution.

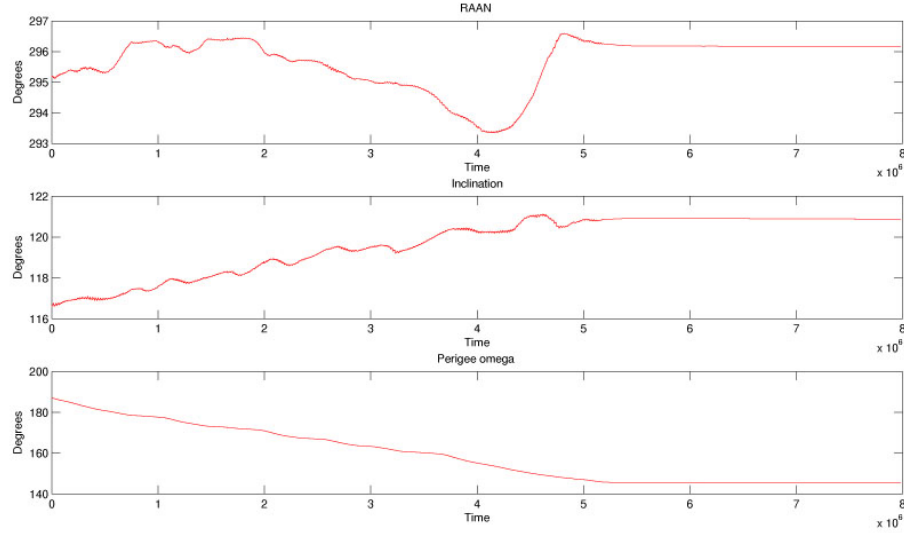


Figure 4.23: Common orbit orientation angles evolution.

- Semi major axis is increased of 199 kilometres
- Eccentricity is decreased of 0.0336107
- Inclination is increased of 4.279816153 degrees
- Perigee omega is decreased of 41.59557898 degrees
- RAAN become almost the same as the satellite number 2
- Mean anomaly become almost the same as the satellite number 2

The fuel consumption for each satellite are respectively: 14.81, 9.88 and 14.61 kilograms. Some considerations have to be made about these values, due to the multiply factor and mainly because the second orbit is similar to the common orbit and almost 10 kgs of fuel mass seems to be wasting the satellite resources. Once it is understood which is the common orbit, the real fuel mass needs to be computed simulating again a simple transfer per each satellite because the destination orbit is well known.

The second simulation involves six of the seven orbits of the FC in Table 4.1. Figures 4.24 and 4.25, show that it is not convenient in terms of time and fuel consumption to group so many satellites of this constellation, mostly due to the RAAN differences. In fact, to generate the common orbit, the algorithm changes the RAAN to all orbits, while moving the equality of the inclination values that are changed in so many different ways.

The simulation was stopped when the mass consumption was around 15/16 kilograms for each satellites and time elapsed 9 million of seconds (2500 hours), but the orientation errors are still away from the desired convergence.

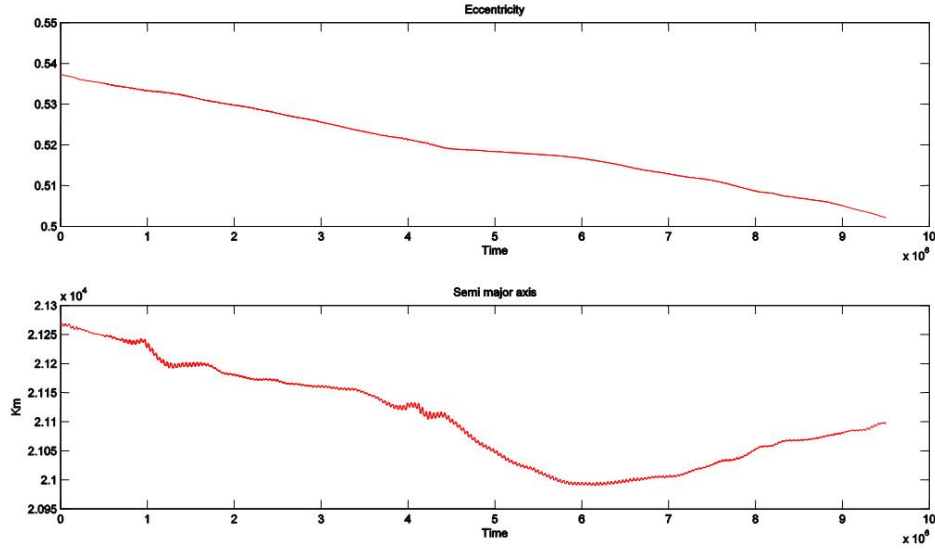


Figure 4.24: Eccentricity and Semi major axis.

4.4 Reconfigurability

Considering a generic reconfiguration, it is possible to need for changing one, or both, shape and orientation. In the most of cases here studied, for one FC the reconfiguration operations require changes in orientation for each orbit. With this motivation, the core of the algorithm has been modified with the addition of some

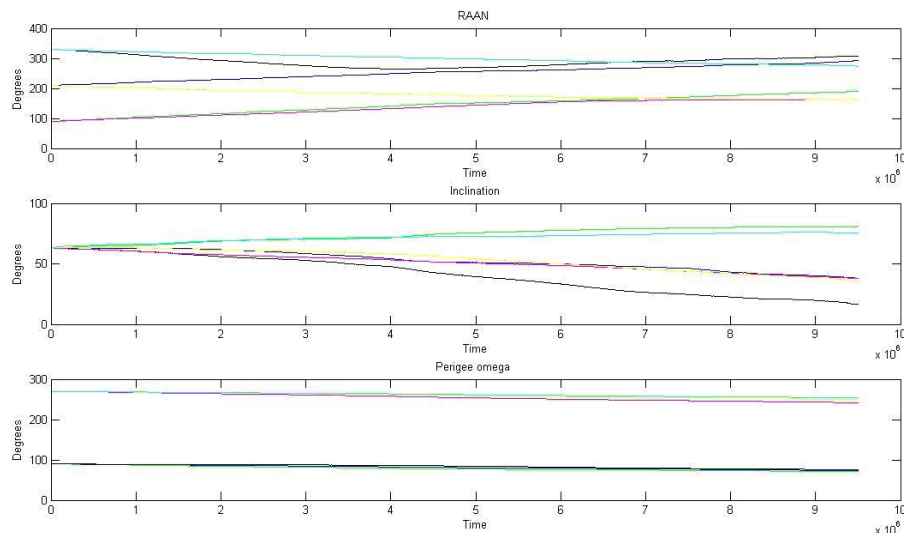


Figure 4.25: Orientation angles.

parameters that allow local worsening to “speed up” the transfers. This means that if the initial and final orbits have the same shape, it is not possible to find a better shape error than zero, as it is for same semi major axis and eccentricity, at least it can be equal to the previous while the orientation error is decreasing very slow. Allowing local worsening, it is possible to have significant decreases of orientation error every time step while the shape error is oscillating between the max local worsening enabled and the shape zero error value.

Reconfiguration could be intended in three different ways:

1. Satellite failure, recover procedure needed to assure continuity of service.
2. Staged deploy: satellites number increment.
3. Changes of area coverage, different services to supply.

These three cases are different in terms of reconfiguration operations, because while in the first 2 the number of satellites change, the third one has only changing of some orbital parameters and this kind of reconfiguration could have been planned even before the deployment.

4.4 Reconfigurability

It is interesting to study the chances of reconfigurability of the two Flower Constellation proposed for Telemedicine services with 7 and 8 satellites (see Table 4.3).

Table 4.3: Flower Constellation for Telemedicine, 8 satellites

Sat no.	a (km)	e	i (deg)	ω (deg)	Ω (deg)	M (deg)
1	12769	0.25932	116.6	187.07	243.77	168
2	12769	0.25932	116.6	187.07	288.77	258
3	12769	0.25932	116.6	187.07	333.77	348
4	12769	0.25932	116.6	187.07	18.77	80
5	12769	0.25932	116.6	187.07	63.77	168
6	12769	0.25932	116.6	187.07	108.77	258
7	12769	0.25932	116.6	187.07	153.77	348
8	12769	0.25932	116.6	187.07	198.77	80

Comparing Tables 4.1 and 4.3, it is possible to see that the two FCs have the same orbit number 1. Also if it might be this is a wanted characteristic, but in general the Flower Constellations may have this possibility.

Before to simulate a complete reconfiguration, it's been investigated different set up of parameters as the local worsening, the time step and the multiply factor of thrust and specific impulse; so the following figures show some simulations for reconfigure the orbit number 2 of Table 4.2 to the orbit number 2 in Table 4.3. Figures 4.26 to 4.30 are obtained from a simulation in which the local worsening is set to 10 km for the shape, the time step is 1 second and the multiply factor is 1000. In Figure 4.26 it is shown that eccentricity decreases rapidly to a value of 0.257 while the semi major axis oscillates until it reaches 12763 km. It means that orbit shape error is positive.

Figure 4.27, shows that the shape error increase and then it oscillates between two values (about 7 km and the LW imposed to 10). The orientation error decreases until it reaches a zero error.

4.4 Reconfigurability

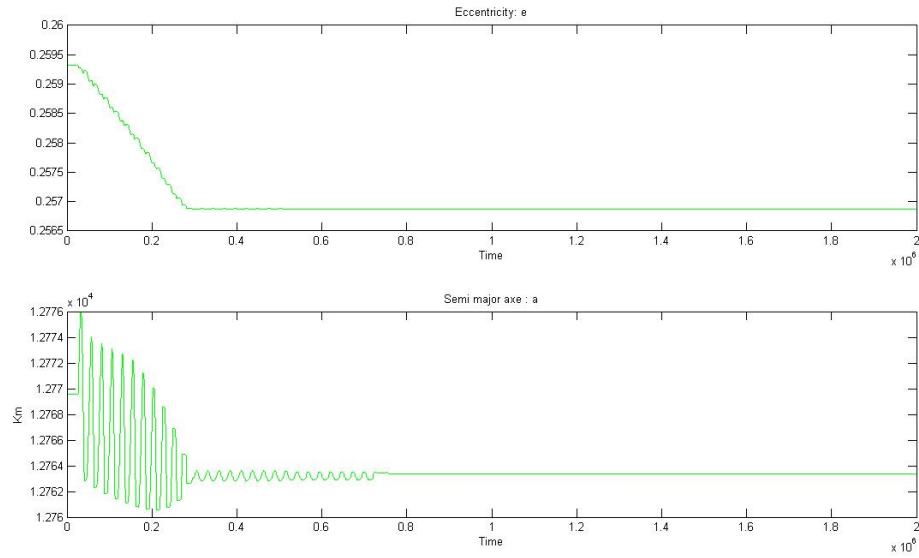


Figure 4.26: Time evolution of eccentricity and semi-major axis.

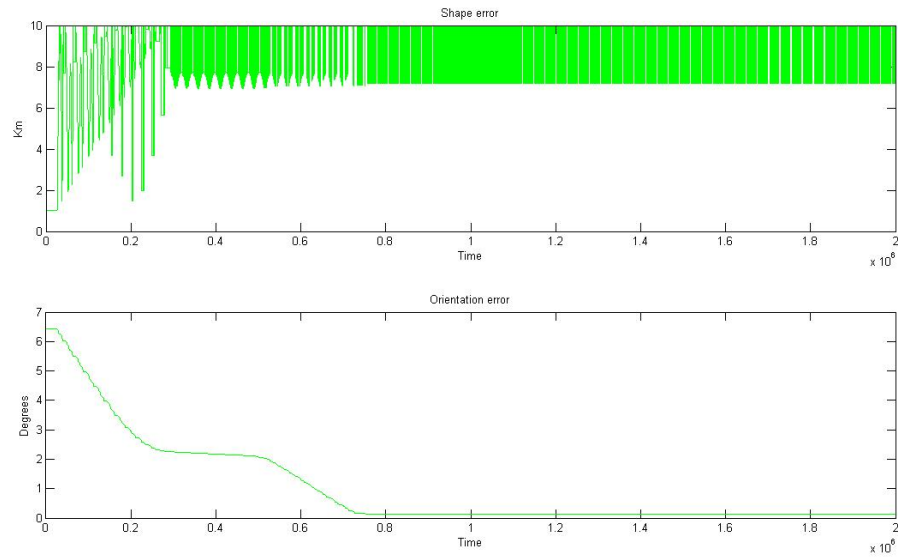


Figure 4.27: Time evolution of shape and orientation errors.

Figure 4.28 shows orientation angles. Inclination and argument of perigee

increase and decrease, oscillating around the correct value, RAAN increases until is reached the designed value.

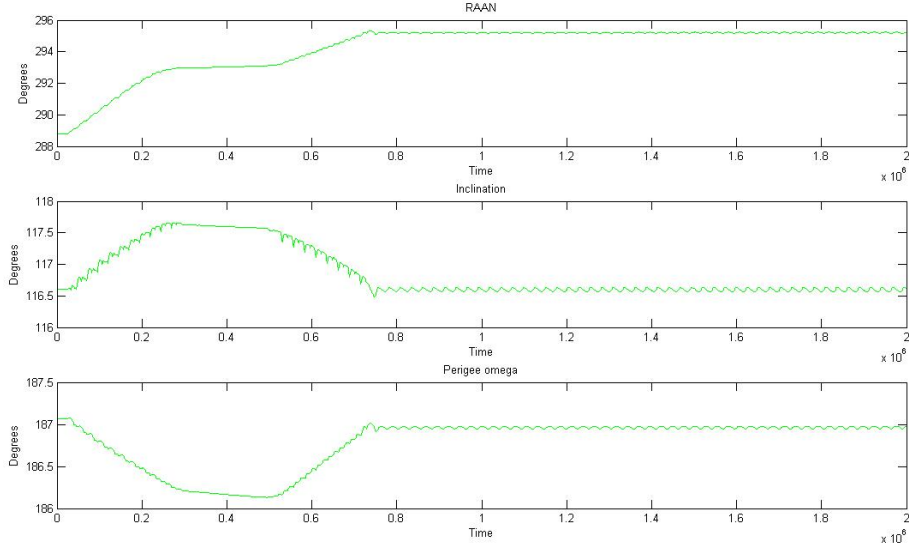


Figure 4.28: Time evolution of RAAN, inclination and argument of perigee.

In Figure 4.31 is depicted the same simulation that has a multiply factor of 100 instead of 1000 for the thrust force and for the Specific impulse. There are visible differences with figure 8, especially for the final Orientation error that it is here bigger than what is wanted: it is possible to say that this is a non convergent simulation.

After the simulation of 1 to 1 case and the time step was fixed to 1 second, four simulations were provided for the complete reconfiguration of 6 satellites, having the multiply factor of 1 (This factor express the engine as it is, in fact the engines available now in the market have a resulting thrust of hundreds of mN), 10 and 100 for the engine thrust and for the specific impulse. All four simulation are confronted in a time window of 400.000 seconds: it is showed what happen to the shape and orientation errors with different multiply factors. It is possible to see (figure 13) that for a multiply factor of 1, the simulation should take long time: Orientation error decrease very slow and the simulation appear to be impossible

4.4 Reconfigurability

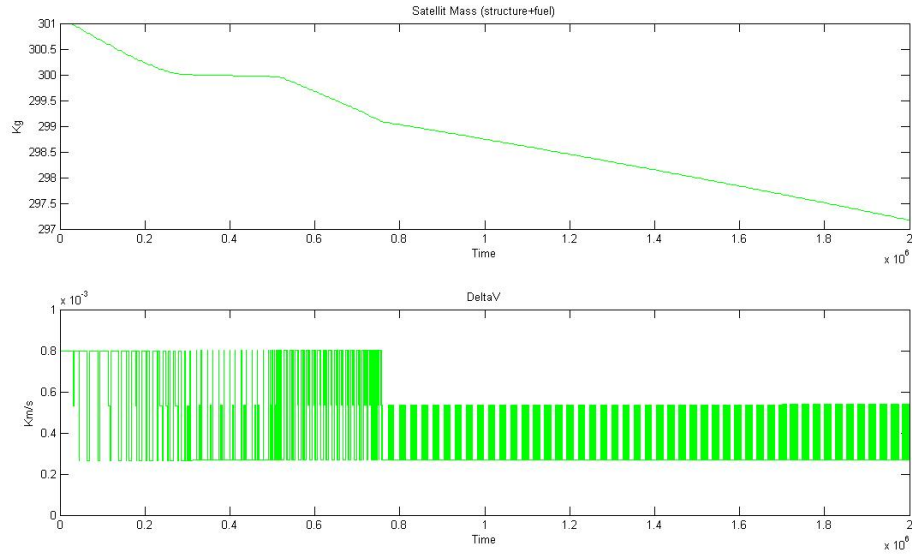


Figure 4.29: Time evolution of satellite mass and delta V .

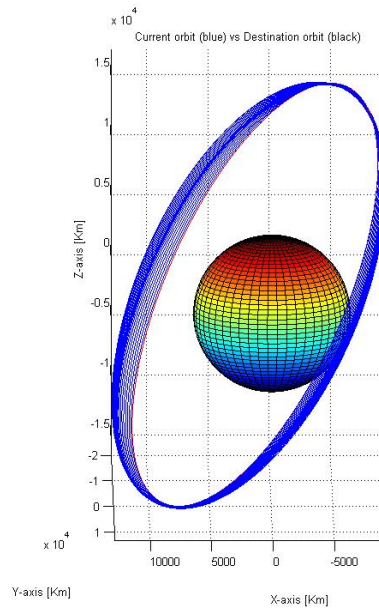


Figure 4.30: Satellite path from initial to the final orbit.

to afford with so low thrust power under effects of the Earth oblateness and the

4.4 Reconfigurability

Local worsening allowed (10 km) is not reached by the shape error.

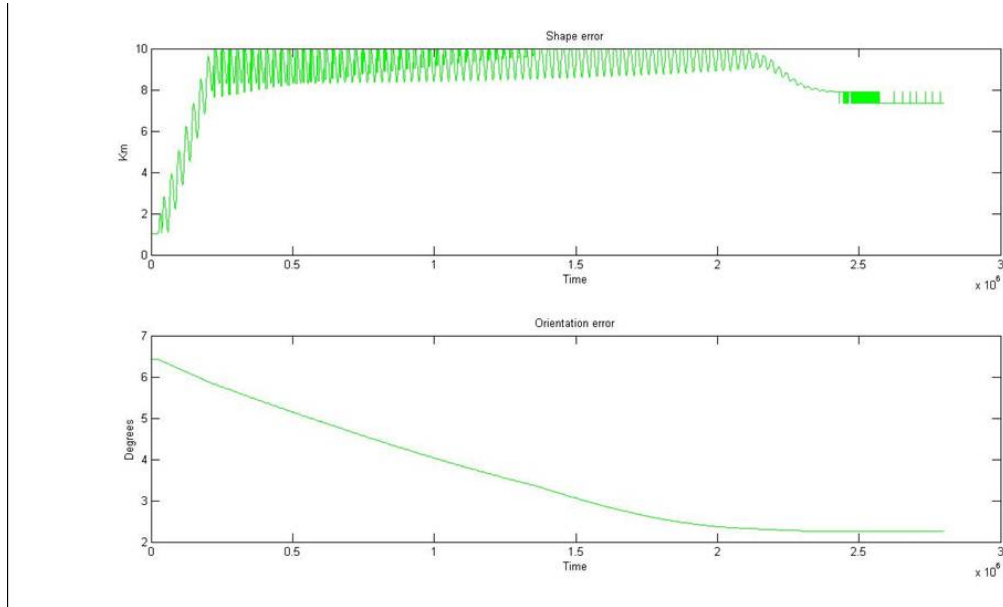


Figure 4.31: Shape and Orientation error when multiply factor is 100.

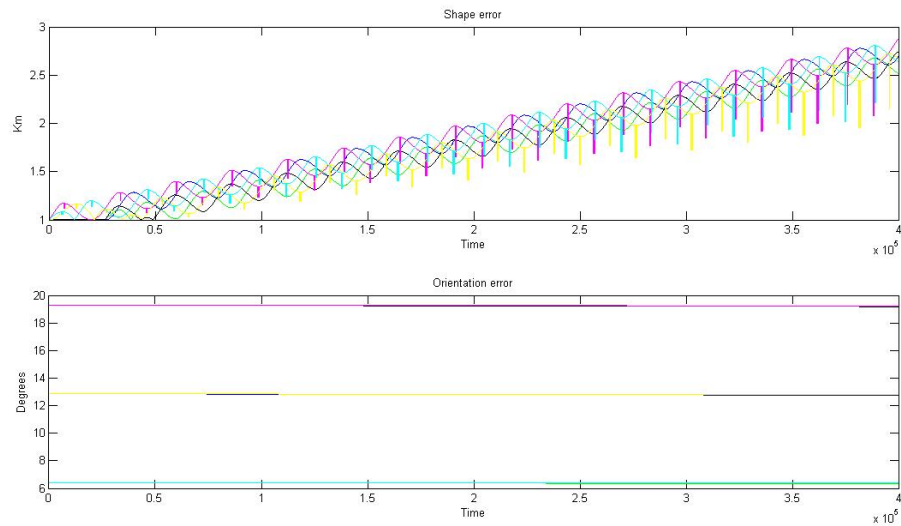


Figure 4.32: Shape and Orientation error for multiply factor equal to 1 (no effect).

In Figure 4.33, the Orientation error and Shape error for a simulation with

multiply factor of 10 are shown: the shape errors reach the maximum value allowed and decrease locally for then increasing again. The Orientation errors, decrease in 400.000 seconds of 1 degree per each satellite.

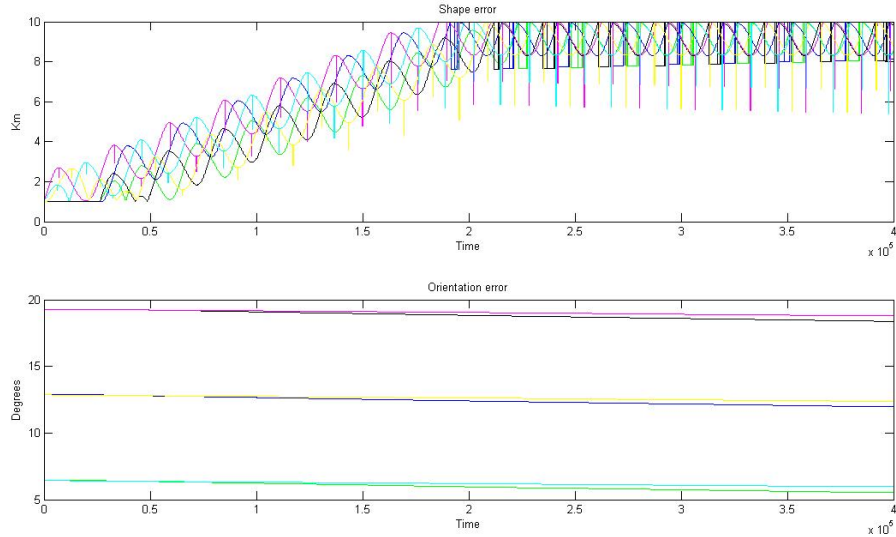


Figure 4.33: Shape and Orientation error for multiply factor equal to 10.

The last simulation is for the 100 multiply factor, where the errors of orientation has a big step in the total simulation time: about 5 degrees for all satellites orientation errors. The time line of the Figure 4.34, it could be divided in two parts: from 0 to 275.000 seconds, orientation errors decrease rapidly because the shape error is oscillating with a big level. In the second part, so after 275.000 seconds, the shape error reduce the oscillations and orientation errors are decreasing slowly.

In conclusions:

- Having a very low thrust it is needed a long time to reconfigure.
- No use of local worsening is optimal in terms of fuel mass consumption but let the reconfiguration be very long in time.

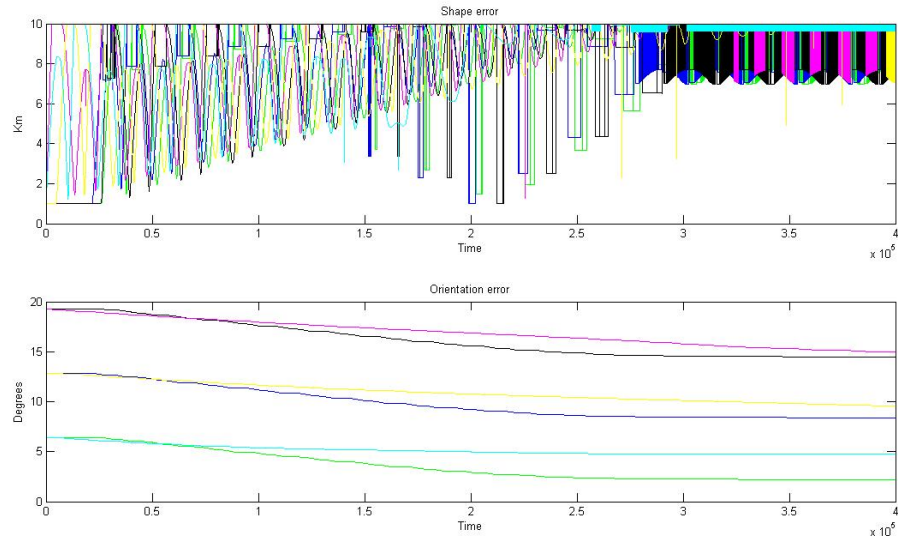


Figure 4.34: Shape and Orientation error for multiply factor equal to 100.

- A smart local worsening usage drive the satellite in non optimal trajectories but reduce the simulation time and the convergence is not always assured: it has to be analyzed the correct value of the maximum local worsening.
- The local worsening does apply to the shape error to reduce the orientation error, while it is not needed in other cases.

Chapter 5

Conclusions

In this report the theory of Flower Constellations has been updated and completed in Chapters 1 by discussing phasing rules, compatible orbits and secondary paths.

Chapter 2 discussed the optimisation process of Flower Constellations that is applied in Chapter 3 to the development of optimised Flower Constellations for different applications. The first example of exploitation of Flower Constellations is related to telemedicine services.

In a first example of application, it has been found that an autonomous Flower Constellation (i.e. provided with inter-satellite links) provides better performance with respect to a Walker constellation in terms of service availability.

The second example of application has shown that, by using Flower Constellations for a planned mission to Mars, large advantages can be achieved with respect to an already developed constellation named 4retro111.

The third example of application is applied to deep space observation by means of multiple satellites for interferometric imaging. The performance of this novel concept of application are shown.

This report ends with a preliminary study about the feasibility in terms of cost for the deployment, control and maintenance of a Flower Constellation.

Appendix A

Flower Constellation Toolbox

This is an help file for the Flower Constellation (FC) toolbox. The FC Toolbox is a collection of functions for the design and optimization of artificial satellite constellations.

List of Functions

- `y = atan3(a, b)`: fourth quadrant inverse tangent.
`a` = sine of angle, `b` = cosine of angle, `y` = angle (radians, $0 \leq c \leq 2\pi$).
- `central_body = c_body(primary_body)`: list of constants for the Planets.
`central_body` = 1 (Earth), `central_body` = 2 (Mars), `central_body` = 3 (Moon).
- `r_sph = cart2sph(r_cart)`: transforms a column vector `r_cart=[x,y,z]` ' represented in cartesian coordinates to a column vector `r_sph=[rho,phi,theta]` ' represented in spherical coordinates where phi and rho are measured in radians.
- `r_eci = ecef2eci(r_ecef,UTC_time)`: transforms a column vector `r_ecef=[x,y,z]` ' represented in cartesian coordinates in a ECEF reference frame to a column vector `r_ecef=[x',y',z']` ' represented in cartesian coordinates in a ECI reference frame. The transformation is computed at time `UTC_time` where `UTC_time` = [year, month, day, hour, minute, second].

-
- `r_ecef = eci2ecef(r_eci, UTC_time)`: transforms a column vector `r_eci=[x,y,z]` represented in cartesian coordinates in a ECI reference frame to a column vector `r_ecef=[x',y',z']` represented in cartesian coordinates in a ECEF reference frame. The transformation is computed at time `UTC_time` where `UTC_time = [year, month, day, hour, minute, second]`.
 - `r_sez_sph = eci2sez(r_sat_eci, lat, long, alt, utctime)`: provides coordinates of a satellite in a SEZ reference frame. `r_sat_eci` = satellite position vector in ECI reference frame and cartesian coordinates, `lat` = geocentric latitude of the observer site (center of the SEZ reference frame), `long` = geocentric longitude of the observer (center of the SEZ reference frame), `alt` = geocentric altitude of the observer (center of the SEZ reference frame), `utctime` = reference time.
 - `optimrepeat`: optimisation of a repeating ground track for the proper coverage of a list of sites. The optimisation process is performed by using Genetic Algorithms.
 - `r_eci = orb2eci(orb)`: computes the position column vector of a satellite in a ECI reference frame from the orbital elements vector `orb`. `orb = [a, e, i, wp, RAAN, TA]`, `a` = semi major axis (km), `e` = eccentricity, `i` = inclination (rad), `wp` = argument of perigee (rad), `RAAN` = Right Ascension of the Ascending Node (rad), `TA` = true anomaly (rad).
 - `[EA,TA] = kepler(MA,ecc)`, solves Kepler's equation, `MA = EA - ecc*sin(EA)` [rad], by using the Mortari method, `MA`: mean anomaly [rad], `ecc`: orbital eccentricity [non-dimensional], `EA`: eccentric anomaly [rad], `TA`: true anomaly [rad]
 - `oe = walker(t, p, f, sma, inc)`: builds a walker constellation for the specified parameters. A Walker constellation consists of a group of satellites that are in circular orbits and have the same period (or, equivalently, radius) and inclination. The pattern of the constellation consists of evenly spaced satellites (`s`) in each of the orbital planes (`p`) specified so that `t = s * p`.

The ascending nodes of the orbital planes are also evenly spaced over a range of right ascensions (RAAN).

t: number of satellites (adim) (integer).

p: number of planes (adim) (integer, $2 \leq p \leq t$).

f: phasing parameter (adim) (integer, $0 \leq f \leq p-1$).

RAANspread: Spreading of the RAAN (deg) ($0 < \text{RAANspread} \leq 360$).

a: semi-major axis (km).

inc: inclination (deg).

oe: orbital elements matrix, $6 \times t$. Each row is the orbital elements of i -th satellite: Semi-major axis, Eccentricity, Inclination, RAAN, Arg of Perigee, Mean anomaly.